

# UNCERTAIN AND ASYMMETRIC FORECASTS <sup>\*</sup>

Eric Vansteenberghe<sup>†</sup>

## Abstract

Measures of inflation uncertainty and directional risk constructed from higher moments of forecast distributions are contaminated by the first moment, but in fundamentally different ways. Using individual density forecasts from the ECB Survey of Professional Forecasters, this paper shows that 42% of the variation in raw forecast variance is explained by the distance of expected inflation from target—a mechanical level effect—while raw asymmetry is too noisy to identify directional risk unless disciplined by the central forecast. We propose two complementary corrections grounded in micro-founded mechanisms. *Normalized Uncertainty* (NU) disentangles the first moment from the second by removing the predictable component of dispersion tied to the policy anchor, recovering genuine belief imprecision. *Asymmetry Coherence* (AC) re-entangles the first and third moments by extracting directional risk only when observed asymmetry is coherent with the central forecast, providing an operational formalization of the balance of risks. These corrections carry first-order consequences for inference. In a replication of Barro (1995), the inflation-volatility effect on growth vanishes once level contamination is removed, and the inflation-level coefficient recovers significance—implying that the growth cost attributed to uncertainty reflects high inflation itself. In a VAR, the sign of the monetary-policy response reverses: raw asymmetry shocks imply easing, whereas coherent upside-risk shocks imply the expected tightening. In the credit channel, properly measured uncertainty genuinely conditions the transmission of monetary policy easing to bank lending: under high inflation uncertainty, pass-through to loan pricing is slower and more incomplete, particularly at longer maturities. A clean division of roles emerges. NU conditions *how* monetary policy is transmitted—governing the state dependence of pass-through to credit conditions. AC informs *why* policy responds—providing directional signals that predict tightening decisions and carry forecasting content for the inflation level. For the second moment, measurement requires disentangling the first from the second; for the third, economic interpretation requires re-linking the third to the first. Higher moments become more informative not when used mechanically, but when measured in a way that separates macroeconomic signals from first-moment contamination.

*Keywords:* Uncertainty, Asymmetry, Balance of Risks, Predictive Distributions, Monetary Policy, Growth.

*JEL codes:* C53, D81, D84, E31, E37, E43, E52.

---

<sup>\*</sup>We are grateful to Olivier de Bandt, Jean Barthélemy, Agnès Benassy-Quéré, Antoine Camous, Laurent Clerc, Jose Fellmann, David Gauthier, Christoph Grosse-Steffen, Sophie Guilloux-Nefussi, Stéphane Lhuissier, Magali Marx, Adrian Penalver, Arthur Saint-Guilhem, Manuel Schick and Elias Wolf for helpful comments and discussions. The views expressed in this paper are solely those of the author and do not necessarily reflect the views of his past, present, or future employers.

<sup>†</sup>Banque de France and Université Paris 1 Panthéon-Sorbonne. E-mail: [eric.vansteenberghe@banque-france.fr](mailto:eric.vansteenberghe@banque-france.fr)

# 1 Introduction

Raw higher moments of forecast distributions do not necessarily identify the economic objects they are commonly taken to measure. When inflation expectations move away from a policy anchor, raw forecast variance increases mechanically—even if genuine belief imprecision does not—so that what is often interpreted as “uncertainty” partly reflects the level of inflation itself (Friedman, 1977; Ball, 1992). Raw skewness poses a related but different challenge: it is difficult to estimate precisely from forecast data, and an asymmetric distribution need not convey a meaningful directional signal about future outcomes. We show that the first moment provides useful discipline for interpreting the third moment and identifying directional risk. Accordingly, the second raw moment embeds a first-moment component large enough to distort inference, whereas the third moment becomes more informative once disciplined by the first moment.

This paper proposes two corrections that recover the objects of interest by appropriately reinterpreting their relationship with the first moment. *Normalized Uncertainty* (NU) disentangles the first and second moments by removing the predictable level component from raw dispersion through a variance-stabilizing transformation anchored in the distance-to-target relationship, thereby recovering genuine belief imprecision. *Asymmetry Coherence* (AC), by contrast, re-links the first and third moments by retaining only the component of asymmetry that is coherent with the central forecast, yielding an operational measure of directional risk and the balance of risks. Both corrections are grounded in micro-founded mechanisms and validated using individual density forecasts from the ECB Survey of Professional Forecasters (ECB-SPF).

The paper makes three contributions. First, on *measurement*: in the ECB-SPF, 42% of the variation in raw forecast variance is explained by the distance from target; NU removes this dependence. Raw asymmetry is strongly related to the first moment: in the ECB-SPF, the correlation between the mean forecast and skewness is 0.64, and individual skewness loads positively on the signed deviation of the forecast from target. Second, on *empirical reassessment*: the corrections can reverse canonical conclusions. In a replication of Barro (1995), the inflation-volatility coefficient vanishes once level contamination is removed, while the inflation-level coefficient recovers significance. In a VAR, raw asymmetry shocks produce a counterintuitive *easing* of the policy rate, whereas AC shocks yield the expected tightening. Third, on *forecasting and interpretation*: adding raw dispersion to inflation forecasting models worsens predictions, while adding AC lowers MSFEs across horizons, with the largest reduction reaching 24% at the four-quarter horizon. More broadly, the corrections are portable across survey data sources and generalizable beyond the inflation setting.

The remainder of the paper is organized as follows. Section 2 formalizes the two identification failures—level dependence and directional-content contamination—and documents their quantitative importance. Section 3 develops NU and AC from micro-founded theory and validates both on ECB-SPF micro data. Section 4 shows how much inference changes once the corrections are applied. Section 5 concludes.

## 1.1 Related literature

This paper connects to several strands of the literature. A common feature of the work surveyed below is that it relies on raw higher moments—uncorrected either for level dependence or for the need to discipline directional content through the first moment—so that some of its conclusions may be affected by the identification problems documented in this paper.

**Measuring macroeconomic uncertainty.** Since uncertainty is not directly observable, economists have developed diverse proxies. News-based indices count uncertainty-related keywords in news-

papers (Baker, Bloom and Davis, 2016; Ahir, Bloom and Furceri, 2022). Market-based measures exploit option-implied volatility to infer the price of aggregate risk. Statistical approaches estimate the expected volatility of the unforecastable component of many macro variables (Jurado, Ludvigson and Ng, 2015). Survey-based approaches, pioneered by Zarnowitz and Lambros (1987), exploit histogram forecasts to distinguish *average individual uncertainty* from *disagreement* (Engelberg, Manski and Williams, 2009). A common feature across all these approaches is that the resulting measures tend to co-move with first-moment movements—option-implied volatility depends on moneyness, GARCH variances absorb regime shifts, and survey dispersion widens when expectations drift from anchors. Our NU measure addresses this level dependence directly: it applies a variance-stabilizing transformation that removes the predictable component of dispersion, yielding a measure of genuine belief imprecision that is portable across data sources.

**Inflation uncertainty and economic performance.** Friedman (1977) was among the first to stress the destabilizing effects of inflation uncertainty on real economic performance. Levi and Makin (1980) document that inflation uncertainty is negatively related to employment; Zarnowitz and Lambros (1987) find adverse effects on growth; and Haa and Sob (2024); Hillenbrand et al. (2025) show that episodes of elevated inflation uncertainty are associated with sizable declines in economic activity, with particularly pronounced effects on investment. A parallel literature links inflation uncertainty to term premia and financial conditions: Wright (2011) documents the impact on the term structure, Rudebusch, Sack and Swanson (2006) finds that lower term premia are associated with stimulus to real activity, Wachter (2006) resolves the expectations puzzle through time-varying bond risk premia linked to the business cycle, and Minoiu, Schneider and Wei (2024) provides evidence that the slope of the yield curve affects economic activity through bank lending. At the micro level, Paloviita and Viren (2013, 2014) show using ECB-SPF data that individual inflation uncertainty systematically lowers the same forecaster’s GDP-growth predictions, consistent with a Lucas-type supply channel, while Fischer, Herler and Schnattinger (2024) confirm in household experiments that higher perceived inflation uncertainty depresses income expectations and planned spending. A key econometric concern running through this literature is that the simultaneous inclusion of the inflation level and its variability is problematic, since the two are inherently correlated (Gordon, 1971; Okun, 1971; Cukierman and Wachtel, 1979). In contrast, survey-level analysis by Abel et al. (2016) finds limited evidence of linkages between forecast uncertainty and the level of inflation, a result we show in Section 2.1 to be largely sample-driven (see also Online Appendix ?? for full replication details). Our NU measure directly addresses the level–variability confound by construction.

**Time-series models of inflation dynamics.** Engle (1982) introduced the ARCH framework applied to inflation data, treating conditional variance as a measure of inflation uncertainty; Grier and Perry (1998) extended this to GARCH specifications to analyze macroeconomic effects. Stock and Watson (2007) proposed the unobserved-components stochastic-volatility (UCSV) model, which decomposes inflation into trend and transitory components with time-varying volatility and provides a foundation for modern state-space approaches to inflation uncertainty. Our theoretical framework extends the UCSV approach by making the innovation variance state-dependent, generating the variance–distance relationship that motivates the NU normalization.

**Asymmetry, directional risk, and the balance of risks.** Skewness is economically important across multiple domains. In asset pricing, Kraus and Litzenberger (1976) establish that coskewness is a priced risk factor; Harvey and Siddique (2000) find that systematic skewness commands a

risk premium; and Barberis and Huang (2008) show that idiosyncratic skewness can be overpriced under prospect theory. In macroeconomics, Neftci (1984) demonstrates that many macro series reject symmetry, Barro (2006) shows that tail asymmetry is central to disaster-risk premia, and Guvenen, Ozkan and Song (2014) documents that labor income changes exhibit countercyclical negative skewness. Artzner et al. (1999) formalize properties of coherent tail-focused risk measures. For inflation specifically, Ball and Mankiw (1995) establish in a menu-cost framework that aggregate inflation is positively related to the skewness of relative price changes; Kitsul and Wright (2013) extract option-implied inflation densities that display pronounced time-varying skewness; and Bianchi, Ludvigson and Ma (2022) document that shifts in the skewness of SPF inflation expectations are informative for subsequent movements in inflation and output. Despite this rich literature, a common shortcoming is that raw asymmetry—whether derived from survey histograms, option-implied densities, or model-based distributions—is often interpreted as a fully informative measure of directional risk. Yet the third moment is notoriously difficult to measure precisely in the settings most often used in practice: survey densities are binned and coarse, option-implied densities are recovered from a limited range of strikes and maturities, and model-based distributions are subject to specification error. Under these conditions, raw skewness can be too noisy to stand on its own as a reliable indicator of the direction of future risks. Our point is therefore to discipline its interpretation. The AC index does so by using the first moment to filter the third moment, retaining only the component of asymmetry that is coherent with the central forecast and therefore more likely to carry economically meaningful directional information. It thus offers an operational statistical formalization of the “balance of risks”—a notion central to monetary policy communication and risk management, but one that has lacked a standard empirical counterpart.

**The inflation–growth nexus.** Barro (1995) establishes two stylized facts in a broad panel of countries—right-skewed inflation distributions and a positive level–volatility relationship—and shows that higher inflation harms long-run growth, with the volatility of inflation entering as a separate damaging channel. Subsequent work has debated the relative roles of inflation levels and inflation variability: Gordon (1971) and Okun (1971) noted early on that the two are inherently correlated, making separate identification difficult; Cukierman and Wachtel (1979) formalized the positive level–variability link. Our replication of Barro (1995) with NU in place of raw inflation standard deviations sheds new light on this debate: the volatility coefficient becomes insignificant once level-corrected uncertainty replaces the raw measure, while the level coefficient recovers its significance. This finding implies that the growth-damaging channel attributed to inflation “uncertainty” in cross-country regressions partly reflects a level effect—high-inflation regimes rather than genuine belief imprecision—consistent with the theoretical predictions of our framework.

## 2 What the literature measures—and why we revisit it

This section documents two identification failures that contaminate the higher moments routinely used as proxies for uncertainty and directional risk. We first describe how each moment is typically constructed and employed, then formalize why the resulting objects do not identify the economic quantities they are intended to measure.

### 2.1 Dispersion as uncertainty

The empirical uncertainty literature relies on four broad classes of proxies, all of which produce measures that co-move with first-moment movements. *Realized-volatility approaches*—beginning with

Engle (1982)’s ARCH framework and its GARCH extensions (Grier and Perry, 1998)—estimate conditional variance from squared residuals, which mechanically inherit regime shifts in the inflation level. *State-space models*, most prominently the unobserved-components stochastic-volatility (UCSV) framework of Stock and Watson (2007), decompose inflation into trend and transitory components with time-varying volatility; the estimated stochastic volatility tracks the scale of shocks but does not separate level-driven from belief-driven variation. *News-based indices* (Baker, Bloom and Davis, 2016; Ahir, Bloom and Furceri, 2022) count uncertainty-related keywords in newspapers; these co-move with inflation episodes because the same macroeconomic conditions that move expectations also generate news coverage. *Survey-based measures* (Zarnowitz and Lambros, 1987; Engelberg, Manski and Williams, 2009) extract the variance of individual forecast distributions from histogram data, providing the most granular proxy—but one that is again mechanically tied to the level of expectations.

The contamination is quantitatively large. In the ECB Survey of Professional Forecasters, regressing raw inflation uncertainty (the cross-sectional mean of individual SPD variances) on the absolute distance of the consensus forecast from the 2% target yields  $R^2 = 0.425$  (Table 3, column 3). Nearly half of what is routinely called “inflation uncertainty” is explained by a single first-moment object. Any regression that uses raw dispersion as an uncertainty proxy is therefore mechanically contaminated by this level dependence—a concern first noted by Gordon (1971) and Okun (1971), formalized by Cukierman and Wachtel (1979), but not systematically corrected in the subsequent literature.

A natural objection is that earlier survey-level evidence found weak or non-significant links between the level of expected inflation and forecast uncertainty. Abel et al. (2016), analyzing ECB-SPF data over 1999–2013, report near-zero slopes and conclude that aggregate point predictions do not co-move with uncertainty. We replicate their specifications on their original sample and confirm their null result ( $\hat{\beta} = 0.029$ ,  $R^2 \approx 0$ ). However, extending the sample to 2025—thereby including the 2021–2023 inflation surge—reverses the conclusion: the slope rises to  $\hat{\beta} = 0.295^{***}$  with  $R^2 = 0.50$  (variance-based measure; Figure 1). The earlier null finding reflects limited statistical power over a period when expectations remained near target, not the absence of a structural relationship. This sample dependence underscores the importance of a correction that is grounded in theory rather than in the absence of a historical episode. Full replication details appear in Online Appendix ???. We now formalize this, previewing the propositions that Section 3 proves in full.

**Level-dependence failure.** Under Bayesian learning about a latent inflation target and stochastic policy-response uncertainty, the conditional predictive variance is not a free parameter: it is a function of the distance  $d_t = |\mu_t - \mu^*|$  of the expected inflation path from the policy anchor. To first order:

$$\text{Var}(X_{t+1} | \mathcal{I}_t) = a + b d_t + V_{\text{genuine},t}, \quad (1)$$

where  $a > 0$  is the baseline variance at target,  $b > 0$  reflects two additive channels (learning and policy-response uncertainty), and  $V_{\text{genuine},t}$  is the residual—the genuine, economically interesting component orthogonal to the level. Any empirical exercise that uses  $\text{Var}(X_{t+1} | \mathcal{I}_t)$  as “uncertainty” confounds the structural component  $a + b d_t$  with  $V_{\text{genuine},t}$ . Proposition 1 in Section 3 provides the micro-founded proof with explicit expressions for  $a$  and  $b$ .

## 2.2 Asymmetry as directional risk

The macroeconomic and finance literatures increasingly use skewness as a proxy for directional risk, tail risk, or the balance of risks. In asset pricing, Kraus and Litzenberger (1976) and Harvey and

Siddique (2000) establish that skewness is a priced risk factor. In macro, Ball and Mankiw (1995) link aggregate inflation to the skewness of relative price changes; Kitsul and Wright (2013) extract option-implied inflation densities with time-varying skewness; and Bianchi, Ludvigson and Ma (2022) show that SPF inflation-skewness shifts predict subsequent inflation and output movements. More recently, De Polis, Melosi and Petrella (2025) use skewness augmentations of UCSV models for density forecasting.

The common assumption across these applications is that observed skewness can be interpreted directly as directional risk. We argue instead that the third moment is often measured too noisily for such a reading to be warranted. In survey data, subjective probability distributions are reported in sparse bins; in option-based settings, densities are recovered from a limited set of strikes and maturities; and in model-based approaches, skewness remains exposed to specification error. In these environments, raw skewness or asymmetry should not be treated as fully informative.

In the ECB-SPF, the first moment is positively related to individual asymmetry, but it explains only a very small fraction of its variation. In Table 4, the signed deviation of the SPD mean from target enters significantly, yet the corresponding  $R^2$  is about 1% in the baseline specification. So the issue is not that raw asymmetry is mechanically driven by the first moment, but that it is too noisy to be interpreted confidently on its own. Our AC measure addresses this problem by using the first moment as a disciplining device: it retains only the component of asymmetry that is coherent with the central forecast, yielding a more operational measure of directional risk and of the balance of risks.

**Directional-content failure.** The problem with raw skewness is not primarily that it is mechanically driven by the first moment. Rather, the problem is interpretability. In many empirical environments, the third moment is difficult to estimate with precision: survey densities are reported on sparse histogram bins, option-implied densities are recovered from a limited range of strikes and maturities, and model-based skewness remains sensitive to specification error. As a result, observed asymmetry often combines a potentially meaningful directional component with substantial measurement noise.

A useful benchmark is the case of *coherent asymmetry*, in which the sign of the third moment agrees with the sign of the deviation of the central forecast from the anchor. Formally, one may write

$$\mu_3(X_{t+1} | \mathcal{I}_t) = c(\mu_t - \mu^*) + \eta_t, \quad (2)$$

where  $c > 0$  and  $\eta_t$  collects measurement error, specification noise, and idiosyncratic shape variation unrelated to the directional signal. When  $\mu_t > \mu^*$ , the case  $c > 0$  implies positive skewness: forecasters not only expect inflation above target, but also assign relatively more probability mass to upside outcomes. From a policy perspective, this is an informative configuration. It suggests that the expected policy response is not perceived as forceful enough to eliminate upside inflation risk. Symmetrically, when  $\mu_t < \mu^*$ , coherent negative skewness indicates perceived downside risk around an already weak central outlook.

Raw skewness alone cannot distinguish this economically meaningful case from a distribution whose estimated asymmetry is large but directionally uninformative. A positive third moment is not necessarily a strong upside-risk signal unless it is read jointly with the location of the distribution. This is why the relevant object is not asymmetry per se, but *asymmetry coherence*: whether the third moment reinforces the message of the first moment or contradicts it. When the first and third moments have the same sign relative to the anchor, the predictive density sends a *strong* directional signal. When they point in opposite directions, the signal is *weak*: the center of the distribution and its tail configuration do not tell the same story. The illustrative figure in Section 3.2.2 makes

this distinction visually by contrasting coherent and incoherent combinations of the first and third moments.

The AC index, developed in Section 3.2.2, operationalizes this idea by filtering raw asymmetry through sign agreement with the central forecast. It therefore does not treat the third moment as fully informative on its own; instead, it extracts the component of asymmetry that is consistent with the directional message conveyed by the first moment. Proposition 2 provides the formal result.

The two failures are conceptually distinct but structurally related. For second moments, the problem is that raw dispersion embeds a first-moment component and therefore overstates genuine uncertainty. For third moments, the problem is that raw asymmetry is often too noisy to be interpreted directly, unless its sign is evaluated jointly with the central forecast. The NU and AC corrections therefore operate on different objects, but both use the first moment as an organizing device. Table 5 in Section 4 summarizes how inference changes once these corrections are imposed.

### 3 Corrected measures

Section 2 documented two identification failures: raw dispersion absorbs level effects, and raw asymmetry is not directly interpretable as directional risk because its directional content is obscured by estimation noise. This section develops the two corrections—Normalized Uncertainty (NU) and Asymmetry Coherence (AC)—from micro-founded mechanisms, defines their construction, and validates both on ECB-SPF micro data.

Label	Definition	Scope
IU	Raw inflation uncertainty (mean of individual subjective probability distribution [SPD] variances)	Inflation
NU	Normalized Uncertainty (generic)	Conceptual
NIU	Normalized Inflation Uncertainty (NU applied to inflation)	Inflation
NGU	Normalized Growth Uncertainty (NU applied to growth)	Growth
Raw asymmetry	Raw quantile-based asymmetry (Bowley’s formula)	All
AC	Asymmetry Coherence (generic)	Conceptual
ACI	Asymmetry Coherence Index (AC applied to inflation)	Inflation
ACG	Asymmetry Coherence of Growth (AC applied to growth)	Growth

Generic labels (NU, AC) are used in conceptual discussion; application-specific labels (NIU, ACI, etc.) are used in all empirical exercises.

#### 3.1 Normalized Uncertainty

Do the macroeconomic effects commonly attributed to inflation uncertainty reflect genuine belief imprecision, or do they largely proxy for high-inflation regimes? If dispersion increases predictably when expectations deviate from a policy anchor, then raw uncertainty measures conflate two conceptually distinct objects: (i) a *structural component*—the predictable widening of the forecast distribution when the expected level drifts from target—and (ii) *genuine uncertainty*—fluctuations in belief precision that are orthogonal to the level of expectations. Disentangling these two components is critical. Without doing so, one cannot determine whether it is inflation uncertainty *per se* that weakens monetary policy transmission, de-anchors expectations, and depresses growth,

or whether these effects merely reflect the level of inflation itself. This contamination problem is not specific to inflation or surveys—it arises whenever variance is used as a state variable in environments where first-moment movements mechanically widen distributions—but it is particularly consequential in the inflation context, where decades of empirical work rest on potentially confounded uncertainty measures.

This section develops a *Normalized Uncertainty* (NU) measure that isolates the genuine component. The construction proceeds in three steps. First, Section 3.1.1 provides micro-founded theoretical mechanisms showing *why* the conditional variance of forecast distributions increases with the distance of expectations from a policy anchor, and derives the affine variance–distance relationship  $\text{Var}(X_{t+1} | \mathcal{I}_t) = a + b |\mu_t - \mu^*|$  as a first-order approximation common to all mechanisms. Second, Section 3.1.2 uses this result to define NU as the natural variance-stabilizing normalization that removes the structural component, yielding an uncertainty indicator that is comparable across survey rounds and largely orthogonal to the level of expected inflation. Third, Section 3.1.3 validates the variance–distance relationship on ECB Survey of Professional Forecasters (ECB-SPF) micro data and documents the empirical properties of the resulting NU measure.<sup>1</sup>

### 3.1.1 Distance-dependent volatility

A robust empirical regularity of survey-based forecast distributions is that dispersion increases when the expected value of the target variable deviates from a policy anchor (Friedman, 1977; Ball, 1992; Brunner and Hess, 1993; Giordani and Söderlind, 2003; Mankiw, Reis and Wolfers, 2003; Lahiri and Liu, 2006; Hartmann, Herwartz and Ulm, 2022). Although Rich and Tracy (2010); Abel et al. (2016) conclude that aggregate forecast uncertainty is not significantly related to the level of expected inflation, the replication exercise reported in Section 2.1 (and in full in Online Appendix ??) shows that this result is largely sample-driven. Re-estimating the specification of Abel et al. (2016) on their original 1999–2013 sample reproduces the insignificant coefficients, but extending the sample to 2025 uncovers a strong and statistically significant relationship, indicating that the earlier null finding largely reflects limited statistical power. This subsection provides micro-founded mechanisms that rationalize modelling the conditional variance as an increasing function of the distance between current expectations and the anchor. We derive two formal channels—Bayesian learning about a latent target and policy-response uncertainty—each of which independently generates a linear variance–distance relationship. Two additional mechanisms, regime-dependent volatility and model ambiguity, reinforce the same qualitative prediction.

Throughout this subsection,  $\text{Var}(X_{t+1} | \mathcal{I}_t)$  denotes the variance of the forecaster’s *subjective* predictive distribution, as elicited by the survey. Forecasters are modelled as Bayesian agents who update a prior over the latent state of the economy using publicly available observations. Under this interpretation, the subjective posterior predictive variance that a rational forecaster reports in the survey coincides with the Kalman-filter predictive variance derived below, so that the theory speaks directly to the object measured in the data.

**Setup and notation.** Let  $X_{t+1}$  denote the variable to be forecast (e.g. inflation),  $\mu^*$  the policy anchor, and define the *distance* of current expectations from the anchor as

$$d_t \equiv |\mu_t - \mu^*|, \quad \mu_t \equiv \mathbb{E}[X_{t+1} | \mathcal{I}_t]. \quad (3)$$

---

<sup>1</sup>The uncertainty measure from the averaged SPDs across heterogeneous forecasters is composed of two components: individual forecasters’ uncertainty and forecasters’ disagreement about the mean (Online Appendix ??). To capture forecaster uncertainty rather than disagreement, we analyze SPDs at the individual forecaster level, accounting for heterogeneity.

We posit from the literature that the conditional variance is a function of this distance,

$$\text{Var}(X_{t+1} | \mathcal{I}_t) = g(d_t), \quad (4)$$

where  $g: \mathbb{R}_{\geq 0} \rightarrow \mathbb{R}_{> 0}$  is differentiable. All economic content lies in establishing *why*  $g'(d) > 0$ ; the mechanisms below provide independent foundations for this inequality.

**Structural foundation.** The additive decomposition  $X_{t+1} = \theta_{t+1} + \phi_{t+1} + \varepsilon_{t+1}$  is the generic reduced-form representation produced by any linearized rational expectations model. To fix ideas, consider the canonical New Keynesian system—Phillips curve, dynamic IS equation, and policy rule—linearized around the steady-state target  $\mu^*$  (Galí, 2015). Writing the system in companion form  $A \mathbb{E}_t z_{t+1} = B z_t + C \eta_t$ , where  $z_t$  collects the macroeconomic state variables, the unique bounded rational expectations solution (Sims, 2001) takes the form  $z_t = \Phi z_{t-1} + \Psi \eta_t$  and implies

$$X_{t+1} = \underbrace{\mu^*}_{\text{anchor}} + \underbrace{s_t}_{\text{systematic deviation}} + \underbrace{\varepsilon_{t+1}^X}_{\text{innovation}}, \quad s_t \equiv c' z_t, \quad (5)$$

where  $c'$  denotes the row of the solution matrix that selects inflation,  $s_t$  is the predictable deviation of inflation from target driven by the current state, and  $\varepsilon_{t+1}^X$  is the one-step-ahead structural innovation.<sup>2</sup>

Since  $\mu_t = \mathbb{E}_t[X_{t+1}] = \mu^* + s_t$ , the distance  $d_t = |s_t|$  measures the magnitude of the predictable state-driven deviation; it is large precisely when macroeconomic conditions push inflation persistently away from target. The maintained assumptions below generalize each NK component. Assumption 1 replaces the fixed intercept  $\mu^*$  with a stochastic, time-varying *short-term implicit target*  $\theta_{t+1}$  that forecasters must filter from noisy observations, rendering the anchor component uncertain. Crucially,  $\theta_t$  is distinct from the publicly announced medium-term target  $\mu^*$ . Central banks such as the ECB define price stability as “inflation of 2% over the medium term” (European Central Bank, 2021), which grants a degree of freedom in the short run: the implicit operational target  $\theta_t$  may temporarily deviate from  $\mu^*$  in response to supply shocks, financial-stability considerations, or other transient factors, provided that the medium-term objective remains credible.<sup>3</sup> Assumption 2 replaces the deterministic state-driven term  $s_t$  with a stochastic Bernoulli correction  $\phi_{t+1}$  whose timing and magnitude remain uncertain even when the gap  $d_t$  is observable. These two departures from the deterministic NK baseline generate the distance-dependent predictive variance formalized in Proposition 1.

**Maintained assumptions.** The formal derivation rests on three maintained assumptions.

**Assumption 1** (Latent target and Bayesian learning). *The short-term implicit target  $\theta_t$  is latent and evolves as a random walk with state-dependent innovation variance:*

$$\theta_t = \theta_{t-1} + \eta_t, \quad \eta_t \sim \mathcal{N}(0, \sigma_{\eta,t}^2), \quad (6)$$

$$\sigma_{\eta,t}^2 = \sigma_{\eta,0}^2 + \gamma d_{t-1}, \quad \gamma \geq 0. \quad (7)$$

<sup>2</sup>Under the standard linear RE solution,  $s_t = c' z_t$  is  $\mathcal{I}_t$ -measurable, so  $\text{Var}(X_{t+1} | \mathcal{I}_t) = \text{Var}(\varepsilon_{t+1}^X)$  is constant and independent of  $d_t$ . The distance-dependent variance of Proposition 1 therefore arises from Assumptions 1 and 2, not from the NK structure itself; equation (5) motivates only the *form* of the decomposition.

<sup>3</sup>The ECB’s 2021 strategy review explicitly acknowledges that “there may be transitory deviations of actual inflation from the target” and that “the medium-term orientation [...] allows for inevitable short-term deviations” (European Central Bank, 2021). Online Appendix ?? formalizes this distinction by replacing the random-walk specification of  $\theta_t$  with a mean-reverting process centred on  $\mu^*$ , parametrized by a persistence parameter  $\rho \in [0, 1)$  that governs the speed of reversion to the medium-term anchor.

The state-dependence in (7) uses the lagged distance  $d_{t-1} = |\mu_{t-1} - \mu^*|$  rather than the current  $d_t$ . Since  $d_{t-1} \in \mathcal{I}_{t-1} \subseteq \mathcal{I}_t$ , the process noise  $\sigma_{\eta,t}^2$  is predetermined at date  $t$  and does not depend on the Kalman-filter output  $\mu_t$ , thereby precluding simultaneity. Forecasters observe the noisy signal

$$X_t = \theta_t + \varepsilon_t, \quad \varepsilon_t \stackrel{\text{i.i.d.}}{\sim} \mathcal{N}(0, \sigma_\varepsilon^2). \quad (8)$$

Since the forecast decomposition of  $X_{t+1}$  includes the policy correction  $\phi_{t+1}$ , consistency requires that the signal in (8) be interpreted as the observation net of realized past policy actions: the central bank announces its interventions, so  $\phi_\tau$  for  $\tau \leq t$  is  $\mathcal{I}_t$ -measurable and can be subtracted from the raw data before filtering  $\theta_t$ .<sup>4</sup> The Gaussianity of  $\eta_t$  ensures tractable Kalman-filter recursions and is maintained for the variance analysis of this section. Section 3.2.1 relaxes this condition by allowing  $\eta_t$  to exhibit state-dependent skewness; the extension affects only third-moment properties and leaves Proposition 1 unaffected, since the latter depends only on the first two moments of  $\eta_t$ .

**Assumption 2** (Policy-response uncertainty). *The stochastic component of the policy correction is*

$$\phi_{t+1} = \begin{cases} \text{sign}(\mu^* - \mu_t) \cdot \Delta & \text{with probability } p_t, \\ 0 & \text{with probability } 1 - p_t, \end{cases} \quad (9)$$

where  $\Delta > 0$  is the magnitude of a decisive correction and

$$p_t = 1 - e^{-\lambda d_t}, \quad \lambda > 0. \quad (10)$$

The exponential specification ensures  $p_t \in [0, 1)$  for all  $d_t \geq 0$ ; for small deviations,  $p_t \approx \lambda d_t$ . The sign convention yields a tightening ( $-\Delta$ ) when inflation exceeds the target and an easing ( $+\Delta$ ) when it falls below, so that  $\text{Var}(\phi_{t+1} | \mathcal{I}_t) = p_t(1 - p_t)\Delta^2$  is symmetric in both directions.<sup>5</sup>

**Assumption 3** (Conditional independence). *Conditional on  $\mathcal{I}_t$ , the Bernoulli draw determining  $\phi_{t+1}$ , the target innovation  $\eta_{t+1}$ , and the fundamental shock  $\varepsilon_{t+1}$  are mutually independent.*

Assumption 3 is the strongest of the three maintained hypotheses. Because the central bank observes its own implicit target  $\theta_t$ , it may condition the probability and direction of a corrective action on the *true* latent deviation  $|\theta_t - \mu^*|$  rather than on the publicly observed distance  $d_t$ . Under such endogenous policy behaviour,  $\phi_{t+1}$  and  $\theta_{t+1}$  are correlated conditional on  $\mathcal{I}_t$  alone, violating Assumption 3. Online Appendix ?? replaces Assumption 3 with the weaker requirement that the three shocks be independent conditional on  $(\theta_t, \mathcal{I}_t)$ , and derives a modified affine approximation (Proposition ??) in which the autoregressive persistence  $\rho$  is replaced by the *net persistence*  $\psi \equiv \rho - \lambda\Delta$ , capturing the endogenous stabilization effect. The key finding is that the corrections to both the intercept and the slope are  $O(\lambda\Delta)$ : for empirically plausible policy-response parameters, Assumption 3 is a useful approximation rather than a structural restriction, and the NU normalization inherits this robustness.<sup>6</sup>

<sup>4</sup>Equivalently, one can define  $\tilde{X}_t \equiv X_t - \phi_t$  and take (8) as the observation equation for  $\tilde{X}_t$ . Because  $\phi_t \in \mathcal{I}_t$ , the Kalman-filter recursions and their steady-state properties are unaffected by this re-definition.

<sup>5</sup>Since  $\mathbb{E}[\phi_{t+1} | \mathcal{I}_t] = p_t \text{sign}(\mu^* - \mu_t)\Delta \neq 0$  in general, the conditional mean of  $\phi_{t+1}$  enters  $\mu_t = \mathbb{E}[X_{t+1} | \mathcal{I}_t]$ , creating a fixed-point relationship between  $\mu_t$  and  $d_t$ . Because  $p_t = O(d_t)$  as  $d_t \rightarrow 0$ , the expected correction vanishes at the anchor and the first-order approximation of Proposition 1—which retains only terms linear in  $d_t$ —is unaffected by this simultaneity.

<sup>6</sup>Specifically, the covariance  $\text{Cov}(\theta_{t+1}, \phi_{t+1} | \mathcal{I}_t) \approx -\rho\lambda\Delta P_{t|t} < 0$  is stabilizing: when the true target exceeds  $\mu^*$ , the central bank is more likely to tighten, partially offsetting the high target. The resulting intercept  $a^\dagger < a_\rho$  and slope  $b^\dagger \approx b_\rho$  preserve the affine form of the variance–distance relationship.

**Channel 1: Bayesian learning about the latent target.** Assumption 1 extends the unobserved-components model of Stock and Watson (2007) by making the innovation variance state-dependent. The economic motivation follows Aoki and Kimura (2007) and Mertens (2016): when  $d_{t-1}$  is large, forecasters rationally assign higher probability to a structural drift in the anchor and accordingly inflate the perceived process noise beyond its baseline  $\sigma_{\eta,0}^2$ . Applying the Kalman filter to (6)–(8), the one-step-ahead predictive variance of the target is

$$\text{Var}(\theta_{t+1} | \mathcal{I}_t) = P_{t|t} + \sigma_{\eta,t+1}^2, \quad (11)$$

where  $P_{t|t}$  is the Kalman-filter posterior variance and  $\sigma_{\eta,t+1}^2 = \sigma_{\eta,0}^2 + \gamma d_t$  is the innovation variance for the transition from  $t$  to  $t+1$ .<sup>7</sup> When  $\gamma = 0$  the process noise is constant and the Riccati recursion for  $P_{t|t}$  converges to the fixed point  $P_\infty$  satisfying  $P_\infty^2 + P_\infty \sigma_{\eta,0}^2 - \sigma_{\eta,0}^2 \sigma_\varepsilon^2 = 0$ , whose positive root is

$$P_\infty = -\frac{\sigma_{\eta,0}^2}{2} + \sqrt{\frac{(\sigma_{\eta,0}^2)^2}{4} + \sigma_{\eta,0}^2 \sigma_\varepsilon^2}, \quad (12)$$

and the steady-state one-step-ahead predictive variance of the target is  $\bar{V} \equiv P_\infty + \sigma_{\eta,0}^2 > 0$ .

For  $\gamma > 0$  but small, a first-order expansion of (11) in  $\gamma$  around zero separates two effects. The *direct* effect operates through  $\sigma_{\eta,t+1}^2 = \sigma_{\eta,0}^2 + \gamma d_t$ , contributing  $\gamma d_t$ . The *indirect* effect operates through  $P_{t|t}$ , whose steady state shifts because the Kalman filter at date  $t$  processes observations generated under the noise level  $\sigma_{\eta,t}^2 = \sigma_{\eta,0}^2 + \gamma d_{t-1}$ ; to first order this contributes  $(\partial P_\infty / \partial \sigma_{\eta,0}^2) \gamma d_{t-1}$ . Combining and writing  $d_{t-1} \approx d_t$  for expectations that evolve smoothly across adjacent periods gives

$$\text{Var}(\theta_{t+1} | \mathcal{I}_t) = \underbrace{\bar{V}}_{\text{baseline}} + \underbrace{\alpha d_t}_{\text{learning}} + O(\gamma^2, |d_t - d_{t-1}|), \quad (13)$$

where

$$\alpha = \gamma \left( 1 + \frac{\partial P_\infty}{\partial \sigma_{\eta,0}^2} \right) > 0. \quad (14)$$

The direct effect ( $\gamma$ ) and the indirect effect ( $\gamma \partial P_\infty / \partial \sigma_{\eta,0}^2$ ) reinforce each other, since  $\partial P_\infty / \partial \sigma_{\eta,0}^2 > 0$ .<sup>8</sup> Channel 1 therefore contributes a strictly positive slope  $\alpha$  to  $g'(d)$ .

**Channel 2: Policy-response uncertainty.** Following Ball (1992) and Cukierman and Meltzer (1986), deviations from the target generate uncertainty about the central bank's corrective response—specifically about its timing and magnitude. At the anchor ( $d_t = 0$ ), there is consensus that no correction is needed, so  $p_t = 0$  and  $\text{Var}(\phi_{t+1} | \mathcal{I}_t) = 0$ . As deviations grow, uncertainty about whether and how swiftly the central bank will act increases, with  $p_t$  rising monotonically in  $d_t$  under (10). The conditional variance of  $\phi_{t+1}$  is

$$\text{Var}(\phi_{t+1} | \mathcal{I}_t) = p_t(1 - p_t) \Delta^2 = (1 - e^{-\lambda d_t}) e^{-\lambda d_t} \Delta^2. \quad (15)$$

Evaluating the derivative at  $d_t = 0$ ,

$$\left. \frac{d}{d d_t} [p_t(1 - p_t) \Delta^2] \right|_{d_t=0} = \lambda \Delta^2, \quad (16)$$

<sup>7</sup>Equation (11) follows from  $\theta_{t+1} = \theta_t + \eta_{t+1}$  and the independence of  $\eta_{t+1}$  from  $\mathcal{I}_t$ :  $\text{Var}(\theta_{t+1} | \mathcal{I}_t) = \text{Var}(\theta_t | \mathcal{I}_t) + \text{Var}(\eta_{t+1}) = P_{t|t} + \sigma_{\eta,t+1}^2$ .

<sup>8</sup>To verify  $\partial P_\infty / \partial \sigma_{\eta,0}^2 > 0$ , set  $Q = \sigma_{\eta,0}^2$  and  $R = \sigma_\varepsilon^2$ . Differentiating  $P_\infty = -Q/2 + \frac{1}{2}(Q^2 + 4QR)^{1/2}$  yields  $\partial P_\infty / \partial Q = -\frac{1}{2} + (Q + 2R)[2(Q^2 + 4QR)^{1/2}]^{-1}$ . Positivity holds if and only if  $(Q + 2R)^2 > Q^2 + 4QR$ , i.e.  $4R^2 > 0$ , which is satisfied for any  $R > 0$ .

so a first-order expansion yields

$$\text{Var}(\phi_{t+1} | \mathcal{I}_t) = \beta d_t + O(d_t^2), \quad \beta \equiv \lambda \Delta^2 > 0. \quad (17)$$

The variance vanishes exactly at  $d_t = 0$  and grows proportionally for small deviations. Channel 2 therefore contributes a second strictly positive slope  $\beta$  to  $g'(d)$ .

**Supporting mechanisms.** Two further mechanisms reinforce  $g'(d) > 0$  while accommodating functional forms beyond strict linearity.

*Regime-dependent volatility* (Brunner and Hess, 1993; Cogley and Sargent, 2005). Let  $r_{t+1} \in \{A, D\}$  index anchored and de-anchored macroeconomic regimes, with within-regime means  $\mu^*$  (A) and  $\mu^* + \delta$  (D) and within-regime variances  $v_A^2 < v_D^2$ . Let  $q_t \equiv \Pr(r_{t+1} = D | \mathcal{I}_t)$  denote the subjective de-anchoring probability and suppose  $q_t \approx \kappa d_t$ ,  $\kappa > 0$ . By the law of total variance,

$$\text{Var}(X_{t+1} | \mathcal{I}_t) \approx v_A^2 + \kappa(v_D^2 - v_A^2 + \delta^2) d_t + O(d_t^2), \quad (18)$$

contributing a strictly positive slope to  $g'(0)$ . Crucially, it is the deviation  $d_t$ —not the inflation level *per se*—that signals the high-volatility regime, since a common latent state simultaneously shifts the mean away from  $\mu^*$  and raises the shock variance.

*Model ambiguity* (Klibanoff, Marinacci and Mukerji, 2005; Ilut and Schneider, 2014). Suppose the forecaster maintains a second-order distribution  $\nu$  over a set of models  $m \in \mathcal{M}$ , each with predictive mean  $\mu_m$  and variance  $\sigma_m^2$ . Under smooth ambiguity preferences, the effective subjective variance admits the second-order approximation (Klibanoff, Marinacci and Mukerji, 2005)

$$\text{Var}_{\text{eff}}(X_{t+1} | \mathcal{I}_t) = \mathbb{E}_\nu[\sigma_m^2] + \chi \cdot \text{Var}_\nu(\mu_m), \quad \chi > 0, \quad (19)$$

where  $\chi$  is proportional to the coefficient of absolute ambiguity aversion. If  $\text{Var}_\nu(\mu_m)$  increases with  $d_t$ —the set of plausible models expands when expectations drift from the anchor—then  $\text{Var}_{\text{eff}}$  inherits this positive dependence, contributing to  $g'(d) > 0$ .

**Local linear approximation.** Each mechanism above establishes  $g'(0) > 0$ . Since  $g(\cdot)$  is differentiable at  $d = 0$ , a first-order Taylor expansion yields

$$\text{Var}(X_{t+1} | \mathcal{I}_t) = a + b d_t + O(d_t^2), \quad a > 0, \quad b > 0. \quad (20)$$

The intercept  $a = g(0)$  is the baseline variance under perfectly anchored expectations; the slope  $b = g'(0)$  reflects the combined sensitivity of uncertainty to anchor deviations. The proposition below provides a structural interpretation of  $a$  and  $b$  in terms of the two formal channels; equations (18) and (19) confirm consistency with (20) for the supporting mechanisms.

**Proposition 1** (Local affine approximation). *Let  $X_{t+1} = \theta_{t+1} + \phi_{t+1} + \varepsilon_{t+1}$ , where the three components satisfy Assumption 3 (conditional independence). Under Assumptions 1 and 2, to first order in  $\gamma$  and in  $d_t$ , and writing  $d_{t-1} \approx d_t$  for expectations that evolve smoothly across periods,*

$$\text{Var}(X_{t+1} | \mathcal{I}_t) = a + b d_t + O(\gamma^2, d_t^2), \quad (21)$$

where

$$a = \bar{V} + \sigma_\varepsilon^2 > 0, \quad b = \alpha + \beta = \alpha + \lambda \Delta^2 > 0. \quad (22)$$

The intercept  $a = P_\infty + \sigma_{\eta,0}^2 + \sigma_\varepsilon^2$  is the sum of the steady-state filtered target uncertainty, baseline process noise, and observation noise; it is strictly positive even when expectations are perfectly anchored. The slope  $b$  pools the two channel contributions:  $\alpha = \gamma(1 + \partial P_\infty / \partial \sigma_{\eta,0}^2)$ , governed by the state-dependence parameter  $\gamma$  and the signal-to-noise ratio  $\sigma_{\eta,0}^2 / \sigma_\varepsilon^2$ ; and  $\beta = \lambda \Delta^2$ , governed by the policy-response intensity  $\lambda$  and the correction magnitude  $\Delta$ .

*Proof.* By Assumption 3, the three components of  $X_{t+1}$  are conditionally independent given  $\mathcal{I}_t$ , so

$$\text{Var}(X_{t+1} | \mathcal{I}_t) = \text{Var}(\theta_{t+1} | \mathcal{I}_t) + \text{Var}(\phi_{t+1} | \mathcal{I}_t) + \sigma_\varepsilon^2. \quad (23)$$

Substituting the Channel 1 approximation (13)—which already incorporates  $d_{t-1} \approx d_t$ —and the Channel 2 expansion (17):

$$\begin{aligned} \text{Var}(X_{t+1} | \mathcal{I}_t) &= (\bar{V} + \alpha d_t) + \beta d_t + \sigma_\varepsilon^2 + O(\gamma^2, d_t^2) \\ &= \underbrace{(\bar{V} + \sigma_\varepsilon^2)}_{=a} + \underbrace{(\alpha + \beta)}_{=b} d_t + O(\gamma^2, d_t^2). \end{aligned} \quad (24)$$

Strict positivity of  $a$  follows from  $\bar{V} > 0$  (since  $P_\infty > 0$  for any  $\sigma_{\eta,0}^2, \sigma_\varepsilon^2 > 0$ ) and  $\sigma_\varepsilon^2 > 0$ . Strict positivity of  $b$  follows from  $\alpha > 0$  for any  $\gamma > 0$  (equation (14) and footnote 8) and  $\beta = \lambda \Delta^2 > 0$ .  $\square$

**Remark 1** (Testable implications). *The decomposition  $b = \alpha + \beta$  carries empirical content. The slope  $b$  should be larger in environments with lower central-bank credibility (higher  $\gamma$ , hence higher  $\alpha$ ) and greater policy-response heterogeneity or opaque communication (higher  $\lambda$  or  $\Delta$ , hence higher  $\beta$ ). Both dimensions are tractable via cross-country or sub-sample variation in institutional characteristics. Online Appendix ?? exploits such variation by comparing the ECB-SPF—which has operated under an explicit 2% target since inception—with the US SPF, where the Federal Reserve adopted a formal numerical target only in January 2012. Consistent with the model, the US variance–distance slope exceeds the ECB slope during the pre-2012 period, and collapses after the Fed’s announcement: a Chow test rejects parameter stability at any conventional level. Post-2012, the two slopes are statistically indistinguishable, supporting the interpretation that  $b$  is structurally determined by the institutional commitment to a numerical inflation target.*

**Remark 2** (Symmetry and asymmetric extensions). *The specification  $d_t = |\mu_t - \mu^*|$  imposes symmetry: uncertainty increases at the same rate whether inflation is above or below target. Both formal channels support this:  $\sigma_{\eta,t}^2$  in Channel 1 depends only on  $|d_{t-1}|$ , and the sign convention in Assumption 2 gives  $\text{Var}(\phi_{t+1} | \mathcal{I}_t) = p_t(1 - p_t)\Delta^2$  identically in both directions. Nonetheless, Hartmann, Herwartz and Ulm (2022) find evidence of asymmetric responses: above-target deviations carry additional uncertainty about the pace and credibility of disinflation, while below-target deviations raise concerns about the effectiveness of conventional expansionary policy. The symmetric specification can be extended by replacing  $b d_t$  with  $b^+(\mu_t - \mu^*)^+ + b^-(\mu_t - \mu^*)^-$ , where the testable restriction  $b^+ = b^-$  nests the symmetric baseline. We maintain symmetry in our baseline but note that asymmetric extensions are straightforward and empirically tractable.*

**Remark 3** (Portability beyond survey densities). *The variance–distance framework derived above is not specific to inflation surveys. The affine relationship  $\text{Var}(X_{t+1} | \mathcal{I}_t) = a + b|\mu_t - \mu^*|$  requires only two structural ingredients: (i) a reference point  $\mu^*$  that anchors expectations, and (ii) economic mechanisms—analogueous to Assumptions 1–2—that generate level-dependent variance. These ingredients are present in many empirical settings. For GDP growth forecasts, the natural anchor is potential output growth, and the resulting Normalized Growth Uncertainty (NGU) is deployed in Online Appendix ?. For option-implied densities, the forward price provides the reference point, and implied volatility exhibits well-documented dependence on the distance of the underlying from key levels. For firm-level expectations on sales, prices, or investment, industry-specific benchmarks or historical means can serve as anchors. More broadly, the NU normalization applies to any predictive distribution in which raw dispersion mechanically co-moves with first-moment deviations from a benchmark—a pervasive feature of economic forecasting environments—and the variance-stabilizing*

transformation of Section 3.1.2 is directly portable. This portability is not merely conceptual: NIU is already used in related work on monetary policy and credit supply (Vansteenberghe, 2025), and it has also been presented in Banque de France policy communication on inflation and growth uncertainty (Vansteenberghe, 2026a).

### 3.1.2 The Normalized Uncertainty measure

Proposition 1 establishes that the raw predictive variance can be decomposed into a structural component and a residual:

$$\begin{aligned} \text{Var}(X_{t+1} | \mathcal{I}_t) &= \underbrace{V_{\text{struct}}(\mu_t)} + V_{\text{genuine},t}, \\ &= a + b d_t \end{aligned} \quad (25)$$

where  $V_{\text{struct}}(\mu_t)$  is the predictable component driven by the distance from the anchor and  $V_{\text{genuine},t}$  is the residual reflecting genuine shocks to belief precision. Raw forecast dispersion therefore conflates these two elements. The *Normalized Uncertainty* (NU) measure removes the structural component:

$$\text{NU}_t \equiv \frac{\sqrt{\text{Var}(X_{t+1} | \mathcal{I}_t)}}{\sqrt{V_{\text{struct}}(\mu_t)}} = \frac{\sqrt{\text{Var}(X_{t+1} | \mathcal{I}_t)}}{\sqrt{a + b |\mu_t - \mu^*|}} = \sqrt{1 + \frac{V_{\text{genuine},t}}{V_{\text{struct}}(\mu_t)}}. \quad (26)$$

When  $V_{\text{genuine},t} = 0$ —all observed dispersion is accounted for by the structural component— $\text{NU}_t = 1$  regardless of  $d_t$ . Deviations above unity identify periods of excess belief dispersion that cannot be attributed to anchor-distance effects. When  $V_{\text{genuine},t} < 0$  (observed dispersion falls below its structural prediction),  $\text{NU}_t < 1$ , indicating unusually compressed uncertainty relative to the structural baseline.

**Connection to variance-stabilizing transformations.** From a statistical perspective,  $\text{NU}_t$  is an instance of the classical variance-stabilizing transformation (VST) (Anscombe, 1948; Nelder and Wedderburn, 1972), belonging to the same family as the Box–Cox power transformation (Box and Cox, 1964). If the variance of a random variable  $X$  depends on its mean through a known function  $\text{Var}(X) = h(\mu)$ , the delta method implies that  $f'(\mu) \propto 1/\sqrt{h(\mu)}$  produces  $\text{Var}(f(X))$  approximately constant to first order. Setting  $h(\mu) = a + b |\mu - \mu^*|$  from the affine variance–distance relationship of Proposition 1 yields  $f'(\mu) = 1/\sqrt{a + b |\mu - \mu^*|}$ , and the ratio  $\sqrt{\text{Var}(X_t)}/\sqrt{a + b |\mu_t - \mu^*|}$  is the resulting stabilized standard deviation.<sup>9</sup> The structural interpretation provided by Proposition 1 adds economic content to this purely statistical device: the denominator of  $\text{NU}_t$  removes the combined effect of Bayesian learning risk ( $\alpha$ ) and policy-response uncertainty ( $\beta$ ), so that  $\text{NU}_t$  isolates belief-precision shocks that are orthogonal to the level of expectations.

**Structural content of the normalization parameters.** In practice,  $a$  and  $b$  are identified from a linear regression of the empirical SPD variance on a constant and  $d_t$ . The structural decomposition  $b = \alpha + \beta$  provides additional content: cross-country or sub-sample variation in central-bank credibility (affecting  $\alpha$ ) and in policy-communication transparency (affecting  $\beta$ ) can in principle be exploited to separately recover the two channel contributions.

---

<sup>9</sup>A simple coefficient of variation  $\sqrt{\text{Var}(X_t)}/|\mu_t|$  is not suitable: inflation values close to zero would cause the measure to diverge. The target-centered VST remains robust to both the dependence on the mean and the near-zero inflation problem, and is equally applicable to economic growth rates where the anchor is potential output.

### 3.1.3 Empirical validation

**Data: the ECB Survey of Professional Forecasters.** We rely on the ECB-SPF, a quarterly survey initiated in 1999 that collects expectations on key euro-area macroeconomic indicators—including inflation (Harmonized Index of Consumer Prices, HICP), real GDP growth, and unemployment—from approximately 90 stable forecasting institutions such as banks and research institutes. Participants provide quantitative forecasts for multiple horizons (one, two, and five years ahead, plus the next quarter) using both rolling and calendar horizon approaches. A distinctive feature is its large sample size (around 60 anonymous respondents quarterly) and the inclusion of subjective probability distributions (SPDs), enabling quantification of forecast uncertainty through assigned probabilities across predefined intervals. These SPDs are predominantly judgment-based, as indicated by special ECB surveys (European Central Bank, 2018), and provide rich insights into forecasters’ central tendencies and associated uncertainty (Garcia, 2003). Individual forecasters allocate positive probability mass to, on average, nearly six distinct bins, yielding a mean normalized entropy of about 0.5. This level of bin usage indicates that respondents meaningfully exploit the probabilistic format rather than concentrating mass on a single interval. Hence, the ECB-SPF SPDs are sufficiently informative to support the construction of dispersion-based uncertainty measures (NIU) as well as asymmetry-based indicators (ACI), and cannot be reduced to degenerate or purely point-forecast representations.

**Survey calendar and date alignment.** The ECB-SPF is conducted four times a year: the Q1 wave is fielded in January–February, the Q2 wave in April–May, the Q3 wave in July–August, and the Q4 wave in October–November; results are typically published by the ECB six to eight weeks after the survey period closes. The microdata files distributed by the ECB label each SPD with the *target period*—defined as the calendar quarter in which the one-year-ahead forecast horizon ends. For instance, the Q1-1999 survey (fielded January–February 1999) targets December 1999 as the endpoint of its twelve-month window, but in regression analyses that join the NIU to monthly or quarterly financial series, it is used as of the field date (1999-01-01), to reflect the uncertainty and asymmetry in professional forecasts at that time.

**Validating the variance–distance relationship.** We estimate the baseline affine model

$$\text{Var}(X_t) = a + b |\mu_t - \mu^*|, \quad a > 0, b \geq 0, \quad (27)$$

on ECB-SPF inflation SPDs, where  $\mu_t = \mathbb{E}[X_t]$  and  $\mu^* = 2\%$ . The model implies that forecast variance should be smallest when expectations coincide with the target and should increase linearly with the absolute gap  $|\mu_t - \mu^*|$ . We distinguish between two datasets: (i) the SPD averaged across all forecasters on each survey date, and (ii) the individual SPDs reported by each forecaster.

**Average SPDs.** The average SPD is obtained by averaging the probability mass in each bin across forecasters and then recomputing the corresponding mean and variance. Because this aggregation smooths idiosyncratic outliers, the full sample of survey dates  $t = 1999 \text{ Q1 to } 2025 \text{ Q3}$  can be used without trimming. To put the estimates in perspective, the mean of the average SPD has ranged between a low of 0.83% in 2015 Q1 and a high of 3.85% in 2023 Q1 over the sample.

Table 6 presents the OLS estimates of equation (27) based on the full sample of averaged SPDs. The estimated intercept,  $\hat{a} = 0.29$  (standard error 0.08), represents the forecast variance when the mean of the average SPD coincides with the inflation target. The slope coefficient,  $\hat{b} = 1.10$  (standard error 0.14), indicates that a one-percentage-point increase in the absolute deviation

$|\mu_t - \mu^*|$  is associated with an increase of about one variance point in the distribution of average forecasts; statistically, the estimate is not significantly different from unity. The  $R^2$  of 0.37 suggests that deviations from the target account for roughly one-third of the variation in forecast variance.

**Individual SPDs.** At the level of individual forecasters the SPD data contain outliers arising from two sources. First, the discrete bins used in the ECB’s survey compress variance when the mean forecast is close to zero or negative (zero-lower bound); second, variance is mechanically undefined for inflation means above about 5% because the upper tail of the histogram is open-ended. To mitigate these issues we exclude SPDs with means below the 30th percentile of the  $\mu$  distribution and cap the sample at  $\mu_t \leq 5$ . This trimmed sample removes observations affected by the zero-lower-bound and by undefined upper-tail variances while leaving the bulk of the data intact.

The OLS results for the trimmed individual SPDs are presented in Table 7. The estimated intercept  $\hat{a} = 0.20$  (standard error 0.02) is the variance of a representative forecaster’s SPD when expected inflation equals the target. The slope  $\hat{b} = 0.86$  (standard error 0.03) implies that each one-percentage-point increase in  $|\mu_t - \mu^*|$  is associated with a roughly 0.86-percentage-point rise in forecast variance. Although the  $R^2$  of 0.19 is lower than that for the average SPD, the F-statistic (710.4) strongly rejects the null of no relationship. The visual scatter plot is presented in Figure 2. These findings confirm the affine variance–distance relationship derived in Section 3.1.1 and justify the NU normalization of Section 3.1.2.

**Choice of normalization parameters.** When the NU normalization developed in Section 3.1.2 is applied to inflation forecast distributions, we refer to the resulting measure as *Normalized Inflation Uncertainty* (NIU); a growth-specific variant, *Normalized Growth Uncertainty* (NGU), is developed analogously in Online Appendix ??.

Although the OLS regressions yield  $\hat{a} = 0.29$ ,  $\hat{b} = 1.10$  for the average SPD and  $\hat{a} = 0.20$ ,  $\hat{b} = 0.86$  for individual SPDs, the empirical construction of NIU sets  $a = 1$  and  $b = 1$ , so the denominator reduces to  $\sqrt{1 + |\mu_t - \mu^*|}$ . This unit calibration is motivated by three considerations.

First, *robustness of the time-series*. The NIU series constructed with  $(a, b) = (1, 1)$  and with  $(a, b) = (1, 1.10)$ —a round-number version of the average-SPD estimate—are virtually indistinguishable: the correlation between the two quarterly series exceeds 0.99 over the full sample. Because the normalization acts multiplicatively on a slow-moving, low-frequency signal, moderate changes in  $b$  leave the dynamics and the cross-sectional ranking of observations essentially unchanged.

Second, *interpretability and dimensional clarity*. With  $a = b = 1$  the denominator equals the standard deviation predicted by a linear model with unit intercept and unit slope, expressed in percentage-point units. This makes the NIU directly comparable across surveys, countries, and horizons without re-estimation, and it avoids the risk that the denominator is driven to near-zero by a small estimated  $\hat{a}$  in periods when the mean is close to target.

Third, *out-of-sample stability*. Plugging in-sample estimates of  $a$  and  $b$  into the normalization introduces a subtle look-ahead bias: as the sample extends and the inflation cycle changes, the fitted regression line shifts, retroactively altering the NIU for historical observations. The unit calibration is sample-free and therefore produces a fixed, reproducible series independent of the estimation window.

**Descriptive statistics.** Figure 3 compares our NIU indicator with the Euro Area Economic Policy Uncertainty (EPU) index. Episodes of heightened political uncertainty closely align with

peaks in the NIU. The indicator remains elevated through mid-2025, well above historical levels, and is only weakly correlated with disagreement, underscoring that individual-level variance contains distinct information.

Figure 4 contrasts normalized inflation uncertainty (NIU) with raw inflation uncertainty (IU), defined as the cross-sectional dispersion of individual SPF variances, plotted on a common scale. While the two measures co-move over time, NIU displays systematically dampened responses during high-dispersion episodes and a smoother profile overall. This visual evidence complements the regression results in Table 3 and illustrates how the normalization compresses regime-driven spikes in raw dispersion, isolating a distinct uncertainty signal that is less mechanically tied to inflation levels or deviations from target.

**What does normalization add?** Table 3 shows that normalized inflation uncertainty (NIU) is closely related to raw inflation uncertainty (IU), but not through a trivial linear rescaling. Column (1) documents a strong positive association between NIU and IU, while column (2) reveals a pronounced and statistically significant nonlinearity: the negative coefficient on  $IU_t^2$  implies that NIU increases with IU at a decreasing rate, compressing high-dispersion regimes. This concavity is consistent with the normalization procedure, which down-weights uncertainty mechanically induced by large deviations of expected inflation from the target.

Columns (3) and (4) further highlight the distinct informational content of NIU. Raw uncertainty is strongly and significantly related to the distance of mean inflation expectations from the target, with  $d_t$  explaining more than 40% of its time-series variation. In contrast, NIU exhibits only a weak and statistically insignificant association with  $d_t$ , and its explanatory power drops sharply. Taken together, these results indicate that NIU removes a substantial regime component of raw dispersion linked to target deviations, yielding an uncertainty measure that is less driven by inflation levels and more reflective of underlying forecast uncertainty.

The same mechanisms that generate distance-dependent variance—Bayesian learning about a latent target and policy-response uncertainty—also produce distance-dependent *skewness*, supplemented by a third channel: state-dependent asymmetry in the innovation distribution. The next section formalizes this parallel structure and develops a complementary measure that extracts directional risk from the third moment.

### 3.2 Asymmetry Coherence

Section 3.1.2 established that the conditional variance of subjective forecast distributions increases with the distance of expectations from the policy anchor, and developed the Normalized Uncertainty (NU) measure to isolate genuine belief imprecision from this structural dependence. Yet variance captures only the *width* of the distribution, not its *shape*. A natural complementary question arises: does the asymmetry of subjective distributions also vary systematically with the deviation of expectations from anchor? If so, the third moment of forecast distributions encodes a structural signal about directional risk—about which side the risks are on, and how coherently—that is conceptually distinct from, and only partly overlapping with, the uncertainty signal captured by NU. In monetary policy communication, financial stability assessments, and risk management, the concept of the “balance of risks” is ubiquitous. Yet there exists no standard statistical operationalization of this concept. This section provides one.

An empirical regularity motivates this investigation. In the ECB-SPF inflation data, the mean and skewness of individual subjective probability distributions are positively correlated (Table 8, Online Appendix Figure ??): higher expected inflation levels are systematically associated with

greater right-tail risk, and lower expectations with left-tail risk. This pattern suggests that forecasters’ perceived asymmetry is not idiosyncratic noise but responds to the position of expectations relative to the inflation target.

This section develops an *Asymmetry Coherence* (AC) measure—an operational formalization of the “balance of risks”—that extracts this directional signal. The construction proceeds in three steps. First, Section 3.2.1 extends the micro-founded framework of Section 3.1.1 to the third moment, establishing conditions under which the conditional skewness of subjective distributions is proportional to the *signed* deviation  $\mu_t - \mu^*$ . Three independent channels contribute to this relationship, two generating coherent skewness and one anti-coherent, with an overall sign that is empirically testable. Second, Section 3.2.2 uses this result to construct the AC index as a signal-extraction device that jointly exploits the first and third moments, yielding a robust directional risk indicator even when survey-based skewness estimates are individually noisy. Third, Section 3.2.3 validates the skewness–deviation relationship on ECB-SPF micro data and documents the empirical properties of AC, including its empirical distinctness from NU.

Working with individual-level subjective probability distributions is essential for this analysis. As demonstrated in Online Appendix ?? and illustrated in Online Appendix Figure ??, averaging SPDs across heterogeneous forecasters can reverse the sign of aggregate skewness relative to the average of individual skewnesses. If two forecasters both report positively skewed distributions but disagree on the location of their central forecast, their averaged SPD may exhibit *negative* skewness, because the disagreement on the mean shifts the mass of each distribution relative to the other and distorts the aggregate asymmetry. Online Appendix Figure ?? confirms that working with granular SPD data preserves both individual variability and the cross-sectional distribution of skewness, which is essential for extracting reliable directional signals. For practical measurement, we rely on Bowley’s skewness—a nonparametric quantile-based measure detailed in Online Appendix Section ??—which is well suited to the sparse probability bins of survey data.<sup>10</sup>

### 3.2.1 Distance-dependent asymmetry

We now extend the framework of Section 3.1.1 from the second to the third moment. Throughout this subsection,  $\mu_3(X_{t+1} | \mathcal{I}_t) \equiv \mathbb{E}[(X_{t+1} - \mu_t)^3 | \mathcal{I}_t]$  denotes the conditional third central moment of the forecaster’s subjective predictive distribution, and we maintain the decomposition  $X_{t+1} = \theta_{t+1} + \phi_{t+1} + \varepsilon_{t+1}$  and the notation of Section 3.1.1.

The second-moment analysis of Section 3.1.1 was symmetric by construction: the variance–distance relationship  $\text{Var}(X_{t+1} | \mathcal{I}_t) = a + b d_t$  depends on the *absolute* distance  $d_t = |\mu_t - \mu^*|$  and is insensitive to the direction of the deviation. The third moment, by contrast, is inherently directional: a positive  $\mu_3$  indicates right-skew (upside risk), a negative  $\mu_3$  left-skew (downside risk). We therefore model the conditional third moment as a function of the *signed* deviation:

$$\mu_3(X_{t+1} | \mathcal{I}_t) = h(\mu_t - \mu^*), \tag{28}$$

where  $h: \mathbb{R} \rightarrow \mathbb{R}$  is differentiable with  $h(0) = 0$ : at the anchor, symmetric distributions carry no directional signal. The slope  $h'(0)$  determines whether skewness increases in the same direction as the deviation (*coherent* asymmetry,  $h'(0) > 0$ ) or in the opposite direction (*anti-coherent* asymmetry,  $h'(0) < 0$ ). The maintained assumptions below provide independent economic channels that determine the sign and magnitude of this slope.

<sup>10</sup>Bowley’s skewness is computed from the three quartiles  $Q_1, Q_2, Q_3$  as  $(Q_3 + Q_1 - 2Q_2)/(Q_3 - Q_1)$ . Unlike moment-based skewness, it is bounded in  $[-1, 1]$  and does not require estimating the third power of deviations from the mean, making it robust to the coarse discretization of survey histograms.

**Maintained assumption.** The following assumption introduces state-dependent asymmetry in the fundamental innovation, complementing Assumptions 1–3 from Section 3.1.1.

**Assumption 4** (State-dependent innovation asymmetry). *The conditional distribution of the fundamental innovation  $\varepsilon_{t+1}$  exhibits state-dependent skewness proportional to the signed deviation of expectations from the anchor:*

$$\mu_3(\varepsilon_{t+1} | \mathcal{I}_t) = \kappa_\varepsilon \sigma_\varepsilon^3 (\mu_t - \mu^*), \quad \kappa_\varepsilon \geq 0, \quad (29)$$

where  $\kappa_\varepsilon$  is a dimensionless asymmetry-sensitivity parameter and  $\sigma_\varepsilon^3$  provides the natural scale.

Assumption 4 posits that the fundamental shocks hitting the economy are not symmetrically distributed when expectations deviate from the policy anchor: when  $\mu_t > \mu^*$ , the innovation distribution is right-skewed ( $\mu_3 > 0$ ), generating further upside risk; when  $\mu_t < \mu^*$ , it is left-skewed. The case  $\kappa_\varepsilon = 0$  nests the standard symmetric baseline. Three independent micro-foundations rationalize  $\kappa_\varepsilon > 0$ .

**Micro-foundation (i): Diagnostic expectations and persistence.** Under diagnostic expectations (Bordalo, Gennaioli and Shleifer, 2018; Bordalo et al., 2020), agents update beliefs by overweighting signals that are representative of the current state relative to a reference distribution. Formally, the diagnostic posterior tilts the predictive density by a likelihood ratio that amplifies outcomes consistent with the recent trend. When the inflation-generating process is persistent—as is the case empirically (Stock and Watson, 2007; Cogley and Sargent, 2005)—a positive deviation  $\mu_t - \mu^* > 0$  means that recent signals have been predominantly above target. Diagnostic agents overweight the right tail of the innovation distribution because extreme positive outcomes are more “representative” of the current high-inflation state than of the unconditional baseline. This representativeness-driven distortion generates positive subjective skewness when  $\mu_t > \mu^*$  and negative skewness when  $\mu_t < \mu^*$ , with the magnitude scaling in the deviation because the representativeness wedge between the current and reference states grows with  $|\mu_t - \mu^*|$ .

**Micro-foundation (ii): Regime-change risk.** When expectations deviate from the anchor, forecasters assign non-trivial probability to a discrete regime change—a structural shift in the inflation-generating process such as central-bank credibility loss, a de-anchoring episode, or a permanent supply-side disruption (Bianchi, Ludvigson and Ma, 2022; Hamilton, 1989). The perceived direction of the regime change aligns with the current deviation: when  $\mu_t > \mu^*$ , the feared alternative regime involves persistently higher inflation (a “Peso problem” in the sense of rare but directional tail risk), generating positive skewness. Symmetrically, when  $\mu_t < \mu^*$ , the feared regime involves a deflationary trap, creating negative skewness. Formally, let  $q_t = \kappa_q |\mu_t - \mu^*|$  denote the subjective probability of the regime change and  $\delta \text{sign}(\mu_t - \mu^*)$  its direction. The law of total skewness implies a contribution to  $\mu_3(\varepsilon_{t+1} | \mathcal{I}_t)$  that is proportional to  $q_t \delta^3 \text{sign}(\mu_t - \mu^*) \propto (\mu_t - \mu^*)$ , consistent with (29).

**Micro-foundation (iii): Asymmetric information processing.** Under rational inattention (Sims, 2003; Maćkowiak and Wiederholt, 2009), agents allocate limited cognitive resources across economic signals. When inflation deviates from target, the salience of inflation-related information increases, but not symmetrically across the outcome space. Outcomes in the direction of the current deviation are more salient—they confirm the prevailing narrative and receive greater media coverage (Coibion and Gorodnichenko, 2015)—causing agents to weight the corresponding tail more heavily in their subjective distributions. This asymmetric processing generates skewness in the direction

of the deviation without requiring any objective asymmetry in the data-generating process: it is a feature of subjective perception under bounded attention.

The three micro-foundations operate through distinct economic mechanisms—belief distortion (diagnostic expectations), tail-risk pricing (regime-change risk), and attentional allocation (rational inattention)—and may coexist. Assumption 4 is agnostic about which mechanism dominates; it summarizes their net contribution through the reduced-form parameter  $\kappa_\varepsilon$ .

**Extension of Assumption 1: non-Gaussian target innovation.** Assumption 1 specifies the target innovation  $\eta_t \sim \mathcal{N}(0, \sigma_{\eta,t}^2)$ , ensuring tractable Kalman-filter recursions for the variance analysis of Section 3.1.1. For the third-moment analysis, we relax the Gaussianity condition by allowing  $\eta_t$  to exhibit state-dependent skewness:

$$\mu_3(\eta_{t+1} | \mathcal{I}_t) = \kappa_\eta \sigma_{\eta,0}^3 (\mu_t - \mu^*), \quad \kappa_\eta \geq 0. \quad (30)$$

This extension does *not* affect Proposition 1, which depends only on the first two moments of  $\eta_t$ . The economic rationale parallels that of Assumption 4: when the implicit target has drifted above  $\mu^*$ , the latent forces generating further drift are more likely to push in the same direction than to reverse, producing positive skewness in the target innovation.<sup>11</sup>

**Three channels for the skewness–deviation relationship.** Under Assumptions 1–3 and 4, the decomposition  $X_{t+1} = \theta_{t+1} + \phi_{t+1} + \varepsilon_{t+1}$  implies—via the additivity of conditional third central moments under independence<sup>12</sup>—three distinct contributions to  $\mu_3(X_{t+1} | \mathcal{I}_t)$ :

$$\mu_3(X_{t+1} | \mathcal{I}_t) = \underbrace{\mu_3(\theta_{t+1} | \mathcal{I}_t)}_{\text{Channel B}} + \underbrace{\mu_3(\phi_{t+1} | \mathcal{I}_t)}_{\text{Channel C}} + \underbrace{\mu_3(\varepsilon_{t+1} | \mathcal{I}_t)}_{\text{Channel A}}. \quad (31)$$

We derive each channel in turn.

**Channel A: Innovation asymmetry (coherent).** This channel follows directly from Assumption 4:

$$\mu_3(\varepsilon_{t+1} | \mathcal{I}_t) = \kappa_\varepsilon \sigma_\varepsilon^3 (\mu_t - \mu^*) \equiv s_A (\mu_t - \mu^*), \quad (32)$$

where  $s_A \equiv \kappa_\varepsilon \sigma_\varepsilon^3 \geq 0$ . Because  $s_A > 0$  when  $\kappa_\varepsilon > 0$ , the innovation channel generates *coherent* skewness: right-skew when expectations exceed the anchor, left-skew when they fall below.

**Channel B: Asymmetric learning drift (coherent).** The latent target  $\theta_{t+1} = \theta_t + \eta_{t+1}$  contributes to  $\mu_3(X_{t+1} | \mathcal{I}_t)$  through the skewness of the target innovation. Under the extension (30), the one-step-ahead third central moment of the target is, to first order in the skewness perturbation,

$$\mu_3(\theta_{t+1} | \mathcal{I}_t) \approx \mu_3(\eta_{t+1} | \mathcal{I}_t) = \kappa_\eta \sigma_{\eta,0}^3 (\mu_t - \mu^*) \equiv s_B (\mu_t - \mu^*), \quad (33)$$

<sup>11</sup>Formally, if  $\theta_t > \mu^*$  because of persistent structural forces, the conditional distribution of  $\eta_{t+1}$  inherits the asymmetry of the underlying structural shocks. This is consistent with a state-dependent generalization of the unobserved-components model of Stock and Watson (2007) and Mertens (2016), where the permanent component of inflation exhibits time-varying higher moments.

<sup>12</sup>Under conditional independence (Assumption 3), the third central moment of a sum of independent random variables equals the sum of their individual third central moments:  $\mu_3(Y_1 + Y_2 + Y_3) = \mu_3(Y_1) + \mu_3(Y_2) + \mu_3(Y_3)$ . This follows from expanding  $(Y_1 + Y_2 + Y_3 - \mathbb{E}[Y_1 + Y_2 + Y_3])^3$  and noting that all cross-terms vanish under independence.

where  $s_B \equiv \kappa_\eta \sigma_{\eta,0}^3 \geq 0$ .<sup>13</sup> Channel B is *coherent*: when the implicit target has drifted above  $\mu^*$ , the forces generating further drift are asymmetrically distributed in the upward direction, adding right-skew to the subjective forecast.

**Channel C: Policy-correction asymmetry (anti-coherent).** The Bernoulli policy correction of Assumption 2 introduces a third contribution whose sign *opposes* the deviation. Under (9),  $\phi_{t+1}$  takes value  $\text{sign}(\mu^* - \mu_t) \cdot \Delta$  with probability  $p_t = 1 - e^{-\lambda d_t}$  and zero otherwise. The third central moment of a two-point distribution with outcomes  $a$  (probability  $p$ ) and 0 (probability  $1 - p$ ) is<sup>14</sup>

$$\mu_3(\phi_{t+1} | \mathcal{I}_t) = p_t(1 - p_t)(1 - 2p_t) [\text{sign}(\mu^* - \mu_t) \cdot \Delta]^3. \quad (34)$$

For small deviations,  $p_t \approx \lambda d_t$  with  $(1 - p_t) \approx 1$  and  $(1 - 2p_t) \approx 1$ , so

$$\mu_3(\phi_{t+1} | \mathcal{I}_t) \approx \lambda d_t \cdot \text{sign}(\mu^* - \mu_t) \cdot \Delta^3 = -\lambda \Delta^3 (\mu_t - \mu^*) + O(d_t^2), \quad (35)$$

where the last equality uses  $d_t \cdot \text{sign}(\mu^* - \mu_t) = -(\mu_t - \mu^*)$ .<sup>15</sup> Defining  $s_C \equiv \lambda \Delta^3 > 0$ , Channel C contributes  $-s_C (\mu_t - \mu^*)$ .

The economic intuition is transparent: when  $\mu_t > \mu^*$ , the policy correction is directed *downward* (toward  $\mu^*$ ), creating probability mass in the left tail of the forecast distribution. The resulting negative skewness opposes the positive deviation—hence the label *anti-coherent*. This channel captures the market perception that the central bank will lean against deviations, generating tail risk in the direction opposite to the current misalignment.

**Asymmetric loss amplification.** The three channels above operate on the *objective* components of the subjective forecast distribution. A fourth mechanism reinforces coherent skewness through the *reporting* stage. If forecasters evaluate outcomes under an asymmetric loss function—such as the LINEX specification of Zellner (1986)—then the reported median (or point forecast) is shifted relative to the conditional mean in the direction of greater perceived risk. When skewness is coherent ( $\mu_3 > 0$  for  $\mu_t > \mu^*$ ), the right tail dominates the loss, pushing the reported median further above target. This shift strengthens the correlation between the reported first moment and the third moment, amplifying the coherence signal that the AC index is designed to detect.<sup>16</sup>

**Skewness–deviation proposition.** The following proposition aggregates the three channels into a single first-order relationship between conditional skewness and the signed deviation, paralleling Proposition 1 for the variance.

**Proposition 2** (Local affine skewness–deviation relationship). *Under Assumptions 1–3 and 4, with  $\eta_t$  exhibiting state-dependent skewness as in (30), the conditional third central moment satisfies, to first order in  $d_t$ ,*

$$\mu_3(X_{t+1} | \mathcal{I}_t) = c(\mu_t - \mu^*) + O(d_t^2), \quad (36)$$

<sup>13</sup>The approximation  $\mu_3(\theta_{t+1} | \mathcal{I}_t) \approx \mu_3(\eta_{t+1} | \mathcal{I}_t)$  holds to first order under weak non-Gaussianity. The Kalman-filter posterior  $\theta_t | \mathcal{I}_t$  is approximately Gaussian when the innovation skewness  $\kappa_\eta$  is small, so  $\mu_3(\theta_t | \mathcal{I}_t) = O(\kappa_\eta^2)$  can be neglected relative to the  $O(\kappa_\eta)$  contribution from  $\eta_{t+1}$ . For formal conditions, see Anderson and Moore (2005).

<sup>14</sup>Let  $m = pa$  denote the mean. Then  $\mu_3 = p(a - m)^3 + (1 - p)(-m)^3 = p(1 - p)a^3[(1 - p)^2 - p^2] = p(1 - p)(1 - 2p)a^3$ .

<sup>15</sup>To verify:  $d_t = |\mu_t - \mu^*|$  and  $\text{sign}(\mu^* - \mu_t) = -\text{sign}(\mu_t - \mu^*)$ , so  $d_t \cdot \text{sign}(\mu^* - \mu_t) = |\mu_t - \mu^*| \cdot (-\text{sign}(\mu_t - \mu^*)) = -(\mu_t - \mu^*)$ .

<sup>16</sup>Under LINEX loss  $L(\varepsilon) = b[\exp(a\varepsilon) - a\varepsilon - 1]$  with  $a > 0$ , the optimal point forecast equals  $\mu_t - (1/a) \ln M_{X_{t+1}}(a)$ , where  $M$  is the moment-generating function. When the predictive distribution is right-skewed,  $M(a) > \exp(a\mu_t + a^2\sigma_t^2/2)$  and the optimal forecast exceeds the mean, reinforcing the median–skewness alignment. See also Elliott, Timmermann and Komunjer (2005) for a general treatment of optimal forecasts under asymmetric loss.

where the net asymmetry coefficient is

$$c = \underbrace{s_A}_{=\kappa_\varepsilon\sigma_\varepsilon^3} + \underbrace{s_B}_{=\kappa_\eta\sigma_{\eta,0}^3} - \underbrace{s_C}_{=\lambda\Delta^3}. \quad (37)$$

The sign of  $c$  determines the nature of the skewness–deviation relationship:

- (i)  $c > 0 \Leftrightarrow$  coherent asymmetry: skewness reinforces the deviation (right-skew when above target, left-skew when below);
- (ii)  $c < 0 \Leftrightarrow$  anti-coherent asymmetry: skewness opposes the deviation, dominated by the policy-correction channel;
- (iii)  $c = 0 \Leftrightarrow$  neutrality: the three channels exactly offset, yielding symmetric forecast distributions regardless of the deviation.

*Proof.* By Assumption 3, the three components  $\theta_{t+1}$ ,  $\phi_{t+1}$ , and  $\varepsilon_{t+1}$  are conditionally independent given  $\mathcal{I}_t$ , so  $\mu_3(X_{t+1} | \mathcal{I}_t) = \mu_3(\theta_{t+1} | \mathcal{I}_t) + \mu_3(\phi_{t+1} | \mathcal{I}_t) + \mu_3(\varepsilon_{t+1} | \mathcal{I}_t)$ . Substituting the Channel A expression (32), the Channel B approximation (33), and the Channel C expansion (35):

$$\begin{aligned} \mu_3(X_{t+1} | \mathcal{I}_t) &= s_B(\mu_t - \mu^*) - s_C(\mu_t - \mu^*) + s_A(\mu_t - \mu^*) + O(d_t^2) \\ &= \underbrace{(s_A + s_B - s_C)}_{=c}(\mu_t - \mu^*) + O(d_t^2). \end{aligned} \quad (38)$$

Coherent asymmetry ( $c > 0$ ) obtains if and only if the combined innovation and drift channels dominate the policy-correction channel:  $s_A + s_B > s_C$ .  $\square$

**Remark 4** (Testable implications and structural content). *The decomposition  $c = s_A + s_B - s_C$  carries empirical content that parallels Remark 1 for the variance slope. First, the sign of  $c$  is testable: regressing an empirical measure of skewness on the signed deviation  $\mu_t - \mu^*$  yields a coefficient whose sign directly identifies whether coherent or anti-coherent asymmetry dominates. A positive and significant slope implies  $c > 0$ , validating the condition for coherent asymmetry assumed in the AC construction of Section 3.2.2. Table 4 confirms this prediction in the ECB-SPF data: the estimated slope is  $\hat{\alpha}_1 = 0.013$  ( $p < 0.01$ ), robustly positive across specifications and sub-samples. Second, the magnitude of  $c$  should vary across institutional environments. In the decomposition  $c = s_A + s_B - s_C$ , a negative  $c$  arises when the policy-correction channel  $s_C$  dominates the innovation and drift channels, implying that forecasters perceive the central bank as responding forcefully enough to deviations that distributions tilt against the direction of departure from target. Online Appendix ?? provides a cross-country comparison using the US SPF (GDP deflator density forecasts). Before the Fed’s adoption of an explicit 2% target in January 2012, the estimated slope is negative and significant ( $\hat{\alpha}_1 = -0.177$ ,  $p < 0.01$ ), suggesting that—despite the absence of a numerical anchor—forecasters perceived a strong Fed reaction function: when expectations drifted above target, the anticipated policy correction was large enough to skew distributions downward. After the formal adoption, the slope shifts toward the ECB value ( $\hat{\alpha}_1 = +0.111$ ), with a statistically significant structural break (Chow  $F = 7.09$ ,  $p < 0.001$ ). One interpretation, consistent with the model, is that the explicit target provided a focal point that strengthened the coherent channels ( $s_A$ ,  $s_B$ )—forecasters now anchoring directional risk perceptions on a publicly stated objective—while potentially reducing the perceived need for aggressive policy corrections ( $s_C$ ). These cross-country patterns are broadly consistent with the decomposition, though the different survey designs (HICP vs. GDP deflator, bin granularity) warrant caution in attributing the full difference to institutional*

factors alone. Third, the anti-coherent channel has a direct policy interpretation: the finding in Section 4 that AC innovations predict tightening decisions is consistent with the central bank reacting to the coherent asymmetry signal—precisely the component that the policy correction is designed to offset.

### 3.2.2 The Asymmetry Coherence measure

Proposition 2 establishes that, under coherent asymmetry ( $c > 0$ ), the conditional skewness of the subjective forecast distribution shares the same sign as the deviation  $\mu_t - \mu^*$ . This provides a theoretical foundation for extracting directional risk signals from expectations data. However, two practical obstacles prevent the direct use of skewness as a policy indicator.

First, skewness estimates are inherently fragile. The third moment is highly sensitive to noise and sample size, particularly when estimated from the sparse probability bins of survey histograms or the discrete strike prices of option-implied densities. Small perturbations in the tail probabilities can produce large swings in skewness, making it unreliable as a standalone signal (Bowley, 1926).

Second, even when individual skewness estimates are informative, the question of *how much confidence* to assign them remains open. A forecaster reporting moderate positive skewness together with a median close to target sends a weaker directional signal than one reporting the same skewness with a median well above target. The former case may reflect noise; the latter is more likely to reflect a genuine perception of upside risk.

Third, coherent asymmetry may itself contain information about the *perceived sufficiency* of monetary policy. When  $c > 0$ , the third moment reinforces the message of the central forecast: above-target inflation expectations are associated with upside tail risk, while below-target expectations are associated with downside tail risk. Such a configuration may be read as indicating that the expected policy response is not sufficiently forceful to neutralize the underlying pressures moving inflation away from target. In that sense, the AC measure is not only a forecasting device but also a policy indicator: it helps detect situations in which forecasters appear to view the anticipated policy reaction as too weak, thereby signalling that the central bank may need either to respond more forcefully or to communicate more clearly that it stands ready to do so. This interpretation echoes the ECB’s own strategy formulation that preserving symmetry around the inflation target may call for an “appropriately forceful or persistent monetary policy action” when inflation deviates from target in a large and sustained manner (European Central Bank, 2025).

**Signal-extraction motivation.** These obstacles motivate a signal-extraction approach—a formalization of the “balance of risks” concept—that combines first- and third-moment information. Under Proposition 2, when  $c > 0$ , both the median deviation  $Q_t - \pi^*$  (a first-moment object, where  $\pi^* \equiv \mu^*$ ) and the asymmetry measure  $A_t$  (a third-moment object) should carry the same directional sign. The degree of sign agreement between the two provides a data-driven confidence weight: when both components point in the same direction, the directional signal is strong; when they disagree, the signal is attenuated.

This logic maps directly onto the structure of a coherent detector. In signal processing, a coherent detector exploits the expected alignment between a noisy signal and a reference to distinguish true directional content from noise. Here,  $Q_t - \pi^*$  serves as the reference signal (the robust first-moment estimate of the deviation) and  $A_t$  serves as the noisy auxiliary signal (the fragile third-moment estimate). Their product  $\tilde{Q}_t \tilde{A}_t$  is positive under coherent asymmetry and negative under incoherent conditions—a natural sign-agreement statistic.

To analyze the strength of directional signals, we assess the alignment between the asymmetry of probability distributions and the median’s deviation from a reference target. A **strong signal**

emerges when skewness and median deviation indicate the same directional expectation: positive skewness with a median above target (strong upward signal) or negative skewness with a median below target (strong downward signal). Conversely, a **weak signal** arises from opposing skewness and median deviation: positive skewness paired with a median below target, or negative skewness with a median above target. Figure 5 illustrates these four scenarios by plotting skew-normal distributions with key quantiles highlighted.

**Construction of the AC index.** The AC index summarizes the directional strength of expectations by jointly exploiting two aggregate statistics extracted from individual SPDs: the cross-sectional median of the forecast distribution, denoted  $Q_t$ , and the cross-sectional mean of individual asymmetry scores (computed via Bowley’s skewness), denoted  $A_t$ .

To ensure comparability across components and robustness to scale differences, both series are normalized using a hyperbolic tangent transformation scaled by their interquartile range (IQR). This normalization preserves signs while bounding magnitudes in  $(-1, 1)$ :

$$\tilde{Q}_t = \tanh\left(\frac{Q_t - \pi^*}{\text{IQR}(Q_t - \pi^*)}\right), \quad \tilde{A}_t = \tanh\left(\frac{A_t}{\text{IQR}(A_t)}\right), \quad (39)$$

where  $\pi^*$  denotes the reference inflation target (equal to  $\mu^*$  in the notation of Section 3.2.1).

The AC index combines these two normalized components through a smooth coherence-based aggregator:

$$\text{AC}_t = \underbrace{\left(\frac{\tilde{Q}_t + \tilde{A}_t}{2}\right)}_{\text{directional signal}} \underbrace{\left(\frac{1 + \tilde{Q}_t \tilde{A}_t}{2}\right)}_{\text{coherence weight}}, \quad (40)$$

which is bounded in  $[-1, 1]$ .

**Structural interpretation.** The two factors in (40) have transparent structural interpretations in the light of Proposition 2.

The first factor,  $(\tilde{Q}_t + \tilde{A}_t)/2$ , is the *signed directional signal*. Under coherent asymmetry ( $c > 0$ ), both  $\tilde{Q}_t$  and  $\tilde{A}_t$  should share the sign of  $\mu_t - \mu^*$ , so their average estimates the direction of the deviation. Taking the average rather than either component alone reduces the variance of the estimator by pooling two noisy proxies for the same latent direction.

The second factor,  $(1 + \tilde{Q}_t \tilde{A}_t)/2$ , is the *coherence weight*. It isolates the extent to which the first and third moments convey a consistent directional message. When both components share the same sign,  $\tilde{Q}_t \tilde{A}_t > 0$  and the weight exceeds  $\frac{1}{2}$ , amplifying the directional signal. When they have opposite signs—indicating that the skewness contradicts the median deviation—the weight falls below  $\frac{1}{2}$ , attenuating the signal. Under perfect anti-coherence ( $\tilde{Q}_t \tilde{A}_t = -1$ ), the weight collapses to zero and  $\text{AC}_t = 0$  regardless of the magnitudes.

For interpretability, we also report the coherence component separately:

$$\text{Coherence}_t = \frac{1 + \tilde{Q}_t \tilde{A}_t}{2}, \quad (41)$$

which lies in  $[0, 1]$  and provides a direct diagnostic of whether the two moments are aligned.

**Formal properties.** The AC index satisfies several desirable properties:

- (i) *Boundedness:*  $\text{AC}_t \in [-1, 1]$  for all  $(\tilde{Q}_t, \tilde{A}_t) \in [-1, 1]^2$ .

- (ii) *Symmetry*:  $AC_t(-\tilde{Q}, -\tilde{A}) = -AC_t(\tilde{Q}, \tilde{A})$ ; reversing the signs of both components reverses the direction of the index.
- (iii) *Coherence monotonicity*: for fixed  $|\tilde{Q}_t|$  and  $|\tilde{A}_t|$ ,  $|AC_t|$  is increasing in  $\tilde{Q}_t\tilde{A}_t$ ; greater sign agreement amplifies the signal.

Online Appendix ?? provides Monte Carlo evidence that the AC formula outperforms alternative aggregation rules—including simple averages and skewness-only indicators—in recovering the true directional state under realistic noise calibrations.

**Remark 5** (Sensitivity to the skewness measure). *The AC construction requires a bounded asymmetry measure  $A_{i,t} \in [-1, 1]$ , a property satisfied by Bowley’s skewness  $B = (Q_3 + Q_1 - 2Q_2)/(Q_3 - Q_1)$ . The Pearson mode skewness  $(\text{mean} - \text{mode})/\sigma$  and the classical moment-based skewness  $m_3/m_2^{3/2}$  are unbounded and more sensitive to outliers in sparse histogram bins. Replacing Bowley’s skewness with either alternative in the AC formula yields qualitatively identical time-series patterns: the quarterly ACI series constructed with Bowley’s formula, Pearson mode, and moment-based skewness exhibit pairwise correlations exceeding 0.95. The quantitative results in this paper are therefore robust to the choice of skewness estimator; we retain Bowley’s measure for its natural boundedness and computational simplicity.*

**Remark 6** (Portability and the balance of risks). *The AC construction is not specific to survey histograms. It applies to any predictive distribution for which one can define (i) a reference point for the central tendency and (ii) a measure of distributional asymmetry. In option-implied densities, the forward price provides the reference and implied skewness the asymmetry signal; AC would then measure whether downside or upside tail risk is coherently aligned with the expected path of the underlying, filtering out smile-interpolation artifacts and maturity-dependent distortions. In firm-level expectation surveys, industry benchmarks or historical means serve as anchors. In GDP growth forecasts, potential output provides the reference. More broadly, AC operationalizes the concept of balance of risks—a notion ubiquitous in central-bank communication, financial stability assessments, and risk management, yet lacking a standard statistical formalization. AC is not merely “better skewness”: it separates shape asymmetry (a statistical property) from decision-relevant directional asymmetry (an economic property), a distinction that matters in any setting where practitioners care about which tail of a distribution is more consequential.*

**Remark 7** (Dependence on first-moment quality). *The signal-extraction power of AC rests on the premise that the first-moment deviation  $Q_t - \pi^*$  is observed more reliably than the third-moment signal  $A_t$ . This premise is well founded in standard inflation-targeting regimes, where the target  $\pi^*$  is publicly announced and the cross-sectional median  $Q_t$  is robustly estimated from a large panel. In low-credibility environments where the anchor itself is ambiguous—for instance, when the central bank lacks an explicit target or when the target is widely believed to be non-binding—the coherence weight  $|\tilde{Q}_t|$  becomes a noisy proxy, and the denoising advantage of AC over raw asymmetry may degrade. In the ECB sample, the two-percent target provides a stable, publicly known reference throughout the estimation period; the AC construction thus operates in a favorable identification environment.*

### 3.2.3 Empirical validation

**Validating the skewness–deviation relationship.** Proposition 2 predicts a linear relationship between skewness and the signed deviation from the anchor. We estimate

$$A_{i,t} = \alpha_0 + \alpha_1 (\mu_{i,t} - \mu^*) + u_{i,t} \tag{42}$$

on individual ECB-SPF inflation SPDs, where  $A_{i,t}$  is Bowley’s skewness for forecaster  $i$  in survey round  $t$  and  $\mu_{i,t}$  is the corresponding SPD mean. A positive and significant  $\hat{\alpha}_1$  validates the coherent-asymmetry condition  $c > 0$ .

Table 4 reports the results. In the baseline specification, the slope is  $\hat{\alpha}_1 = 0.013$  ( $t = 7.26$ ,  $p < 0.001$ ; standard errors clustered by survey date), confirming that forecasters who expect inflation further above target tend to report more positively skewed distributions, and vice versa—consistent with the positive mean–skewness correlation documented in Table 8. The coefficient strengthens with time fixed effects ( $\hat{\alpha}_1 = 0.015$ , column 2), showing that the relationship holds within each survey round and is not driven by common time variation. It remains significant when trimming extreme deviations ( $p = 0.03$  in the most demanding specification, column 4). The low  $R^2$  reflects the inherent noisiness of individual survey-based skewness estimates—precisely the signal-extraction problem that the AC construction addresses through the coherence weight.

**Descriptive application to the ECB-SPF.** When the AC construction is applied to inflation forecast distributions, we denote the resulting measure the *Asymmetry Coherence Index* for inflation (ACI); a growth-specific counterpart (ACG) is developed in Online Appendix ??.

We apply the AC index to one-year-ahead inflation forecasts from the ECB-SPF, Figure 6. Prior to the Global Financial Crisis, the first-moment component  $\hat{Q}_t$  and the asymmetry component  $\hat{A}_t$  display little systematic coherence, indicating weak directional signals in inflation expectations. During the Zero Lower Bound (ZLB) period, forecasters exhibit a pronounced and persistent downside signal, reflecting sustained concerns about below-target inflation. By contrast, during the recent euro-area inflation surge, expectations initially display strong upside risk signals, which gradually dissipate by the end of 2023. Notably, changes in distributional asymmetry anticipate shifts in the median forecast, suggesting that skewness contains early information about emerging inflation risks. While ECB-SPF forecasts are not designed to deliver direct predictive accuracy, they provide a structured and timely signal to the central bank regarding perceived inflation risks. Over the sample, these signals are broadly consistent with the credibility of the ECB’s commitment to stabilizing inflation around its target, with the notable exception of periods constrained by the ZLB.

**Distinctness from Normalized Uncertainty.** Using one-year-ahead inflation forecasts from the ECB-SPF, the AC measure is only moderately correlated with the skewness component ( $r = 0.55$ ,  $R^2 = 0.30$ ), leaving a substantial share of its variation unexplained by skewness alone. By contrast, AC is tightly associated with the median component ( $r = 0.89$ ,  $R^2 = 0.79$ ), indicating that it primarily reflects movements of the central tendency relative to the inflation target, while incorporating skewness through sign coherence. Regressing standardized inflation AC (ACI) on standardized normalized inflation uncertainty (NIU) yields a positive and significant coefficient ( $\beta = 0.46$ ) but a low explanatory power ( $R^2 = 0.22$ ), implying substantial non-overlap between the two measures. A time-series decomposition corroborates this result, showing that only a limited portion of ACI fluctuations is captured by NIU. Taken together, these findings indicate that ACI is not redundant with uncertainty measures but captures a complementary dimension of inflation expectations related to directional asymmetry around the target. Jointly, NIU and ACI exploit information from the first three moments of subjective probability distributions in a parsimonious and robust manner, allowing informative inference despite the limited granularity of survey-based distributions.

**Monte Carlo validation.** The theoretical predictions of Propositions 1 and 2 are validated jointly in a controlled simulation environment designed to test whether the corrected measures recover the intended latent objects better than raw moments under known contamination. Online Appendix ?? generates an economy with a latent inflation target (random walk with state-dependent drift), AR(1) genuine uncertainty  $u_t$ , and AR(1) directional risk  $\delta_t$ , observed through a panel of 30 heterogeneous forecasters. Three core results emerge from 500 Monte Carlo replications (Table 9). First, NU—as a decontaminated uncertainty measure—tracks genuine uncertainty 43% better than raw IU ( $R^2 = 0.83$  vs. 0.58) and is 4.6 times less contaminated by the distance artifact ( $R^2 = 0.09$  vs. 0.44). Second, the most powerful diagnostic replicates the Barro pattern: in a data-generating process (DGP) where growth depends on the distance from target but *not* on genuine uncertainty, raw IU produces spurious significance in 58% of replications (Newey–West HAC standard errors); adding the distance as a control collapses the rejection rate to its nominal 5% level for both raw IU and NU, confirming that the entire spurious relationship operates through the level channel. Third, AC—as a coherence-adjusted directional-risk measure—recovers the true coherent signal with  $R^2 = 0.94$  (vs. 0.78 for raw asymmetry) and delivers a 4.9% reduction in out-of-sample inflation forecast error using expanding-window (real-time) normalisation with no look-ahead (median relative MSFE of 0.951), while neither raw IU nor NU improve inflation level forecasts—confirming the division of roles. The advantage of the corrected measures is not knife-edge: it survives substantial misspecification of both normalising parameters and functional forms, and grows with noise (Online Appendix ??). Figure 7 makes the contamination visible: when the latent target drifts from its anchor, raw IU spikes even if genuine uncertainty is stable (artifact episodes shaded in red), while NU tracks the truth closely.

While NIU captures *how uncertain* forecasters are, ACI captures *the balance of risks*—whether risks are perceived as coherently tilted toward upside or downside outcomes. The two dimensions are conceptually distinct—one reflects the width of beliefs, the other their directional shape—and may interact differently with monetary policy. Importantly, the two corrections differ in kind: NU removes a documented *bias* (level contamination that systematically inflates raw dispersion when expectations deviate from anchor), while AC addresses a *noise* problem (raw asymmetry is fragile and often uninformative about directional risk). The corrections are parallel in purpose but distinct in mechanism. Section 4 deploys both measures in a unified set of applications that exploits this complementarity.

## 4 Policy implications

The preceding sections documented two identification failures and proposed corrections for each. This section demonstrates that these corrections carry first-order consequences for how policymakers should interpret—and act on—higher-moment information extracted from survey forecasts. The evidence is organized around a simple diagnostic principle. When the same regression or VAR is estimated with both the raw and the corrected measure, two outcomes are possible: if the conclusions agree, the result is robust to the identification failure; if they diverge, the raw result was driven by the artifact, and the corrected result is the economically relevant one. Three broad policy implications emerge. First, the long-standing view that inflation uncertainty independently depresses growth needs to be reconsidered: the true growth cost comes predominantly from high inflation itself, reinforcing the primacy of price stability in central-bank mandates (Section 4.2). Second, inflation uncertainty—once properly measured—is a key state variable for the transmission of monetary policy to credit conditions, with direct implications for how central banks should calibrate the pace and communication of policy adjustments (Section 4.3). Third, the balance of risks, as cap-

tured by the Asymmetry Coherence Index (ACI), provides an operationally useful signal for both inflation forecasting and the assessment of policy-rate responses, making it a natural candidate for inclusion in central-bank monitoring frameworks (Section 4.4). Section 4.1 first summarizes these comparisons in a single diagnostic table; Section 4.5 synthesizes the policy-relevant findings. Additional applications—including the response of perceived de-anchoring to monetary-policy shocks, the credit transmission channel, and growth expectations—appear in Online Appendix ??.

#### 4.1 Diagnostic overview: raw versus corrected measures

Table 5 assembles the central evidence of this paper in a single object: for each empirical exercise, it reports the conclusion obtained with the raw higher moment alongside the conclusion obtained with the corrected measure. The first two rows are diagnostic: they confirm that the corrections succeed in removing the contamination documented in Section 2. Raw inflation uncertainty (IU) loads heavily on the distance from target ( $R^2 = 0.425$ ); normalized inflation uncertainty (NIU) does not ( $R^2 = 0.057$ ). Raw asymmetry correlates with the consensus mean ( $\rho = 0.64$ ); ACI captures a distinct, only partially overlapping dimension relative to NIU.

The remaining rows show what happens to substantive inference—and, by extension, to the policy conclusions drawn from it. In the Barro growth–inflation setting, the raw volatility coefficient is strongly significant; with NIU, it vanishes, and mean inflation recovers significance—implying that the policy priority should be price stability rather than uncertainty reduction per se. In the pre-2020 VAR, raw IU shocks produce a significant contraction in industrial production; NIU shocks do not—the apparent real cost of uncertainty was an artifact of level contamination. Raw asymmetry shocks predict a *decrease* in the policy rate; ACI shocks predict the expected *increase*—a sign reversal with direct implications for how central banks should read balance-of-risks signals. In the inflation forecasting horse race, augmenting the AR with raw IU worsens accuracy, while ACI lowers MSFEs relative to the baseline, especially at the four-quarter horizon, though these gains are only suggestive in two-sided Diebold–Mariano tests.

The diagnostic principle is straightforward: when a finding reverses, the raw result was driven by the artifact that the correction removes. When a finding survives—as with the DFR response to ACI shocks—it reflects a genuine economic mechanism that policymakers can rely on. The subsections below develop each comparison in detail, organized around three policy themes.

#### 4.2 Inflation uncertainty and long-run growth: the primacy of price stability

The classic interpretation of the inflation-uncertainty–growth nexus holds that unpredictable inflation depresses long-run growth through an independent “uncertainty channel” (Barro, 1995). This interpretation has had a lasting influence on policy design: if uncertainty per se harms growth, then central banks should target not only the level of inflation but also the dispersion of inflation expectations. Yet if raw inflation uncertainty embeds a level component, this prescription may rest on a measurement artifact: what appears as an uncertainty effect could instead reflect the well-documented damage caused by high inflation itself. Replacing raw volatility with NIU re-evaluates the classic interpretation by removing the component of dispersion that is mechanically tied to the inflation level; any residual growth effect can then be attributed to genuine belief imprecision rather than to high-inflation regimes.

**Two stylized facts and the motivation for NIU.** *Fact 1: The distribution of inflation rates is highly right-skewed.* Figure 8 replicates Figure 1 of Barro (1995) using a balanced cross-country panel drawn from the Global Macro Data (GMD) database, covering the period 1960–2019 with

Table 1: Raw versus corrected higher moments: how inference changes

Application	Raw	Result	Corrected	Result	Diagnostic
Distance dependence ( $R^2$ )	IU on $d_t$	$R^2 = 0.425$	NIU on $d_t$	$R^2 = 0.057$	Level contamination removed
Mean–asymmetry correlation	Raw asym. $A_t$	$\rho = 0.64$	ACI	Distinct from NIU	Directional noise filtered
Growth (Barro)	regression $\sigma_\pi$	$-0.0009^{***}$	NIU	$-0.0015$ (n.s.)	Effect vanishes
Mean inflation in Barro	With $\sigma_\pi$	$0.0001$ (n.s.)	With NIU	$-0.0003^{***}$	Recovers significance
VAR: IP $\leftarrow$ uncertainty	IU shock	IP contracts**	NIU shock	IP insignificant	Contraction was artifact
VAR: DFR $\leftarrow$ asymmetry	Raw asym. shock	DFR <i>decreases</i>	ACI shock	DFR <i>increases</i> *	Sign reversal
Forecasting (MSFE, $h = 4$ )	AR + IU	Deteriorates	AR + ACI	$0.759$ (DM n.s.)	Suggestive improvement

*Notes:* IU = raw inflation uncertainty (cross-sectional mean of individual SPD variances); NIU = Normalized Inflation Uncertainty (§3.1.2); ACI = Asymmetry Coherence Index (§3.2.2);  $d_t = |\bar{\mu}_t - \pi^*|$  is the distance of the consensus forecast from target. Pre-2020 subsample for VAR rows. Significance: \*\*\* $p < 0.01$ , \*\* $p < 0.05$ , \* $p < 0.1$ ; n.s. = not significant. For the forecasting row, the two-sided Diebold–Mariano test against the AR(AIC) benchmark yields  $p = 0.109$  at  $h = 4$ .

annual observations trimmed to the range  $[-20\%, 200\%]$  to exclude extreme deflation and hyperinflation episodes. The histogram reveals the familiar right skewness of the cross-sectional distribution of inflation: the vast majority of country-year observations cluster at low and moderate rates, while a thin but consequential right tail captures high-inflation and near-hyperinflationary episodes.

*Fact 2: Inflation uncertainty increases with the inflation level.* Figure 9 replicates Figure 2 of Barro (1995), plotting decade-average inflation against within-decade inflation volatility (standard deviation) for each country–decade cell. We overlay an OLS fit, a robust Huber M-estimator, and a nonparametric LOWESS smoother. All three confirm the strong positive relationship between the level and the uncertainty of inflation: high-inflation decades are systematically more volatile, consistent with the theoretical arguments of Ball (1992).

These two facts jointly motivate the NIU normalization. Since raw inflation uncertainty ( $\sigma_\pi$ ) systematically increases with the inflation level ( $\bar{\pi}$ ), a regression of growth on raw  $\sigma_\pi$  conflates two conceptually distinct channels: a *level effect* (high inflation itself reduces growth, as in Barro, 1995) and a *genuine uncertainty effect* (unpredictability of inflation conditional on the level). By dividing  $\sigma_\pi$  by  $\sqrt{a + b|\bar{\pi} - \pi^*|}$ , NIU removes the predictable component of uncertainty attributable to the level, isolating the residual dispersion that is orthogonal to expected inflation.

**Barro–Lee cross-country growth regressions.** We replicate Table 2, column (1) of Barro (1995) using the Barro–Lee panel of 138 countries organized in five-year subperiod averages over 1960–1989 (six subperiods, indexed  $x = 1, \dots, 6$ , corresponding to 1965–69 through 1985–89). The outcome variable is real GDP per capita growth ( $\text{grwb}_x$ ); controls include initial income ( $\log \text{gdpwb}_{xx}$ ), male and female schooling ( $\text{humanm}_{xx}$ ,  $\text{humanf}_{xx}$ ), life expectancy ( $\log \text{lifee0}_x$ ), fertility ( $\log \text{fert}_x$ ), government consumption ( $\text{govsh5}_x$ ), education spending ( $\text{geetot}_x$ ), the black-market premium ( $\text{bmp}_x$ ), terms-of-trade shocks ( $\text{tot}_x$ ), investment ratio ( $\text{invsh5}_x$ ), and the political-

rights index (country constant, averaged over available waves). To match the decade structure of the inflation data (drawn from GMD), we aggregate the five-year Barro–Lee subperiods to decades, matching each decade’s inflation moments to the corresponding Barro–Lee decade. All specifications include decade fixed effects and country-clustered standard errors.

Table 10 presents five specifications. Column (1) confirms the baseline Barro finding: mean decade inflation carries a negative and statistically significant coefficient ( $-0.0004^{***}$ ), implying that a one-percentage-point increase in average inflation reduces annual growth by approximately 0.04 percentage points. Column (2) adds the within-decade standard deviation; the mean-inflation coefficient becomes statistically negligible (0.0001), while inflation uncertainty enters with a strongly negative coefficient ( $-0.0009^{***}$ ), suggesting that it is the unpredictability of inflation rather than its level that harms growth once both are included. Column (3) introduces the full Barro–Lee control set, retaining raw uncertainty: the latter remains negative and significant at 10% ( $-0.0005^*$ ).

Columns (4) and (5) replace raw uncertainty with the NIU measure. In both cases, NIU enters with a negative sign ( $-0.0015$  and  $-0.0022$  respectively) but is *not statistically significant*, while the mean-inflation coefficient recovers its significance. This pattern is informative: it implies that, once inflation uncertainty is level-normalized, residual uncertainty does not independently reduce long-run growth in the Barro–Lee sample. The coefficient on mean inflation reappearing significant ( $-0.0003^{***}$ ) when NIU replaces raw uncertainty further confirms that Barro’s uncertainty effect partially reflects a level component: raw  $\sigma_\pi$  proxies for high-inflation regimes, which NIU has removed by construction. The remaining negative sign on NIU, while imprecisely estimated, is directionally consistent with a genuine uncertainty channel; the absence of significance likely reflects the limited size of the Barro–Lee sample (93 countries over three decades in the full-controls specification) rather than the absence of any underlying effect. A Monte Carlo exercise confirms this interpretation: in a simulated economy where growth depends on the distance from target but not on genuine uncertainty, raw IU produces spurious significance in 58% of replications (using Newey–West HAC standard errors), whereas adding distance as a control collapses the rejection rate to its nominal 5% level for both raw IU and NU—the same pattern as the Barro regressions (Online Appendix ??).

**Policy implication: price stability as the primary growth mandate.** The reinterpretation has a direct bearing on how policymakers should prioritize their objectives. If inflation uncertainty were an independent drag on growth, central banks would face a dual task: stabilizing both the level and the dispersion of inflation expectations. Our results indicate that the growth cost attributed to uncertainty largely reflects the damage caused by high inflation itself. This does not imply that uncertainty is irrelevant—as the credit transmission results below demonstrate, it plays a material role in conditioning how policy is transmitted—but it does imply that, for long-run growth, the first-order policy prescription remains price stability. Central banks that succeed in anchoring inflation close to target simultaneously eliminate the component of measured uncertainty that harms growth, without needing a separate instrument or communication strategy aimed at reducing forecast dispersion per se.

### 4.3 Monetary policy transmission and credit conditions

The previous subsection established that the growth cost of inflation uncertainty is largely attributable to the inflation level. This subsection turns to a domain where properly measured uncertainty plays a genuine and independent role: the transmission of monetary policy to credit conditions. For central banks, understanding the state dependence of their own policy transmission is essential for calibrating the pace and magnitude of rate adjustments. We first present VAR

evidence on the macro-dynamic effects of uncertainty and then examine the credit channel in detail.

**VAR evidence: uncertainty and real activity.** The Barro exercise shows that the level-contamination artifact distorts cross-country inference; a VAR exercise tests whether it also distorts macro-dynamic conclusions within a single economy. The key question for policymakers is whether inflation uncertainty shocks have genuine real effects or whether the apparent contractionary impact is an artifact of mismeasurement. We estimate a quarterly VAR on approximately 108 ECB-SPF observations, ordering  $(EPU_t, NGU_t, NIU_t, \pi_t, DFR_t, u_t, \log IP_t)$ , where  $NGU_t$  is normalized growth uncertainty and  $NIU_t$  is normalized inflation uncertainty. The system also includes the EPU index (Baker, Bloom and Davis, 2016), the ECB deposit facility rate ( $DFR$ ), and industrial production ( $IP$ ). Identification relies on a recursive (Cholesky) decomposition; the lag order is selected by AIC.

Figure 10 reports the NIU impulse responses: innovations to  $NIU_t$  foreshadow movements in realized inflation, consistent with uncertainty acting as a leading indicator of inflationary risk, but have limited effects on employment, industrial production, or the policy rate. Full details on the EPU and NGU blocks appear in Online Appendix ??.

The sharpest evidence that mismeasured uncertainty distorts policy-relevant inference comes from the pre-2020 subsample ( $\leq 2019Q4$ ). Replacing NIU with raw inflation uncertainty (IU) yields a significant negative response of industrial production to IU shocks, whereas the corresponding NIU response is insignificant (Online Appendix Figure ??). This directly reinforces the Barro reinterpretation: once level contamination is removed, the contractionary real effect attributed to inflation uncertainty becomes statistically insignificant. The implication for central banks is consequential: policymakers who monitor raw dispersion may overestimate the real cost of uncertainty shocks and, as a result, overreact to episodes of widening forecast distributions that reflect high inflation rather than genuine belief imprecision.

### **Credit transmission: inflation uncertainty as a state variable for policy pass-through.**

We now show that, while inflation uncertainty does not independently depress real activity, it genuinely conditions the transmission of monetary policy to non-financial corporations' (NFCs) financing conditions—a finding with direct implications for how central banks should calibrate the pace of rate adjustments in different uncertainty environments. Recent work emphasizes that monetary policy transmission is state dependent due to banks' balance-sheet constraints and deposit pricing, with the effectiveness of policy varying across interest-rate environments (Eichenbaum et al., 2025; Volk, 2026). We complement this literature by showing that belief-based states—uncertainty and directional risk—govern the transmission of policy easing even when balance-sheet conditions are held constant. The empirical challenge in credit-market applications is that loan outcomes are typically jointly determined at origination: quantities, rates, maturities, and collateral are co-chosen by banks and borrowers, and their responses to policy shocks may confound price adjustments with selection in contract characteristics. To minimize this multidimensional endogeneity, we focus on overdrafts as in Vansteenberghe (2025), which are close to pure price-quantity contracts at an overnight horizon and thus provide a cleaner environment to isolate pricing responses.

Our main variable of interest is the overnight overdraft rate charged to NFCs in France, and we complement it with the overnight deposit rate received by NFCs. Combining the two, we construct an *overnight NFC spread* defined as the difference between the overdraft rate and the deposit rate. This spread can be interpreted as a representative wedge between an ultra-liquid borrowing margin (NFC liabilities) and an ultra-liquid remuneration on deposits (NFC assets) within the

same institutional setting. As such, it summarizes the net cost of immediate liquidity for NFCs, abstracting from longer-term contract features, Figure 11.

We estimate local projections to quantify how this spread responds to exogenous monetary policy innovations, using “pure” monetary policy shocks (Jarociński and Karadi, 2020). Our interactions are between our uncertainty measure,  $\text{NIU}_t$ , and the monetary policy shocks in order to assess whether the impulse response is state dependent along the uncertainty dimension. We translate the interaction estimates into impulse responses evaluated at low and high uncertainty, corresponding to one standard deviation below and above average  $\text{NIU}_t$ .

Our main specification is given by

$$y_{t+h} = \alpha_h + \beta_h \varepsilon_t^{\text{MP}} + \theta_h \left( \varepsilon_t^{\text{MP}} \times \widetilde{\text{NIU}}_t \right) + \Gamma'_h Z_t + \sum_{j=1}^{p=6} \Phi_{h,j} y_{t-j} + u_{t+h}, \quad (43)$$

where  $y_{t+h}$  denotes the outcome of interest at horizon  $h$  up to  $H = 24$ , namely the overnight NFC spread,  $\varepsilon_t^{\text{MP}}$  is the exogenous monetary policy shock, and  $\widetilde{\text{NIU}}_t \equiv \text{NIU}_t - \mathbb{E}[\text{NIU}_t]$  is the de-measured inflation uncertainty measure. The uncertainty measure  $\text{NIU}_t$  is constructed at quarterly frequency and interpolated to a monthly series using time-based linear interpolation. In the interaction specification,  $\widetilde{\text{NIU}}_t$  enters both directly as a control and interacted with the monetary policy shock, so that  $\theta_h$  captures genuine state dependence rather than omitted-level effects of uncertainty. The vector  $Z_t$  collects monthly control variables, including year-on-year HICP inflation, NFC overnight deposit volumes, the level of  $\widetilde{\text{NIU}}_t$ , and month-of-year fixed effects.

De-meaning  $\text{NIU}_t$  implies that  $\beta_h$  identifies the impulse response to a monetary policy shock at average uncertainty, while  $\theta_h$  captures how the transmission of monetary policy varies with the level of uncertainty. Each horizon- $h$  regression is estimated by OLS, and inference is based on heteroskedasticity- and autocorrelation-consistent standard errors, implemented using Newey–West corrections with a horizon-dependent lag truncation ( $\text{maxlags} = h + 1$ ). Impulse responses at low and high uncertainty are constructed using the delta method, exploiting the full HAC covariance matrix of  $(\beta_h, \theta_h)$  to form confidence intervals.

The key result, Figure 12, is that the transmission of a contractionary monetary policy shock depends on inflation uncertainty. In particular, at *low* uncertainty, a positive monetary policy shock reduces the overnight NFC spread. This pattern is consistent with an incomplete pass-through on the overdraft (liability) side relative to the deposit (asset) side: when banks’ inflation uncertainty is low, tightening is not fully reflected in NFC overdraft pricing, thereby mitigating the increase in NFCs’ marginal cost of ultra-short-term liquidity.

**Maturity-dependent pass-through and the role of uncertainty.** We next examine whether inflation uncertainty also shapes the *speed* of monetary policy transmission along the maturity dimension of NFC loan pricing. Using monthly French MIR data on new business loans below one million euros (Figure 13), we consider two benchmark rates: short-maturity loans with an initial rate fixation below one year and long-maturity loans with an initial fixation above five years. For each maturity  $m \in \{\text{S}, \text{L}\}$ , we construct a policy-relevant spread defined as the difference between the NFC loan rate and the ECB deposit facility rate (DFR),

$$s_t^m \equiv r_t^m - \text{DFR}_t, \quad m \in \{\text{S}, \text{L}\}, \quad (44)$$

where  $r_t^{\text{S}}$  denotes the monthly NFC loan rate with  $\text{PFIT} < 1$  year,  $r_t^{\text{L}}$  denotes the monthly NFC loan rate with  $\text{PFIT} > 5$  years, and  $\text{DFR}_t$  is the monthly average ECB deposit facility rate. We then focus on the maturity differential in spreads,

$$\Delta s_t \equiv s_t^{\text{L}} - s_t^{\text{S}}, \quad (45)$$

which summarizes, at each date, how much more (or less) long-maturity new lending is priced relative to short-maturity new lending, after netting out the contemporaneous stance of monetary policy.

Our objective is not to isolate “pure” monetary policy shocks, but to quantify the *dynamic pass-through of observed DFR changes* to loan pricing, and to test whether this transmission differs systematically between easing and tightening *cycles*. Let  $\Delta\text{DFR}_t$  denote the monthly change in the policy rate, and let  $D_t^E$  and  $D_t^T$  be indicators for easing and tightening cycles.<sup>17</sup> For each horizon  $h = 0, \dots, H$  (with  $H = 24$  months), we estimate the horizon-specific local projection

$$\Delta s_{t+h} = \alpha_h + \beta_h^E (\varepsilon_t^{\text{MP}} \times D_t^E) + \beta_h^T (\varepsilon_t^{\text{MP}} \times D_t^T) + \Gamma'_h Z_t + \sum_{j=1}^p \Phi_{h,j} \Delta s_{t-j} + u_{t+h}, \quad (46)$$

where  $Z_t$  collects controls (including inflation and seasonality),  $p = 6$  is the number of lags, and inference relies on Newey–West HAC standard errors with horizon-dependent lag truncation. Equation (46) allows the impulse response of the maturity differential to differ between easing and tightening cycles.

To connect the horizon-by-horizon estimates to the cumulative objects reported in the figures, define the state-specific impulse responses of  $\Delta s$  as  $\widehat{\text{IRF}}_h^E \equiv \widehat{\beta}_h^E$  and  $\widehat{\text{IRF}}_h^T \equiv \widehat{\beta}_h^T$ . We then report the *cumulative differential adjustment*,

$$\widehat{\text{CUM}}_h^k \equiv \sum_{\tau=0}^h \widehat{\text{IRF}}_\tau^k, \quad k \in \{E, T\}, \quad (47)$$

with confidence bands computed by the delta method using the HAC covariance matrix of the stacked horizon-specific coefficients, Figure 14.

Standard theories of bank pricing under interest rate risk and refinancing considerations predict asymmetric dynamics: during easing cycles, long-maturity loan rates should adjust more sluggishly than short-maturity rates, reflecting duration risk, prepayment uncertainty, and the option value of delaying repricing. During tightening episodes, pass-through is typically faster and more homogeneous across maturities, as higher policy rates can be transmitted quickly to both short- and long-term contracts through repricing clauses and risk premia. Consistent with these priors, we find that during easing episodes the cumulative difference between long- and short-maturity spreads widens significantly, whereas no statistically meaningful differential emerges during tightening episodes. This asymmetry reflects the downward rigidity of long-term lending rates and confirms that banks smooth the transmission of accommodative policy at longer horizons.

We then turn to our central question: does inflation uncertainty affect the *timing* of maturity-dependent pass-through during easing? To this end, we augment the easing-state local projections with interactions between monetary policy shocks and inflation uncertainty. Let  $\text{NIU}_t$  denote the normalized inflation uncertainty indicator, and define its de-measured version  $\widetilde{\text{NIU}}_t \equiv \text{NIU}_t - \mathbb{E}[\text{NIU}_t]$ . We estimate, for each horizon  $h$ ,

$$\Delta s_{t+h} = \alpha_h + \beta_h^E (\varepsilon_t^{\text{MP}} \times D_t^E) + \theta_h^E (\varepsilon_t^{\text{MP}} \times D_t^E \times \widetilde{\text{NIU}}_t) + \Gamma'_h Z_t + \sum_{j=1}^p \Phi_{h,j} \Delta s_{t-j} + u_{t+h}, \quad (48)$$

where  $\widetilde{\text{NIU}}_t$  is also included in  $Z_t$  (in levels) so that  $\theta_h^E$  captures genuine state dependence rather than level effects of uncertainty. Impulse responses are evaluated at low and high uncertainty,

$$\widehat{\text{IRF}}_h^E(\text{low}) \equiv \widehat{\beta}_h^E + \widehat{\theta}_h^E (\mu_{\text{NIU}} - \sigma_{\text{NIU}} - \mu_{\text{NIU}}) = \widehat{\beta}_h^E - \widehat{\theta}_h^E \sigma_{\text{NIU}}, \quad \widehat{\text{IRF}}_h^E(\text{high}) \equiv \widehat{\beta}_h^E + \widehat{\theta}_h^E \sigma_{\text{NIU}}, \quad (49)$$

<sup>17</sup>In the empirical implementation, these states are constructed from the sign of the contemporaneous policy rate change,  $D_t^E = \mathbb{1}\{\Delta\text{DFR}_t < 0\}$  and  $D_t^T = \mathbb{1}\{\Delta\text{DFR}_t > 0\}$ .

and cumulative responses are constructed as in (47). The resulting objects are plotted in Figure 15, with confidence intervals again obtained by the delta method using the full HAC covariance matrix of  $(\beta_h^E, \theta_h^E)$ .

Splitting easing episodes by the level of inflation uncertainty, we uncover a sharp state dependence. Under low uncertainty, the cumulative difference between long- and short-maturity spreads is short-lived and largely resolves within four months, indicating a relatively rapid and orderly transmission of policy easing across the maturity spectrum. Under high uncertainty, by contrast, the initial response of the two spreads is indistinguishable, but after approximately four months the differential becomes statistically significant and grows for the next six months. The cumulative gap under high uncertainty is substantially larger than under low uncertainty. This pattern implies that elevated inflation uncertainty slows the pass-through of policy easing even at short maturities and induces banks to delay repricing more strongly at long maturities. In such environments, banks appear reluctant to commit to lower rates for extended horizons, consistent with heightened concern about future inflation realizations and the risk of being locked into low-yield contracts.

**Policy implication: calibrating the pace of easing under uncertainty.** These results suggest that central banks should account for the prevailing level of inflation uncertainty when designing easing cycles. In high-uncertainty environments, the standard transmission mechanism is impaired: banks delay repricing, particularly at longer maturities, so that intended stimulus reaches the real economy more slowly and less completely. This calls for a more patient and possibly front-loaded approach to easing when uncertainty is elevated—or, alternatively, for complementary forward guidance aimed at reducing uncertainty itself, thereby unblocking the credit channel. Monitoring NIU rather than raw dispersion is essential in this context, since raw measures conflate the level of inflation with genuine uncertainty and would therefore overstate the degree of transmission impairment during high-inflation episodes that are not genuinely uncertain.

#### 4.4 The balance of risks: forecasting and policy-rate responses

While uncertainty governs how monetary policy is transmitted, the balance of risks—as captured by the Asymmetry Coherence Index (ACI)—informs *why* policy responds. This subsection presents two complementary pieces of evidence: the forecasting content of directional risk signals and the VAR response of the policy rate to coherent balance-of-risks shocks. Together, they suggest that ACI provides an operationally useful signal for central-bank risk assessment and communication.

**The balance of risks as a forecasting signal.** Uncertainty measures capture the *width* of the forecast distribution and are not necessarily expected to improve point predictions of the level—their role is to condition the transmission of shocks, not to predict their direction. Directional-coherence measures, by contrast, encode information about *which side the risks are on* and should therefore carry forecasting content for the level of inflation. This conceptual distinction implies a testable prediction: neither raw nor corrected uncertainty should improve level forecasts, whereas ACI—if it captures a genuine balance-of-risks signal—should. We test this in a pseudo out-of-sample horse race following the design of Stock and Watson (2007); Online Appendix ?? reports a complementary density evaluation exercise embedding ACI in the UCSV framework of De Polis, Melosi and Petrella (2025).

**Pseudo out-of-sample horse race.** We compare models at horizons  $h \in \{1, 2, 4\}$  quarters ahead: an autoregressive benchmark with Akaike information criterion (AIC)-selected lag order [AR(AIC)]; the Atkeson–Ohanian random walk on inflation levels [AO, Atkeson, Ohanian et al.,

2001]; an integrated moving-average model with fixed coefficient [IMA( $\theta = 0.65$ )]; AR models augmented with NIU, with ACI, and with both; and—to implement the raw-versus-corrected diagnostic—AR models augmented with raw inflation uncertainty (IU) and raw asymmetry. All models are estimated recursively, with direct  $h$ -step-ahead projections and Newey–West standard errors (bandwidth  $h - 1$ ). The out-of-sample evaluation begins in 2003Q1. Table 11 reports mean squared forecast errors (MSFEs) normalized to the AR(AIC) baseline, together with Diebold–Mariano  $p$ -values for equal predictive accuracy against the AR(AIC).

The results confirm the predicted division of roles. Uncertainty measures—whether raw or corrected—do not improve level forecasts: adding raw IU to the AR *worsens* accuracy (relative MSFE of 1.267 at  $h = 4$ ), and corrected NIU similarly deteriorates it (1.136 at  $h = 4$ ). This is not a failure of the correction: it is consistent with the conceptual role of uncertainty as a state variable that conditions transmission rather than predicting the direction of future inflation. Raw asymmetry is equally uninformative: AR+Asym. produces a relative MSFE of 0.995 at  $h = 4$ , indistinguishable from the baseline.

The coherence-filtered measure tells a different story. Adding ACI to the AR model reduces mean squared forecast errors at every horizon: relative MSFE declines from 0.951 at  $h = 1$  to 0.859 at  $h = 2$  and 0.759 at  $h = 4$ , with the largest reduction occurring at the four-quarter horizon. AR+ACI outperforms every other benchmark at  $h = 4$ , including the IMA(1,1) (relative MSFE of 0.821;  $p = 0.029$ ). The contrast between raw asymmetry (uninformative) and ACI (lower MSFEs across horizons) is the forecasting analogue of the VAR sign reversal: the coherence filter does not merely refine a noisy signal—it separates signal from noise. The MSFE gains do not reach conventional significance under two-sided Diebold–Mariano tests ( $p = 0.109$  at  $h = 4$ ), partly reflecting the limited Euro Area quarterly sample; the density evaluation in Online Appendix ?? points in the same direction but remains modest, with Brier score improvements for tail events that are significant only at the 10% level. The forecasting horse race thus suggests that the two corrections serve distinct purposes: uncertainty captures width, while directional coherence captures predictive content for the level of inflation.

**VAR evidence: the balance of risks and the policy rate.** To complement the forecasting evidence, we estimate a second quarterly VAR ordering ( $EPU_t$ ,  $NIU_t$ ,  $ACI_t$ ,  $\pi_t$ ,  $DFR_t$ ,  $u_t$ ,  $\log IP_t$ ). Figure 16 shows that a positive ACI innovation is followed by a statistically meaningful increase in the ECB deposit facility rate, with no robust effect on real activity or inflation dynamics. This pattern is economically intuitive: periods of coherent upside inflation risk—a median above target aligned with positive asymmetry—are precisely episodes in which the central bank is more likely to tighten.

The pre-2020 subsample reveals a striking sign reversal that underscores the importance of proper measurement for interpreting central-bank behavior. Replacing ACI with raw aggregate asymmetry produces a counterintuitive *decrease* in the deposit facility rate following a positive skewness shock—the opposite of what standard Taylor-rule logic would predict when upside inflation risk is signaled. With ACI, this puzzle is resolved: a short-lived positive DFR response appears, consistent with the central bank tightening in response to coherent upside inflation risk (Online Appendix Figure ??). The coherence filter removes incoherent skewness observations—positive skewness with a median below target—that otherwise confound the aggregate signal. This finding demonstrates that the AC construction does not merely refine a noisy measure: it reverses a qualitative conclusion about the link between distributional asymmetry and monetary policy.

**Maturity-dependent pass-through and the role of asymmetry coherence.** We next assess whether directional inflation risk, captured by the Asymmetry Coherence Index (ACI), affects the *timing* of monetary policy pass-through across loan maturities. We estimate a specification analogous to (48), replacing the interaction with de-meaned inflation uncertainty by the de-meaned coherence component of ACI, while retaining NIU in the control set to isolate second-moment effects. This design allows us to distinguish precautionary behavior driven by overall uncertainty from adjustments driven by the perceived direction of inflation risks.

Figure 17 summarizes the overnight spread results. When the ACI is low—corresponding to a pronounced perception of downside inflation risk—the response of the overnight NFC spread to a contractionary monetary policy shock is weak and statistically insignificant, and if anything slightly negative. Conversely, when ACI is high, reflecting strong perceptions of upside inflation risk, the spread response is also statistically insignificant, suggesting limited state dependence of short-term lending spreads with respect to directional inflation risk.

Figure 18 reports the maturity-dependent results for easing episodes. When ACI is high, indicating strong upside inflation risk perceptions, the cumulative response of the long–short maturity spread to a policy easing, has a lag, and is then larger. This pattern is consistent with banks anticipating that tightening policy will be longer-lasting to lean on this higher inflation risk and therefore being reluctant to lower long-maturity lending rates quickly. By contrast, when ACI is low, corresponding to dominant downside risk perceptions, maturity-dependent pass-through is faster and the cumulative differential remains limited.

**Robustness.** A joint 9-variable VAR including both uncertainty dimensions (NGU, NIU) and both asymmetry dimensions (ACG, ACI) simultaneously produces qualitatively unchanged NIU and ACI impulse responses, confirming that these measures carry distinct information (Online Appendix Figures ?? and ??).

**Policy implication: operationalizing the balance of risks.** The balance of risks is a concept that pervades central-bank communication—the ECB’s Governing Council, for instance, routinely characterizes risks to the inflation outlook as “tilted to the upside,” “tilted to the downside,” or “broadly balanced.” Yet this assessment has lacked a standard empirical counterpart derived from survey expectations. Our results suggest that ACI can serve this role. It provides a quantitative, real-time signal of whether the perceived direction of inflation risk is coherent with the central forecast—precisely the object that risk-tilting language aims to capture. The forecasting evidence shows that ACI carries predictive content for the level of inflation at policy-relevant horizons, while the VAR evidence confirms that the ECB’s actual policy-rate decisions align with coherent balance-of-risks signals rather than with raw distributional asymmetry. For central banks, this implies that monitoring ACI—or an analogous coherence-filtered measure constructed from their own survey infrastructure—would provide a disciplined empirical anchor for the qualitative risk assessments that already feature prominently in policy communication. It would also guard against the risk of acting on incoherent asymmetry signals that, as the sign-reversal evidence shows, can point in the wrong direction.

## 4.5 Summary of policy-relevant findings

The diagnostic principle applied throughout this section yields a clear partition of existing empirical conclusions into artifacts and genuine effects, with distinct policy implications for each. Table 2 synthesizes the findings.

**Conclusions that require reinterpretation.** Three established results do not survive the raw-to-corrected transition, and the policy prescriptions built on them should be reconsidered. The Barro (1995) finding that inflation uncertainty reduces growth is driven by the level component of raw uncertainty; once NIU replaces raw  $\sigma_\pi$ , the coefficient becomes insignificant and mean inflation recovers its explanatory power. The policy implication is that the growth cost historically attributed to uncertainty is better understood as a cost of high inflation itself—reinforcing, rather than supplementing, the case for price stability. The contractionary real effect of inflation uncertainty shocks on industrial production (VAR 1, pre-2020 subsample) is an artifact of the same contamination: policymakers should not interpret widening raw forecast distributions as an independent threat to real activity. The counterintuitive decrease of the deposit facility rate following a positive raw asymmetry shock (VAR 2, pre-2020 subsample) reflects incoherent asymmetry observations that the AC filter removes: using raw skewness to read central-bank reaction functions would produce misleading conclusions about the policy response to directional risk.

**Conclusions with genuine policy content.** The DFR tightening response to ACI shocks survives and indeed sharpens with the correction: the central bank reacts to coherent upside risk, not to raw distributional shape. This validates the use of coherence-filtered asymmetry as an indicator of policy-relevant directional risk. The forecasting results for ACI, while only suggestive under two-sided Diebold–Mariano tests, contrast with the noise added by raw asymmetry: ACI lowers MSFEs, whereas raw asymmetry does not—suggesting that central-bank staff forecasting models could benefit from incorporating coherence-filtered balance-of-risks measures. The credit transmission channel also survives: NIU genuinely conditions the magnitude and timing of monetary policy pass-through to bank lending, confirming that level-purified uncertainty is a real state variable for the macroeconomy. This result is particularly relevant for central banks during easing cycles, when impaired transmission under high uncertainty may require adjustments to the pace or communication of rate cuts.

**EPU diagnostic.** A further confirmation comes from the correlation between inflation uncertainty and the EPU index of Baker, Bloom and Davis (2016). If the correction merely destroyed signal, one would expect it to weaken the EPU correlation; instead,  $\rho(\text{EPU}, \text{NIU}) = 0.84$  substantially exceeds  $\rho(\text{EPU}, \text{IU}) = 0.66$ . Level contamination *dilutes* rather than reinforces the EPU signal: the mechanical variance component tied to deviations from target adds noise uncorrelated with the political-uncertainty sources captured by EPU. Online Appendix Table ?? reports the full correlation matrix and Figure ?? provides the time-series overlay. For policymakers who already track EPU as part of their monitoring toolkit, this finding provides reassurance that NIU is more aligned with the broader uncertainty environment they seek to assess.

**The division of roles: a framework for central-bank monitoring.** Across all exercises, a clean separation emerges that maps directly onto distinct dimensions of central-bank decision-making. Normalized Uncertainty (NU) conditions *how* monetary policy is transmitted—governing the magnitude, timing, and state dependence of pass-through to credit conditions. Asymmetry Coherence (AC) informs *why* policy responds—providing coherent directional signals that predict tightening decisions and carry forecasting content for the inflation level. This division of roles suggests that central banks would benefit from monitoring both dimensions separately: NU as a state variable for transmission assessment, and AC as a signal for risk-tilting and forward guidance. Additional applications in Online Appendix ??—including the de-anchoring response, growth expectations, and the NU-only VAR—further corroborate this pattern.

Table 2: Policy-relevant findings: which conclusions survive artifact correction

Application	Raw result	Corrected result	Policy verdict
Barro growth–inflation	$\sigma_\pi$ : $-0.0009^{***}$	NIU: $-0.0015$ (n.s.)	Growth cost reflects inflation level, not uncertainty
VAR: IP $\leftarrow$ uncertainty	IU shock contracts IP**	NIU shock: insignificant	No independent real cost of uncertainty
VAR: DFR $\leftarrow$ asymmetry	Raw asym. shock $\Rightarrow$ DFR <i>decreases</i>	ACI shock $\Rightarrow$ DFR <i>increases*</i>	Raw skewness misleads on policy reaction
Inflation forecasting	AR+IU worsens; AR+Asym. uninformative	AR+ACI: lower MSFE (DM n.s.)	ACI useful for staff projections
EPU correlation	$\rho(\text{EPU}, \text{IU}) = 0.66$	$\rho(\text{EPU}, \text{NIU}) = 0.84$	NIU better aligned with broader uncertainty
DFR $\leftarrow$ ACI	—	DFR increases*	ECB reacts to coherent upside risk
Credit transmission	—	NIU conditions pass-through	Uncertainty impairs easing transmission

## 5 Conclusion

This paper shows that commonly used measures of inflation uncertainty and directional risk are contaminated by the first moment of forecast distributions and proposes two corrections grounded in micro-founded mechanisms. In the ECB Survey of Professional Forecasters, nearly half of the variation in raw forecast dispersion is explained by the distance of expected inflation from target, while raw asymmetry is too noisy to be interpreted as directional risk unless disciplined by the central forecast. Normalized Uncertainty (NU) removes the predictable level component from raw dispersion through a variance-stabilizing transformation, recovering genuine belief imprecision. Asymmetry Coherence (AC) extracts directional risk by retaining only the component of asymmetry that is coherent with the first moment, providing an operational formalization of the balance of risks.

These corrections materially change inference, and the evidence organizes around a clean division of roles. NU conditions *how* monetary policy is transmitted. In a replication of the Barro (1995) growth–inflation regressions, the inflation–volatility coefficient—long interpreted as evidence that uncertainty independently depresses growth—vanishes once level contamination is removed, while the mean–inflation coefficient recovers its significance. The growth cost historically attributed to uncertainty is better understood as a cost of high inflation itself, reinforcing the primacy of price stability in central-bank mandates. In a VAR exercise, the apparent contractionary effect of inflation uncertainty shocks on industrial production likewise disappears with the corrected measure, confirming that policymakers who monitor raw dispersion risk overestimating the real cost of uncertainty.

AC informs *why* policy responds. In the pre-2020 VAR, replacing raw asymmetry with the Asymmetry Coherence Index (ACI) reverses the sign of the policy-rate response: raw asymmetry shocks produce a counterintuitive easing, whereas coherent upside-risk shocks produce the expected tightening—consistent with the central bank reacting to genuine directional risk rather than to distributional noise. In a pseudo out-of-sample forecasting horse race, adding raw dispersion or raw asymmetry to inflation models worsens or leaves unchanged predictive accuracy, while ACI lowers mean squared forecast errors across horizons, with the largest reduction reaching 24% at the

four-quarter horizon.

The credit transmission channel provides a further domain where properly measured uncertainty plays a genuine and independent role. Using local projections on overnight NFC spreads and maturity-differentiated loan pricing, we show that the pass-through of monetary policy easing to bank lending conditions is state-dependent along the uncertainty dimension. Under low inflation uncertainty, easing transmits relatively quickly across the maturity spectrum; under high uncertainty, banks delay repricing—particularly at longer maturities—consistent with heightened concern about future inflation realizations. This finding implies that central banks should account for the prevailing level of inflation uncertainty when calibrating the pace of easing cycles, and that monitoring NIU rather than raw dispersion is essential to avoid overstating transmission impairment during high-inflation episodes that are not genuinely uncertain.

The two corrections are portable beyond the ECB-SPF setting. The NU normalization applies to any dispersion measure—survey-based, option-implied, or model-based—for which a reference anchor is available. The AC construction requires only a central-tendency estimate and a measure of distributional asymmetry, making it applicable to option-implied densities, firm-level expectation surveys, GDP growth forecasts, and supervisory applications such as Vansteenberghe (2026*b*). Cross-country evidence from the US SPF confirms that the skewness–deviation relationship varies with the institutional environment, with a structural break around the Fed’s adoption of an explicit inflation target. More broadly, the signal-extraction logic—using the first moment to discipline the interpretation of higher moments—may prove useful in any setting where raw higher moments are too noisy or too contaminated by level effects to be taken at face value.

Survey distributions become more informative not when higher moments are used mechanically, but when they are measured in a way that separates macroeconomic signals from first-moment contamination. For central banks, this implies a two-dimensional monitoring framework: Normalized Uncertainty as a state variable governing the magnitude and timing of policy transmission, and Asymmetry Coherence as a signal for risk-tilting assessments and forward guidance. Uncertainty and the balance of risks are not the same object, and treating them as such—as the literature has often done—leads to conclusions that do not survive proper measurement.

## References

- Abel, Joshua, Robert Rich, Joseph Song, and Joseph Tracy.** 2016. “The measurement and behavior of uncertainty: evidence from the ECB survey of professional forecasters.” *Journal of Applied Econometrics*, 31(3): 533–550.
- Ahir, Hites, Nicholas Bloom, and Davide Furceri.** 2022. “The world uncertainty index.” National bureau of economic research.
- Anderson, Brian DO, and John B Moore.** 2005. *Optimal filtering*. Courier Corporation.
- Anscombe, Francis J.** 1948. “The transformation of Poisson, binomial and negative-binomial data.” *Biometrika*, 35(3/4): 246–254.
- Aoki, Kosuke, and Takeshi Kimura.** 2007. “Uncertainty about perceived inflation target and monetary policy.” Deutsche Bundesbank Discussion Paper Series 1: Economic Studies.
- Artzner, Philippe, Freddy Delbaen, Jean-Marc Eber, and David Heath.** 1999. “Coherent measures of risk.” *Mathematical finance*, 9(3): 203–228.
- Atkeson, Andrew, Lee E Ohanian, et al.** 2001. “Are Phillips curves useful for forecasting inflation?” *Federal Reserve bank of Minneapolis quarterly review*, 25(1): 2–11.
- Baker, Scott R, Nicholas Bloom, and Steven J Davis.** 2016. “Measuring economic policy uncertainty.” *The quarterly journal of economics*, 131(4): 1593–1636.
- Ball, Laurence.** 1992. “Why does high inflation raise inflation uncertainty?” *Journal of Monetary Economics*, 29(3): 371–388.
- Ball, Laurence, and N Gregory Mankiw.** 1995. “Relative-price changes as aggregate supply shocks.” *The Quarterly Journal of Economics*, 110(1): 161–193.
- Barberis, Nicholas, and Ming Huang.** 2008. “Stocks as lotteries: The implications of probability weighting for security prices.” *American Economic Review*, 98(5): 2066–2100.
- Barro, Robert J.** 1995. “Inflation and economic growth.”
- Barro, Robert J.** 2006. “Rare disasters and asset markets in the twentieth century.” *The Quarterly Journal of Economics*, 121(3): 823–866.
- Bianchi, Francesco, Sydney C Ludvigson, and Sai Ma.** 2022. “Belief distortions and macroeconomic fluctuations.” *American Economic Review*, 112(7): 2269–2315.
- Bordalo, Pedro, Nicola Gennaioli, and Andrei Shleifer.** 2018. “Diagnostic expectations and credit cycles.” *The Journal of Finance*, 73(1): 199–227.
- Bordalo, Pedro, Nicola Gennaioli, Yueran Ma, and Andrei Shleifer.** 2020. “Overreaction in macroeconomic expectations.” *American Economic Review*.
- Bowley, Arthur Lyon.** 1926. *Elements of statistics*. King.
- Box, George EP, and David R Cox.** 1964. “An analysis of transformations.” *Journal of the Royal Statistical Society: Series B (Methodological)*, 26(2): 211–252.

- Brunner, Allan D, and Gregory D Hess.** 1993. “Are higher levels of inflation less predictable? A state-dependent conditional heteroscedasticity approach.” *Journal of Business & Economic Statistics*, 11(2): 187–197.
- Cogley, Timothy, and Thomas J Sargent.** 2005. “Drifts and volatilities: monetary policies and outcomes in the post WWII US.” *Review of Economic dynamics*, 8(2): 262–302.
- Coibion, Olivier, and Yuriy Gorodnichenko.** 2015. “Information rigidity and the expectations formation process: A simple framework and new facts.” *American Economic Review*.
- Cukierman, Alex, and Allan H Meltzer.** 1986. “A theory of ambiguity, credibility, and inflation under discretion and asymmetric information.” *Econometrica: journal of the econometric society*, 1099–1128.
- Cukierman, Alex, and Paul Wachtel.** 1979. “Differential inflationary expectations and the variability of the rate of inflation: theory and evidence.” *The American Economic Review*, 69(4): 595–609.
- De Polis, Andrea, Leonardo Melosi, and Ivan Petrella.** 2025. “The taming of the skew: Asymmetric inflation risk and monetary policy.” Working Paper.
- Eichenbaum, Martin S, Federico Puglisi, Sergio Rebelo, and Mathias Trabandt.** 2025. “Banks and the State-Dependent Effects of Monetary Policy.” National Bureau of Economic Research.
- Elliott, Graham, Allan Timmermann, and Ivana Komunjer.** 2005. “Estimation and testing of forecast rationality under flexible loss.” *The Review of Economic Studies*, 72(4): 1107–1125.
- Engelberg, Joseph, Charles F Manski, and Jared Williams.** 2009. “Comparing the point predictions and subjective probability distributions of professional forecasters.” *Journal of Business & Economic Statistics*.
- Engle, Robert F.** 1982. “Autoregressive conditional heteroscedasticity with estimates of the variance of United Kingdom inflation.” *Econometrica: Journal of the econometric society*, 987–1007.
- European Central Bank.** 2018. “Results of the Third Special Survey.” Accessed: 2024-10-09.
- European Central Bank.** 2021. “The ECB’s Monetary Policy Strategy Statement.” European Central Bank. Adopted 8 July 2021.
- European Central Bank.** 2025. “The ECB’s monetary policy strategy statement (2025).” [https://www.ecb.europa.eu/mopo/strategy/strategy-review/ecb.strategyreview202506\\_strategy\\_statement.en.html](https://www.ecb.europa.eu/mopo/strategy/strategy-review/ecb.strategyreview202506_strategy_statement.en.html), Accessed 17 March 2026.
- Fischer, Johannes, Christoph Herler, and Philip Schnattinger.** 2024. “The effect of inflation uncertainty on household spending.” mimeo.
- Friedman, Milton.** 1977. “Nobel lecture: inflation and unemployment.” *Journal of political economy*, 85(3): 451–472.
- Gali, Jordi.** 2015. *Monetary Policy, Inflation, and the Business Cycle*. . 2nd ed., Princeton University Press.

- Garcia, Juan A.** 2003. “An introduction to the ECB’s survey of professional forecasters.” *ECB Occasional Paper*.
- Giordani, Paolo, and Paul Söderlind.** 2003. “Inflation forecast uncertainty.” *European Economic Review*, 47(6): 1037–1059.
- Gordon, Robert J.** 1971. “Steady anticipated inflation: Mirage or oasis?” *Brookings Papers on Economic Activity*, 1971(2): 499–510.
- Grier, Kevin B, and Mark J Perry.** 1998. “On inflation and inflation uncertainty in the G7 countries.” *Journal of International Money and Finance*, 17(4): 671–689.
- Guvenen, Fatih, Serdar Ozkan, and Jae Song.** 2014. “The nature of countercyclical income risk.” *Journal of Political Economy*, 122(3): 621–660.
- Haa, Jongrim, and Inhwon Sob.** 2024. “The Economic Effects of Global Inflation Uncertainty.” *International Journal of Central Banking*.
- Hamilton, James D.** 1989. “A new approach to the economic analysis of nonstationary time series and the business cycle.” *Econometrica: Journal of the econometric society*, 357–384.
- Hartmann, Matthias, Helmut Herwartz, and Maren Ulm.** 2022. “Inflation targeting under inflation uncertainty—Multi-economy evidence from a stochastic volatility model.” *Macroeconomic Dynamics*, 26(5): 1302–1337.
- Harvey, Campbell R, and Akhtar Siddique.** 2000. “Conditional skewness in asset pricing tests.” *The Journal of finance*, 55(3): 1263–1295.
- Hillenbrand, Sebastian, Viral V Acharya, Venky Venkateswaran, and Margaret Underwood.** 2025. “Inflation Uncertainty: Measurement, Causes, and Consequences.” *Causes, and Consequences (September 11, 2025)*.
- Ilut, Cosmin L, and Martin Schneider.** 2014. “Ambiguous business cycles.” *American Economic Review*, 104(8): 2368–2399.
- Jarociński, Marek, and Peter Karadi.** 2020. “Deconstructing monetary policy surprises—the role of information shocks.” *American Economic Journal: Macroeconomics*, 12(2): 1–43.
- Jurado, Kyle, Sydney C Ludvigson, and Serena Ng.** 2015. “Measuring uncertainty.” *American Economic Review*, 105(3): 1177–1216.
- Kitsul, Yuriy, and Jonathan H Wright.** 2013. “The economics of options-implied inflation probability density functions.” *Journal of Financial Economics*, 110(3): 696–711.
- Klibanoff, Peter, Massimo Marinacci, and Sujoy Mukerji.** 2005. “A smooth model of decision making under ambiguity.” *Econometrica*, 73(6): 1849–1892.
- Kraus, Alan, and Robert H Litzenberger.** 1976. “Skewness preference and the valuation of risk assets.” *The Journal of finance*, 31(4): 1085–1100.
- Lahiri, Kajal, and Fushang Liu.** 2006. “Modelling multi-period inflation uncertainty using a panel of density forecasts.” *Journal of Applied Econometrics*, 21(8): 1199–1219.

- Levi, Maurice D, and John H Makin.** 1980. “Inflation uncertainty and the Phillips curve: Some empirical evidence.” *The American Economic Review*, 70(5): 1022–1027.
- Maćkowiak, Bartosz, and Mirko Wiederholt.** 2009. “Optimal sticky prices under rational inattention.” *American Economic Review*, 99(3): 769–803.
- Mankiw, N Gregory, Ricardo Reis, and Justin Wolfers.** 2003. “Disagreement about inflation expectations.” *NBER macroeconomics annual*, 18: 209–248.
- Mertens, Elmar.** 2016. “Measuring the level and uncertainty of trend inflation.” *Review of Economics and Statistics*, 98(5): 950–967.
- Minoiu, Camelia, Andres Schneider, and Min Wei.** 2024. “Why does the yield curve predict GDP growth? The role of banks.” *The Role of Banks\*(March 19, 2024)*.
- Neftci, Salih N.** 1984. “Are economic time series asymmetric over the business cycle?” *Journal of political economy*, 92(2): 307–328.
- Nelder, John Ashworth, and Robert WM Wedderburn.** 1972. “Generalized linear models.” *Journal of the Royal Statistical Society Series A: Statistics in Society*, 135(3): 370–384.
- Okun, Arthur M.** 1971. “The mirage of steady inflation.” *Brookings papers on economic activity*, 1971(2): 485–498.
- Paloviita, Maritta, and Matti Viren.** 2013. “Are individual survey expectations internally consistent?” *National Bank of Poland Working Paper*.
- Paloviita, Maritta, and Matti Viren.** 2014. “Inflation and output growth uncertainty in individual survey expectations.” *Empirica*.
- Rich, Robert, and Joseph Tracy.** 2010. “The relationships among expected inflation, disagreement, and uncertainty: evidence from matched point and density forecasts.” *The Review of Economics and Statistics*, 92(1): 200–207.
- Rudebusch, Glenn D, Brian P Sack, and Eric T Swanson.** 2006. “Macroeconomic implications of changes in the term premium.” *FRB of San Francisco Working Paper*.
- Sims, Christopher A.** 2001. “Solving Linear Rational Expectations Models.” *Computational Economics*, 20: 1–20.
- Sims, Christopher A.** 2003. “Implications of rational inattention.” *Journal of monetary Economics*, 50(3): 665–690.
- Stock, James H, and Mark W Watson.** 2007. “Why has US inflation become harder to forecast?” *Journal of Money, Credit and banking*, 39: 3–33.
- Vansteenberghe, Eric.** 2025. “Monetary Policy, Uncertainty, and Credit Supply.” *arXiv preprint arXiv:2512.12255*.
- Vansteenberghe, Eric.** 2026a. “Inflation and growth: professional forecasters continue to express high levels of uncertainty.” *Banque de France Eco Notepad No. 436*, Published February 27, 2026.
- Vansteenberghe, Eric.** 2026b. “Insurance supervision under climate change: a pioneer detection method.” *The Geneva Papers on Risk and Insurance-Issues and Practice*, 51(1): 176–207.

Abel (2016) Eqs.(8)-(9): Full sample vs Abel (1999-2013Q4) regressions

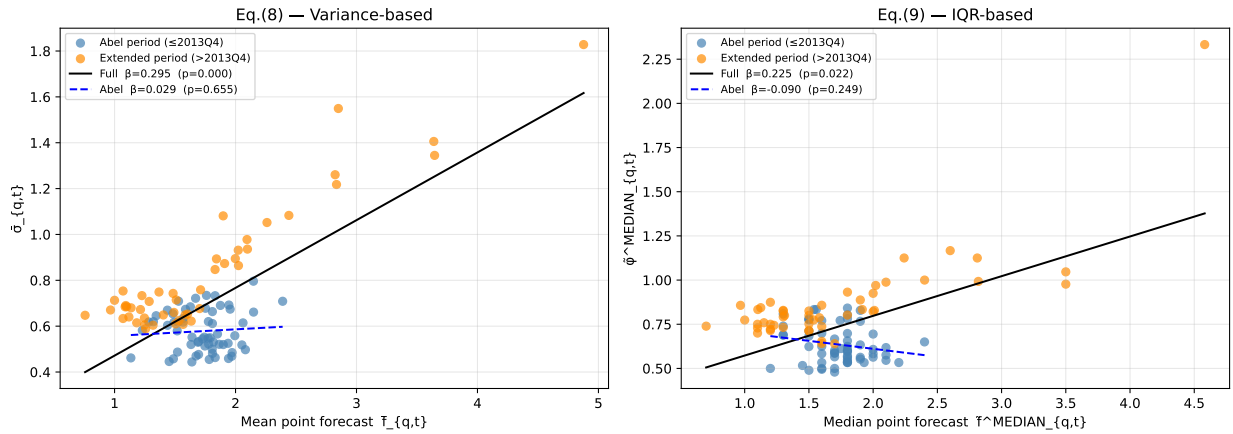


Figure 1: Inflation uncertainty versus aggregate point forecast: replication of Abel et al. (2016) and sample extension. **Left:** Variance-based measure  $\bar{\sigma}_{q,t}$  (cross-sectional mean of individual SPD standard deviations) against mean point forecast  $\bar{f}_{q,t}$ . **Right:** IQR-based measure  $\tilde{\phi}_{q,t}^{\text{MEDIAN}}$  (cross-sectional median of individual interquartile ranges) against median point forecast  $\tilde{f}_{q,t}^{\text{MEDIAN}}$ . Blue: 1999Q1–2013Q4 (Abel et al., 2016 sample); orange: 2014Q1–2025Q4 (extension). Solid line: OLS fit, full sample; dashed line: OLS fit, Abel sample only. Newey–West HAC standard errors (4 lags).

**Volk, Matjaž.** 2026. “Pricing Risk or Rationing Credit? Bank Behaviour in a Tightening Monetary Cycle.” *Banka Slovenije Working Papers*.

**Wachter, Jessica A.** 2006. “A consumption-based model of the term structure of interest rates.” *Journal of Financial economics*, 79(2): 365–399.

**Wright, Jonathan H.** 2011. “Term premia and inflation uncertainty: Empirical evidence from an international panel dataset.” *American Economic Review*, 101(4): 1514–1534.

**Zarnowitz, Victor, and Louis A Lambros.** 1987. “Consensus and uncertainty in economic prediction.” *Journal of Political economy*.

**Zellner, Arnold.** 1986. “Bayesian estimation and prediction using asymmetric loss functions.” *Journal of the American Statistical Association*, 81(394): 446–451.

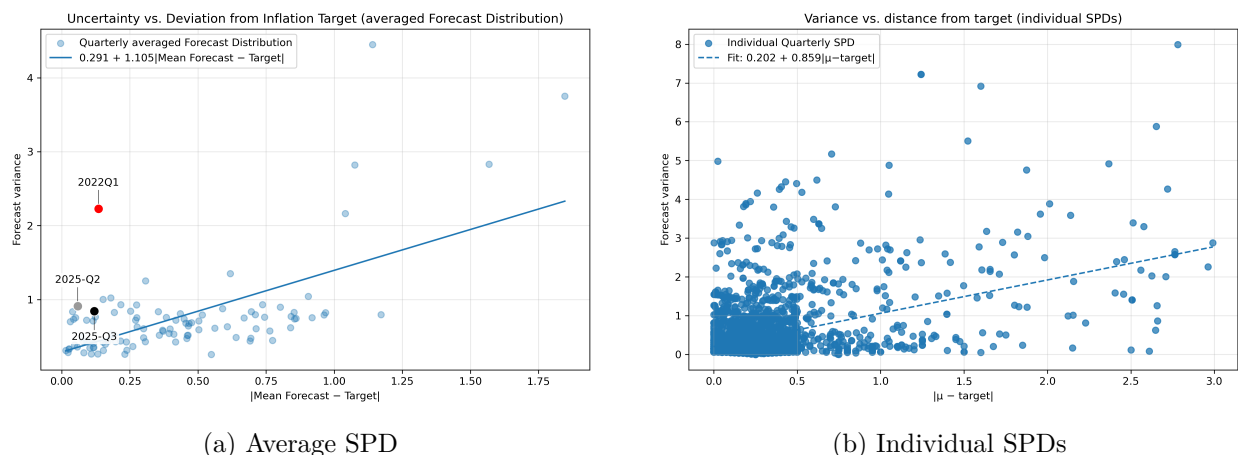


Figure 2: Variance–distance relationship in ECB-SPF inflation forecasts. The left panel plots the variance of the average SPD against  $|\mu_t - \pi^*|$ ; the right panel plots individual SPD variances against the same distance. Solid lines show OLS fits with regression coefficients reported in the legends. For the individual-level panel, observations with SPD means below the 30th percentile are excluded to mitigate zero-lower-bound effects, and means above 5% are trimmed in line with the ECB-SPF bin design.

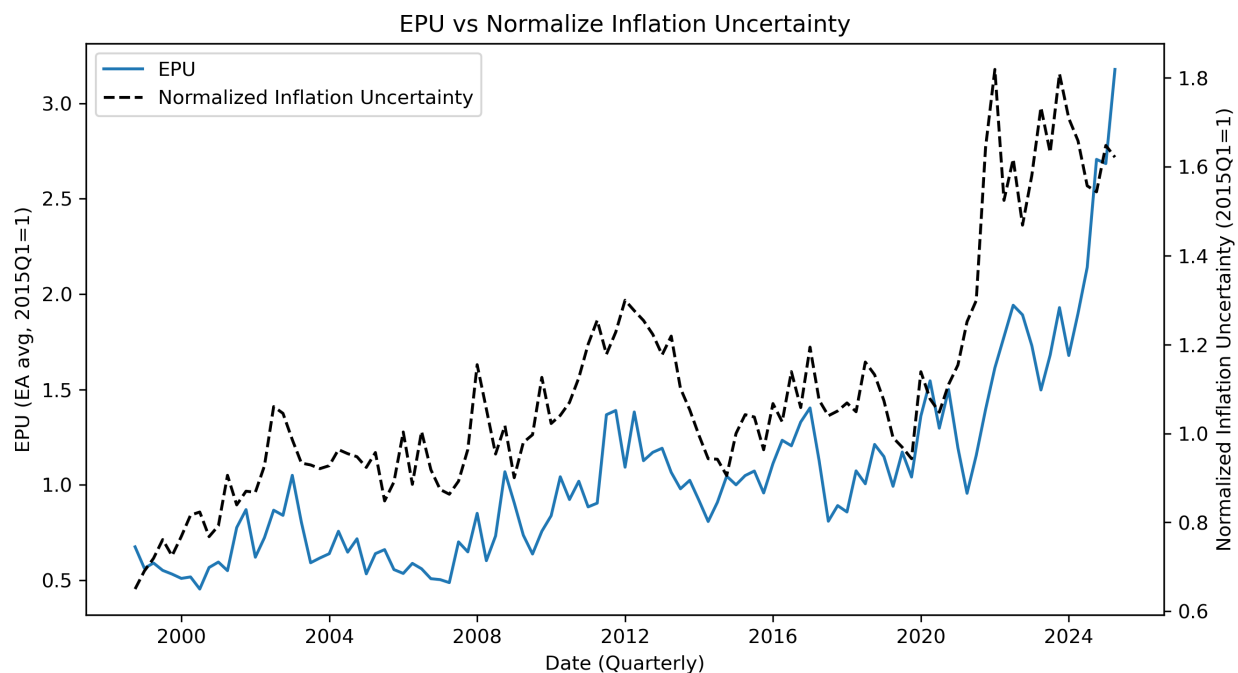


Figure 3: Economic Policy Uncertainty versus Normalized Inflation Uncertainty. The EPU index is the average of the Baker, Bloom and Davis (2016) country-level indices for six euro-area countries. NIU is the cross-sectional mean of individual  $CV^*$  computed from ECB-SPF one-year-ahead inflation density forecasts. Both series are quarterly.

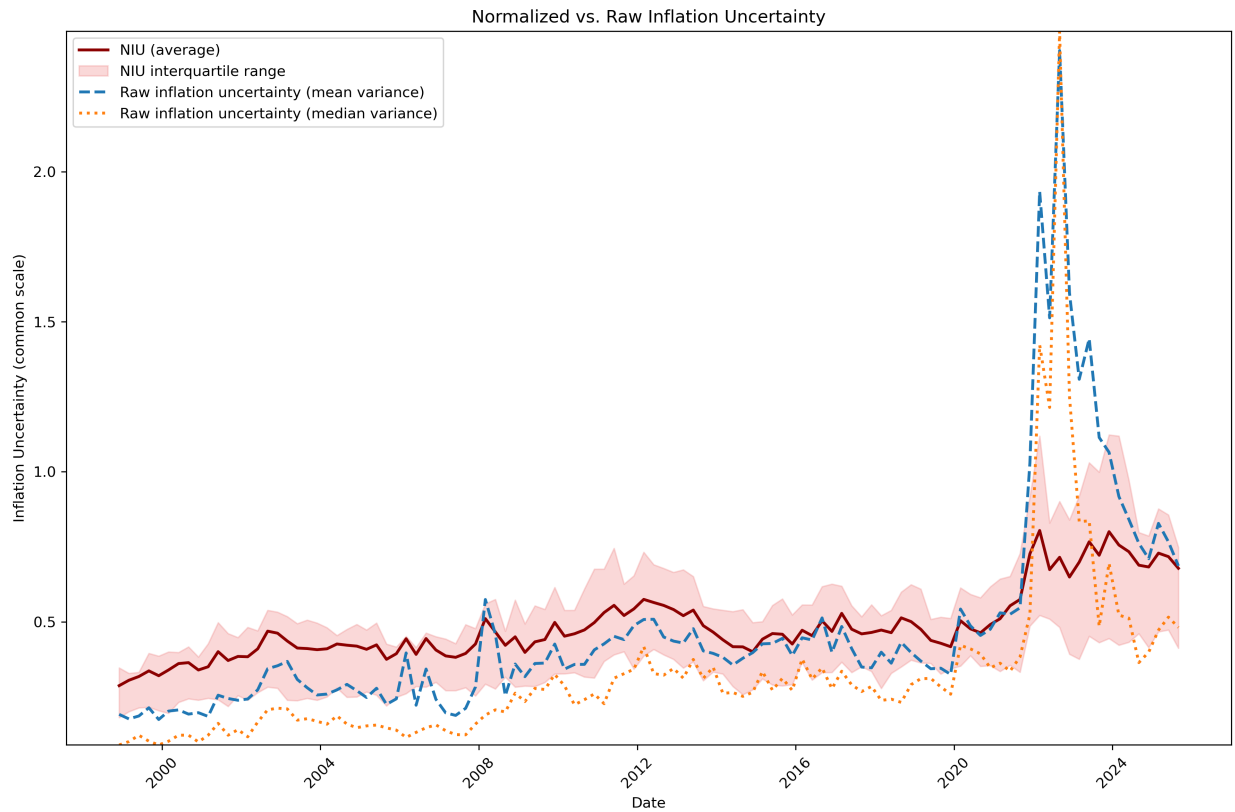
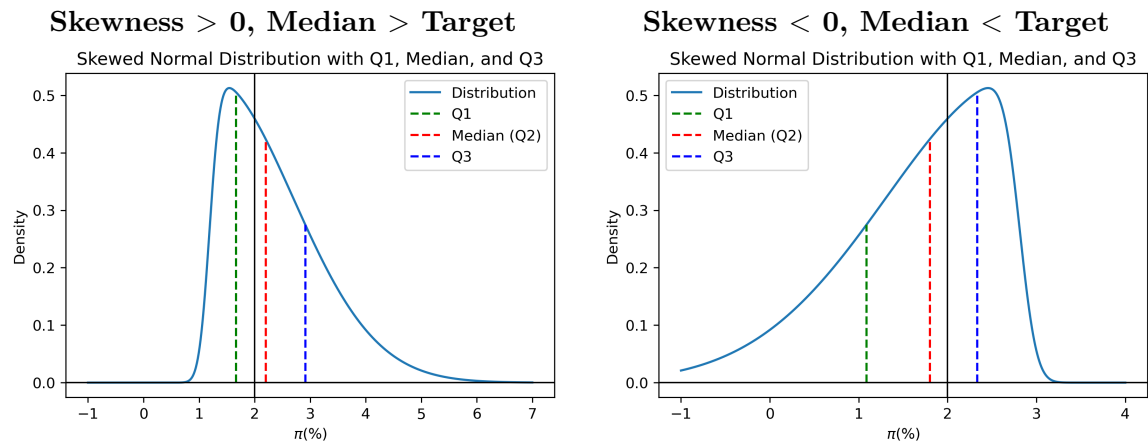


Figure 4: Normalized Inflation Uncertainty (NIU) versus raw inflation uncertainty (IU). NIU (solid line) is shown with its interquartile range (shaded area). Raw uncertainty is measured as the cross-sectional mean and median of individual SPD variances from the ECB-SPF one-year-ahead inflation forecast distributions.

### COHERENT ASYMMETRY (strong directional signal)



### INCOHERENT ASYMMETRY (weak directional signal)

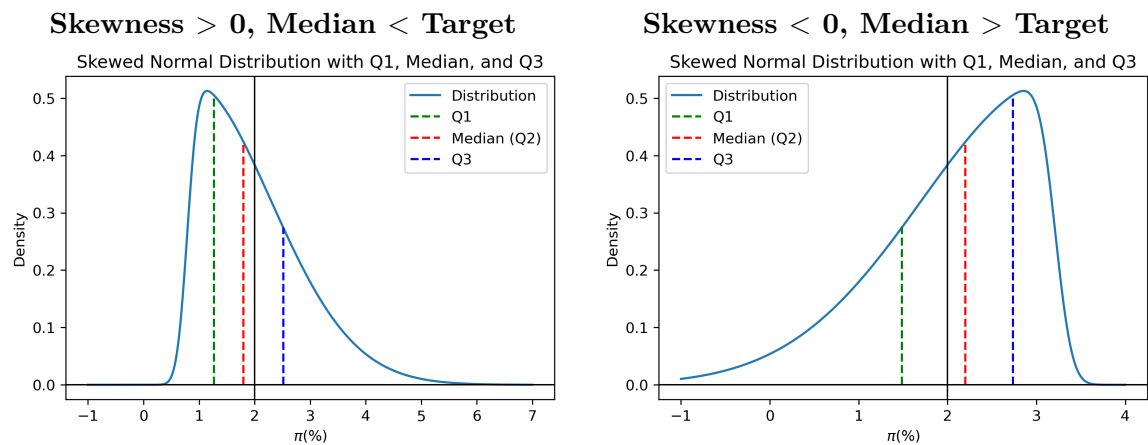


Figure 5: Illustration of coherent versus incoherent asymmetry. Skew-normal distributions with  $Q_1$  (green dashed), median (red dashed), and  $Q_3$  (blue dashed) marked; the solid black vertical line indicates the 2% inflation target ( $\pi^*$ ). **Top row:** coherent cases—the sign of skewness agrees with the direction of the median deviation from target, producing a strong directional signal. **Bottom row:** incoherent cases—skewness and median deviation point in opposite directions, producing a weak or uninformative signal.

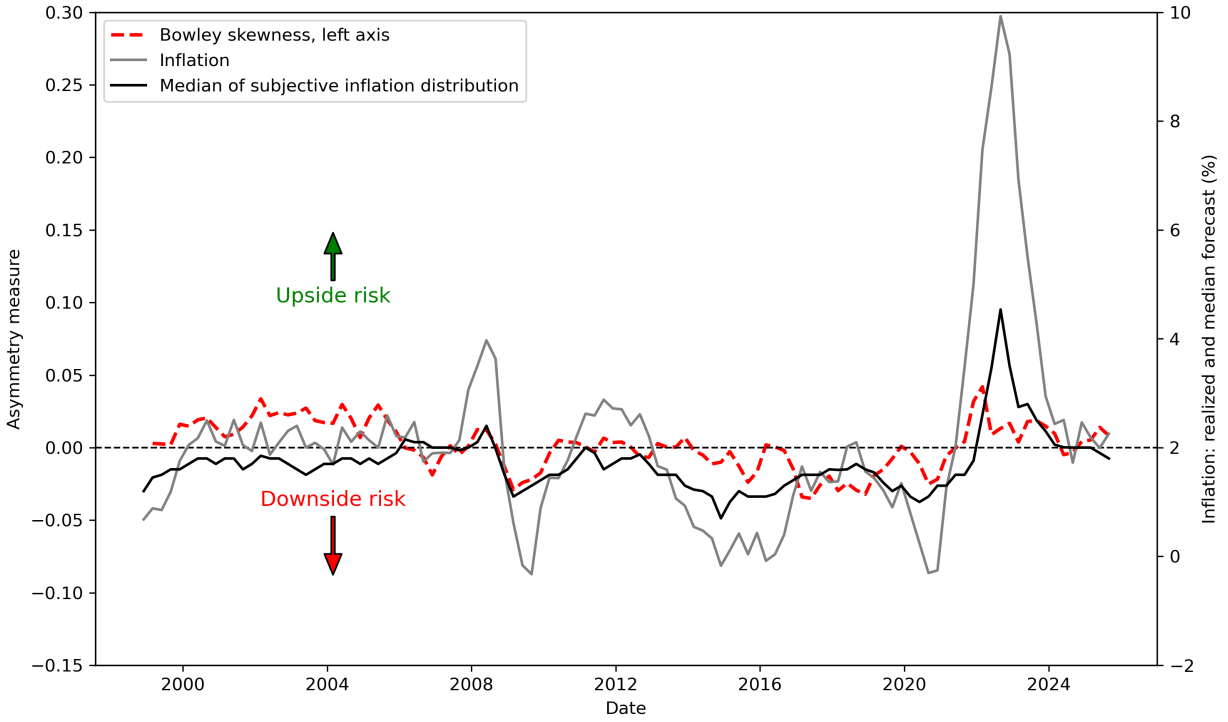


Figure 6: Asymmetry Coherence Index (ACI) and median inflation expectations: ECB-SPF one-year-ahead forecasts.

*Notes:* The right-hand axis reports  $\bar{Q}_t$ , the cross-forecaster median of individual SPD medians for one-year-ahead inflation expectations. The left-hand axis reports  $\bar{A}_t$ , the cross-sectional mean of individual Bowley's skewness computed from subjective probability distributions. Positive (negative) values indicate predominant upside (downside) inflation risk relative to the center of the distribution. Both series are aligned to forecast formation dates by shifting observations back by one year. The asymmetry series is smoothed using a short moving average to emphasize medium-run dynamics. The ECB-SPF probability bins change in 2024Q4: prior to that date, distributions are defined over 14 coarse inflation intervals; from 2024Q4 onward, the survey introduces a refined grid with narrower bins around zero inflation. Quartiles and skewness are computed by linear interpolation within bins, selecting the appropriate bin structure in each regime.

Strategy E: Period-by-period four-moment decomposition

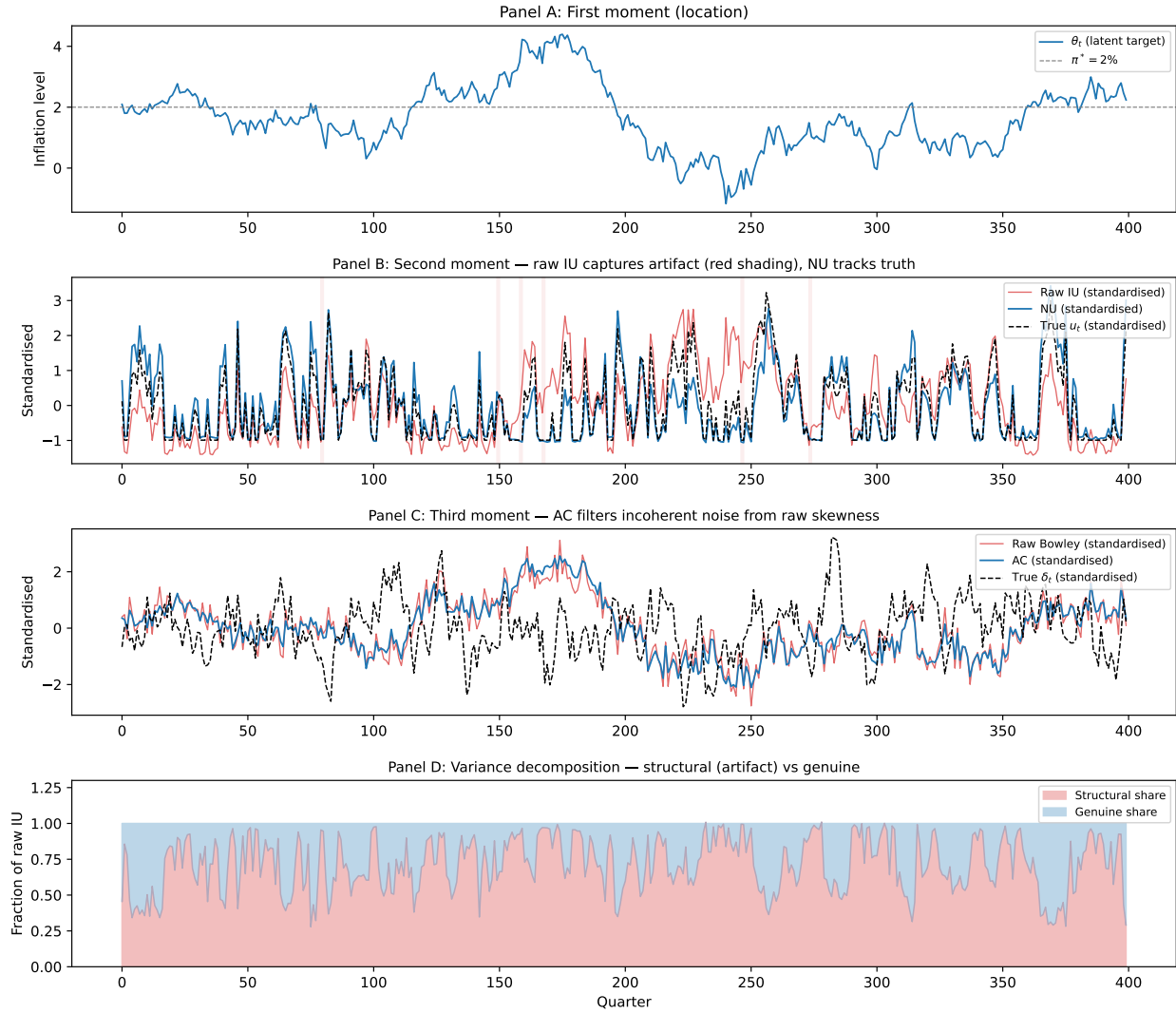


Figure 7: Period-by-period decomposition of raw and corrected moments (Monte Carlo, single extended run,  $T = 400$ ). **Panel A:** Latent inflation target  $\theta_t$  relative to the anchor  $\pi^*$  and raw mean forecast  $\mu_t$ . **Panel B:** Raw IU captures the artifact—it rises whenever  $\theta_t$  drifts from  $\pi^*$  even when genuine uncertainty  $u_t$  is stable (artifact episodes shaded in red)—while NU tracks the true  $u_t$  closely. **Panel C:** AC filters incoherent noise from raw asymmetry, tracking the true directional risk  $\delta_t$ . **Panel D:** Variance decomposition showing that 50–80% of raw IU is structural artifact at any given time. All series in Panels A–C are standardized.

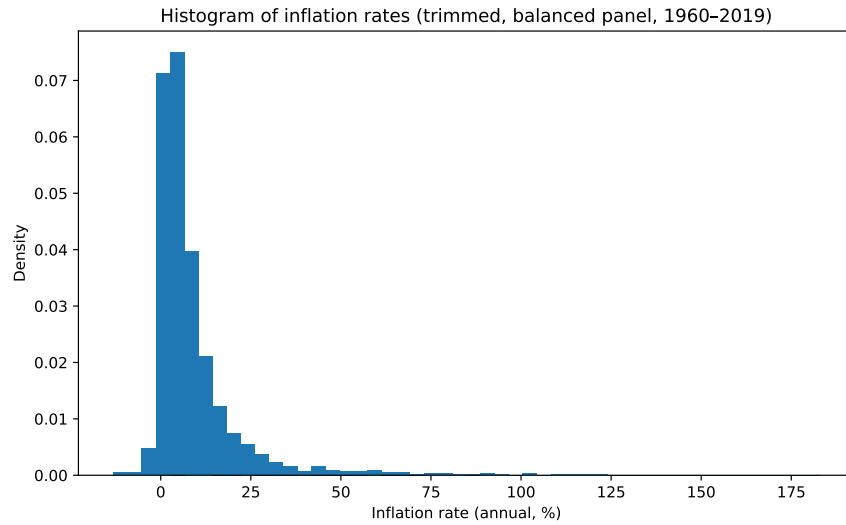


Figure 8: Distribution of annual inflation rates: replication of Barro (1995), Figure 1. *Notes:* Annual CPI inflation from the Global Macro Data (GMD) database, balanced panel, 1960–2019, trimmed to  $[-20\%, 200\%]$  to exclude extreme deflation and hyperinflation. The histogram confirms the well-documented right skewness of the cross-country inflation distribution.

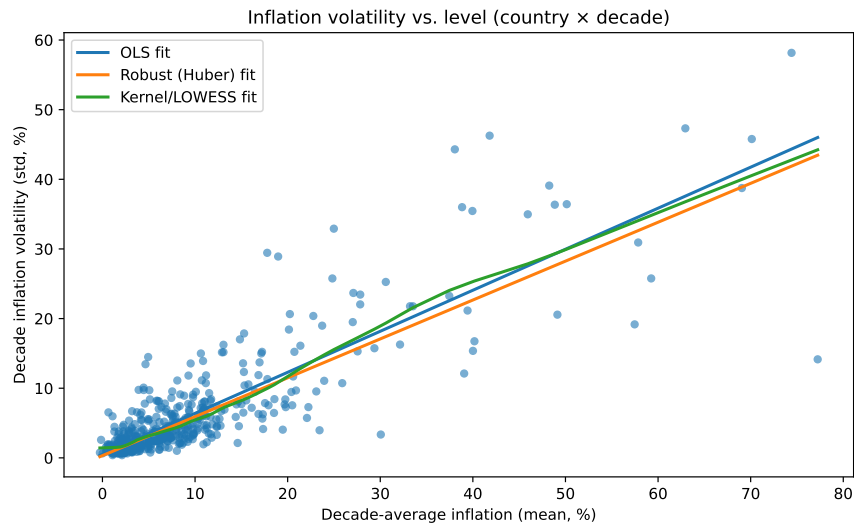


Figure 9: Inflation volatility versus inflation level: replication of Barro (1995), Figure 2. *Notes:* Each point is a country–decade observation (GMD, 1960–2019). Three fitted curves are overlaid: OLS (linear), robust Huber M-estimator, and LOWESS (frac = 0.30). All three confirm the strong positive relationship between the level and the volatility of inflation.

Table 3: Raw versus normalized inflation uncertainty: regression evidence

	(1)	(2)	(3)	(4)
	NIU <sub>t</sub>	NIU <sub>t</sub>	IU <sub>t</sub>	NIU <sub>t</sub>
Constant	0.359*** (0.026)	0.226*** (0.024)	0.239*** (0.066)	0.458*** (0.030)
IU <sub>t</sub>	0.266*** (0.061)	0.713*** (0.084)		
IU <sub>t</sub> <sup>2</sup>		-0.224*** (0.035)		
$d_t =  \bar{\mu}_t - \pi^* $			0.524*** (0.164)	0.062 (0.042)
Observations	108	108	108	108
$R^2$	0.688	0.894	0.425	0.057
HAC lags	4	4	4	4

Notes: NIU<sub>t</sub> is Normalized Inflation Uncertainty (cross-sectional mean of individual CV<sup>\*</sup>). IU<sub>t</sub> is raw inflation uncertainty (cross-sectional mean of individual SPD variances).  $d_t = |\bar{\mu}_t - \pi^*|$  is the absolute distance of the mean SPF point forecast from the inflation target  $\pi^* = 2\%$ . Column (3) documents the level-dependence failure: 42.5% of the variation in raw IU is explained by the distance from target. Column (4) shows that NIU removes this dependence ( $R^2 = 0.057$ ). Standard errors are Newey–West HAC (maxlags = 4). \*\*\* $p < 0.01$ , \*\* $p < 0.05$ , \* $p < 0.1$ .

Table 4: Skewness–deviation regression: individual ECB-SPF inflation forecasts

	(1)	(2)	(3)	(4)
Constant	0.005*** (0.002)	0.004 (0.011)	0.005** (0.002)	0.000 (0.011)
$\mu_{i,t} - \mu^*$	0.013*** (0.002)	0.015*** (0.003)	0.013*** (0.003)	0.011** (0.005)
Observations	4,538	4,538	4,461	4,461
$R^2$	0.012	0.057	0.006	0.053
Time fixed effects	No	Yes	No	Yes
Sample	Full	Full	$ d  \leq 2$	$ d  \leq 2$
SE clustering	Date	Forecaster	Date	Forecaster

Notes: OLS regressions of individual asymmetry  $A_{i,t}$  (Bowley’s skewness) on the signed deviation of the SPD mean from the inflation target  $\mu^* = 2\%$ :  $A_{i,t} = \alpha_0 + \alpha_1(\mu_{i,t} - \mu^*) + u_{i,t}$ . Data: ECB-SPF one-year-ahead inflation density forecasts (108 survey dates, 107 forecasters, 1999Q1–2025Q3). The positive and significant  $\hat{\alpha}_1$  validates the coherent-asymmetry condition ( $c > 0$ ) of Proposition 2. The low  $R^2$  reflects the noisiness of individual survey-based skewness—precisely the signal-extraction problem that the AC construction addresses. Columns (3)–(4) trim observations with  $|\mu_{i,t} - \mu^*| > 2$  pp. \*\*\* $p < 0.01$ , \*\* $p < 0.05$ , \* $p < 0.1$ .

Table 5: Raw versus corrected higher moments: how inference changes

Application	Raw	Result	Corrected	Result	Diagnostic
Distance dependence ( $R^2$ )	IU on $d_t$	$R^2 = 0.425$	NIU on $d_t$	$R^2 = 0.057$	Level contamination removed
Mean–asymmetry correlation	Raw asym. $A_t$	$\rho = 0.64$	ACI	Distinct from NIU	Directional noise filtered
Growth (Barro)	regression $\sigma_\pi$	$-0.0009^{***}$	NIU	$-0.0015$ (n.s.)	Effect vanishes
Mean inflation in Barro	With $\sigma_\pi$	$0.0001$ (n.s.)	With NIU	$-0.0003^{***}$	Recovers significance
VAR: IP $\leftarrow$ uncertainty	IU shock	IP contracts**	NIU shock	IP insignificant	Contraction was artifact
VAR: DFR $\leftarrow$ asymmetry	Raw asym. shock	DFR <i>decreases</i>	ACI shock	DFR <i>increases</i> *	Sign reversal
Forecasting (MSFE, $h = 4$ )	AR + IU	Deteriorates	AR + ACI	$0.759$ (DM n.s.)	Suggestive improvement

Notes: IU = raw inflation uncertainty (cross-sectional mean of individual SPD variances); NIU = Normalized Inflation Uncertainty (§3.1.2); ACI = Asymmetry Coherence Index (§3.2.2);  $d_t = |\bar{\mu}_t - \pi^*|$  is the distance of the consensus forecast from target. Pre-2020 subsample for VAR rows. Significance: \*\*\* $p < 0.01$ , \*\* $p < 0.05$ , \* $p < 0.1$ ; n.s. = not significant. For the forecasting row, the two-sided Diebold–Mariano test against the AR(AIC) benchmark yields  $p = 0.109$  at  $h = 4$ .

Table 6: Variance–distance regression: average SPD (full sample)

	Coef.	Std. err.	$t$	$p$ -value
Constant	0.291	0.078	3.75	0.000
$ \mu - \pi^* $	1.105	0.142	7.78	0.000
Observations		106		
$R^2$		0.368		

Notes: OLS regression of the variance of the average SPD on the absolute distance of the mean forecast from the inflation target  $\pi^* = 2\%$ :  $\text{Var}(\bar{X}_t) = a + b|\bar{\mu}_t - \pi^*| + e_t$ . Data: ECB-SPF one-year-ahead inflation forecasts, 106 quarterly survey rounds.

Table 7: Variance–distance regression: individual SPDs (trimmed sample)

	Coef.	Std. err.	$t$	$p$ -value
Constant	0.202	0.015	13.64	0.000
$ \mu - \pi^* $	0.859	0.032	26.65	0.000
Observations		3,083		
$R^2$		0.187		
$F$ -statistic		710.4		

Notes: OLS regression of individual SPD variance on the absolute distance of the forecaster’s mean from the inflation target  $\pi^* = 2\%$ :  $\text{Var}_{i,t} = a + b|\mu_{i,t} - \pi^*| + e_{i,t}$ . The sample is trimmed by excluding SPDs with means below the 30th percentile or above 5%, consistent with the ECB-SPF bin design. Data: ECB-SPF one-year-ahead inflation individual density forecasts.

Table 8: Correlation matrix of individual SPD moments: ECB-SPF one-year-ahead inflation forecasts

	Mean	CV	Skewness	Kurtosis
Mean	1.00	-0.49	0.64	0.48
CV	-0.49	1.00	-0.30	0.12
Skewness	0.64	-0.30	1.00	0.16
Kurtosis	0.48	0.12	0.16	1.00

*Notes:* Pairwise correlations of the four statistical moments—Mean, Coefficient of Variation (CV), Bowley’s Skewness, and Moors’ Kurtosis—computed from individual subjective probability distributions (SPDs) of one-year-ahead inflation forecasts in the ECB-SPF. The positive mean–skewness correlation ( $\rho = 0.64$ ) motivates the Asymmetry Coherence construction: higher expected inflation is systematically associated with greater right-tail risk.

Table 9: Monte Carlo simulation: raw versus corrected moments

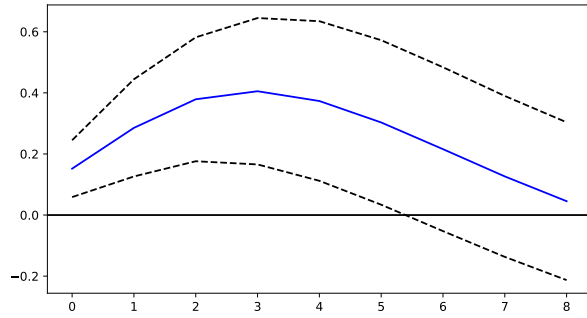
Strategy	Metric	Raw	Corrected
<i>Panel A: Normalized Uncertainty</i>			
A. Oracle $R^2$ : tracking $u_t$	$R^2(\cdot, u_t)$	0.581	<b>0.829</b>
A. Artifact exposure: tracking $d_t$	$R^2(\cdot, d_t)$	0.437	<b>0.094</b>
B. Spurious rejection (HAC, growth $\sim$ measure)	% reject at 5%	57.6%	23.6%
B. Controlled (HAC, growth $\sim$ measure + $d$ )	% reject at 5%	4.6%	<b>4.6%</b>
<i>Panel B: Asymmetry Coherence</i>			
A. Coherent signal recovery	$R^2(\cdot, AC^{nf})$	0.780	<b>0.941</b>
D. Inflation forecasting (real-time AC)	Median rel. MSFE	0.982	<b>0.951</b>

*Notes:* Monte Carlo simulation with 500 replications,  $T = 200$  periods,  $N = 30$  forecasters. The DGP is an extended UCSV model with a latent inflation target (mean-reverting with state-dependent drift,  $\kappa_\theta = 0.02$ ), AR(1) genuine uncertainty  $u_t$ , and AR(1) directional risk  $\delta_t$ . Raw: cross-sectional mean of individual variances (IU) or raw asymmetry (Bowley’s formula). Corrected:  $NU = \sqrt{\text{Var}}/\sqrt{a + b|\mu - \mu^*|}$  or  $AC = [(\tilde{Q} + \tilde{A})/2] \cdot [(1 + \tilde{Q}\tilde{A})/2]$ .  $AC^{nf}$ : noise-free AC computed from structural and genuine Bowley components (without incoherent noise). Strategy B uses Newey–West (HAC) standard errors; Strategy D uses expanding-window (real-time) AC normalisation with no look-ahead. Bold: the measure with better performance. Full results in Online Appendix ??.

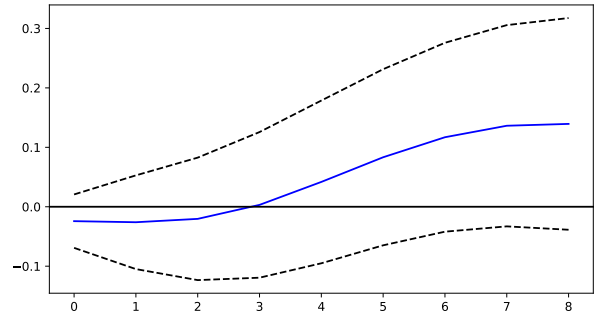
Table 10: Decade-averaged growth regressions: Barro–Lee panel with NIU

	(1)	(2)	(3)	(4)	(5)
Mean inflation (decade)	−0.0004*** (0.0001)	0.0001 (0.0002)	−0.0001 (0.0001)	−0.0003*** (0.0001)	−0.0003*** (0.0001)
Std. dev. inflation (decade)		−0.0009*** (0.0003)	−0.0005* (0.0003)		
NIU = $\sigma_\pi / \sqrt{1 +  \bar{\pi} - 2 }$				−0.0015 (0.0013)	
NIU <sub>alt</sub> = $\sigma_\pi / \sqrt{1 +  \bar{\pi} }$					−0.0022 (0.0014)
log Real GDP per capita			−0.0000 (0.0005)	0.0000 (0.0005)	0.0000 (0.0005)
Male schooling years (age 25+)			0.0041* (0.0021)	0.0039* (0.0021)	0.0041* (0.0021)
Female schooling years (age 25+)			−0.0054*** (0.0016)	−0.0054*** (0.0016)	−0.0055*** (0.0016)
log Life expectancy at birth			0.0281* (0.0161)	0.0291* (0.0158)	0.0294* (0.0158)
log Fertility rate			−0.0138* (0.0076)	−0.0138* (0.0077)	−0.0133* (0.0077)
Government consumption / GDP			−0.0263 (0.0307)	−0.0286 (0.0310)	−0.0272 (0.0309)
Gov. education spending / GDP			0.0497 (0.1323)	0.0429 (0.1327)	0.0461 (0.1323)
Black market premium			−0.0042 (0.0027)	−0.0044* (0.0026)	−0.0044* (0.0026)
Terms-of-trade shock			0.0465 (0.0425)	0.0434 (0.0436)	0.0428 (0.0433)
Investment / GDP			0.0500 (0.0304)	0.0513* (0.0301)	0.0500* (0.0300)
Political rights index			0.0136*** (0.0039)	0.0136*** (0.0039)	0.0137*** (0.0039)
Political rights <sup>2</sup>			−0.0015*** (0.0005)	−0.0015*** (0.0005)	−0.0015*** (0.0005)
Constant	0.0287*** (0.0025)	0.0301*** (0.0025)	−0.0871 (0.0642)	−0.0889 (0.0639)	−0.0911 (0.0635)
Decades			1960, 1970, 1980		
Decade fixed effects			Yes		
Country-clustered SE			Yes		
Observations	343	343	237	237	237
Countries	124	124	93	93	93
R <sup>2</sup>	0.143	0.171	0.432	0.427	0.431

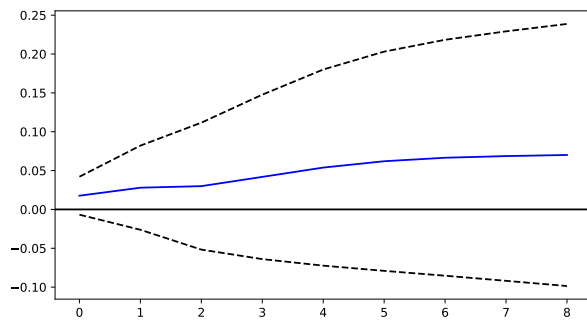
*Notes:* Dependent variable: decade-averaged real GDP per capita growth (Barro–Lee  $\text{grwb}_x$ ). Within-decade inflation moments are computed from GMD annual CPI inflation (trimmed to [−20%, 200%]). Pooled OLS with decade fixed effects; standard errors clustered at the country level. Columns (1)–(3) use raw inflation volatility ( $\sigma_\pi$ , within-decade standard deviation); columns (4)–(5) replace it with Normalized Inflation Uncertainty. NIU =  $\sigma_\pi / \sqrt{1 + |\bar{\pi} - 2|}$  normalizes by the distance of mean inflation from the 2% target; NIU<sub>alt</sub> =  $\sigma_\pi / \sqrt{1 + |\bar{\pi}|}$  uses an untargeted normalization. The raw volatility coefficient is significant in columns (2)–(3) but vanishes with NIU in columns (4)–(5), while mean inflation recovers significance. Data: Barro–Lee panel (138 countries, six quinquennial subperiods 1965–1990, aggregated to decades); GMD inflation matched by ISO3 code. \*\*\* $p < 0.01$ , \*\* $p < 0.05$ , \* $p < 0.1$ .



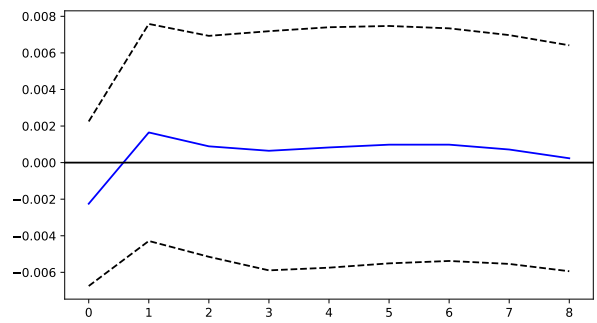
(a) Response of inflation (INFL)



(b) Response of the ECB deposit facility rate (DFR)



(c) Response of unemployment (UNEMP)



(d) Response of industrial production (log IP)

**Figure 10: Impulse responses to a normalized inflation uncertainty shock (VAR 1).** Orthogonalized impulse responses (Cholesky identification) from a quarterly VAR with ordering  $(EPU_t, NGU_t, NIU_t, \pi_t, DFR_t, u_t, \log IP_t)$ . The shock is a one-standard-deviation innovation to standardized NIU.

*Notes:* NIU denotes Normalized Inflation Uncertainty (cross-sectional mean of individual  $CV^*$  from ECB-SPF one-year-ahead inflation density forecasts), standardized prior to estimation. INFL is quarterly average year-on-year HICP inflation; DFR is the end-of-quarter ECB deposit facility rate; UNEMP is the quarterly average euro-area unemployment rate; log IP is the quarterly average of log industrial production. Lag order is selected by AIC (maxlags = 3). Shaded areas denote Monte Carlo error bands (1000 replications, 10% significance level). Horizon: 8 quarters.

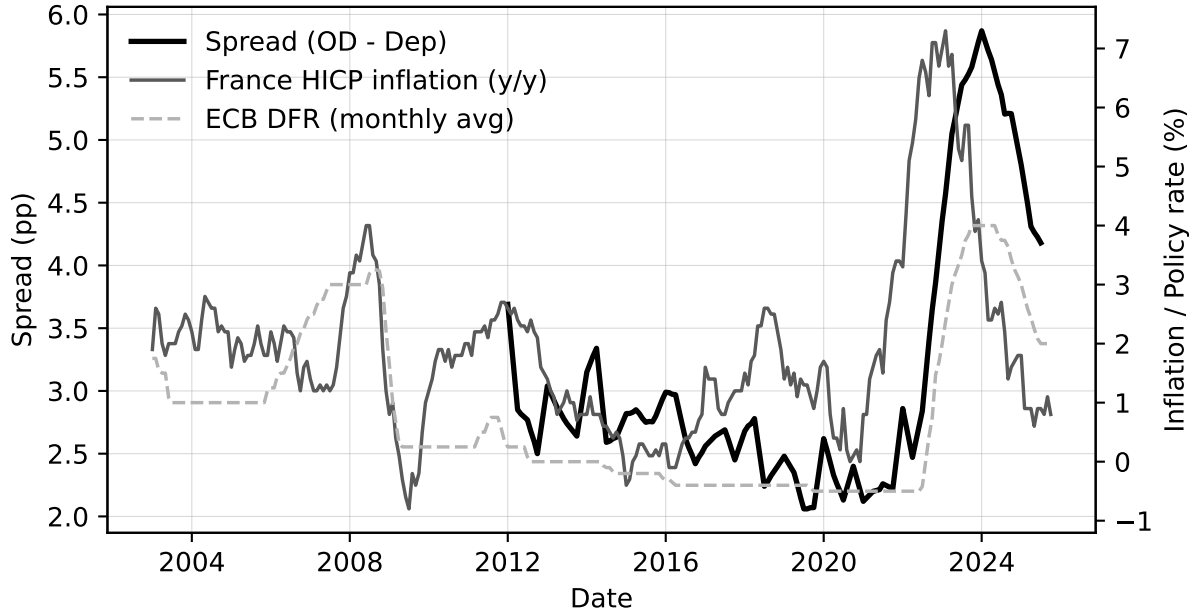


Figure 11: France: NFC overnight overdraft–deposit spread, HICP inflation, and the ECB deposit facility rate

*Notes:* The solid line (left axis) reports the spread between the NFC overnight overdraft rate and the NFC overnight deposit rate,  $\text{Spread}_t \equiv r_t^{\text{od}} - r_t^{\text{dep}}$ . The right axis reports France year-on-year HICP inflation (all items) and the ECB deposit facility rate (monthly average of daily observations). Source: Banque de France Webstat and ECB.

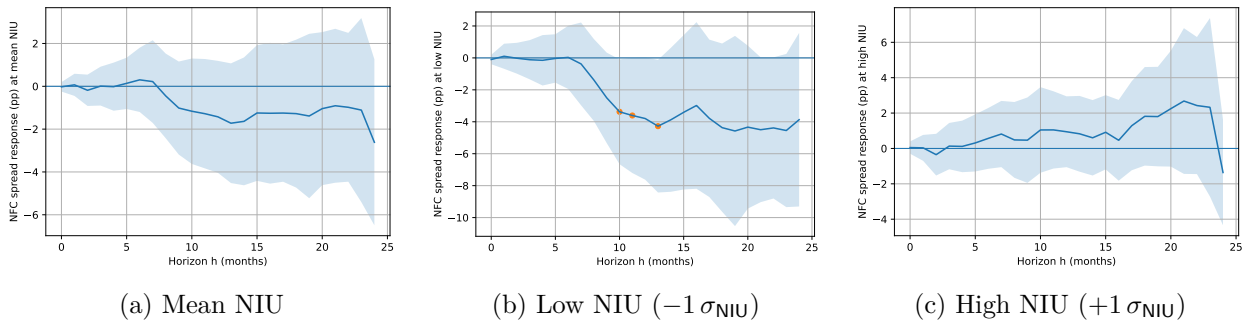


Figure 12: Local projections: response of the NFC overnight overdraft–deposit spread to a monetary policy shock across inflation-uncertainty states. Impulse responses are evaluated at average NIU (left), one standard deviation below (center), and one standard deviation above (right). Monetary policy shocks are “pure” shocks from Jarociński and Karadi (2020). Horizon: 24 months; Newey–West HAC standard errors with horizon-dependent lag truncation.

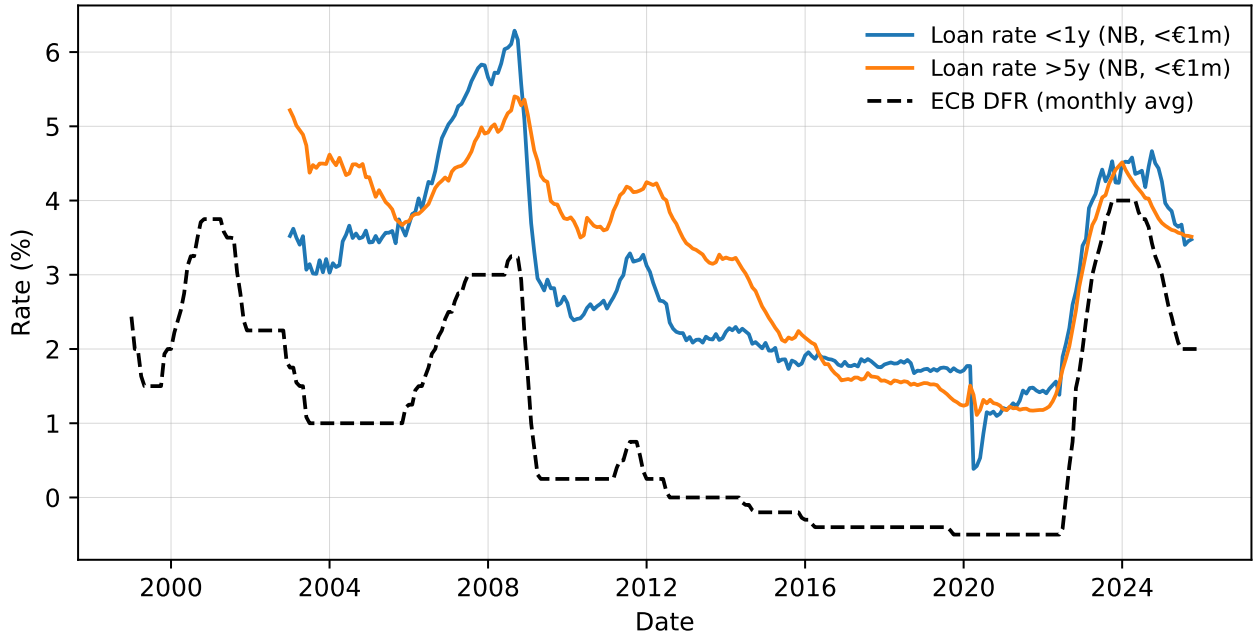
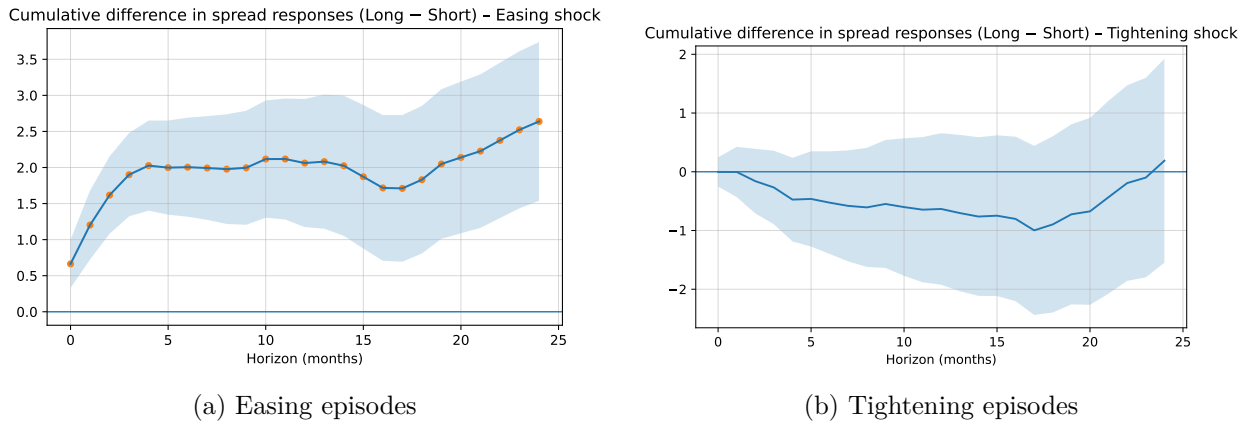


Figure 13: NFC loan rates by maturity and the ECB deposit facility rate

*Notes:* Monthly interest rates on new business loans to non-financial corporations (NFCs) in France with loan amounts below €1m, by initial period of rate fixation (PFIT). Solid lines correspond to PFIT < 1 year and PFIT > 5 years. The dashed black line reports the ECB deposit facility rate (monthly average). Source: Banque de France MIR statistics and ECB. Rates are expressed in percent per annum.



(a) Easing episodes

(b) Tightening episodes

Figure 14: Cumulative maturity differential in policy-rate-adjusted NFC loan spreads: easing versus tightening episodes. The plotted series is  $\sum_{\tau=0}^h (\hat{\beta}_{\tau}^L - \hat{\beta}_{\tau}^S)$ , the cumulative difference between the long-maturity (> 5 years) and short-maturity (< 1 year) spread responses to monetary policy shocks. Spreads are defined as  $s_t^m = r_t^m - \text{DFR}_t$ . Easing (tightening) shocks are identified from negative (positive) DFR changes. 95% confidence bands from Newey–West HAC standard errors with horizon-dependent lag truncation ( $\text{maxlags} = h$ ); markers indicate horizons where the cumulative difference is significant at the 5% level. Horizon: 24 months; 6 lags; controls include HICP inflation and month-of-year fixed effects. Source: Banque de France MIR and ECB.

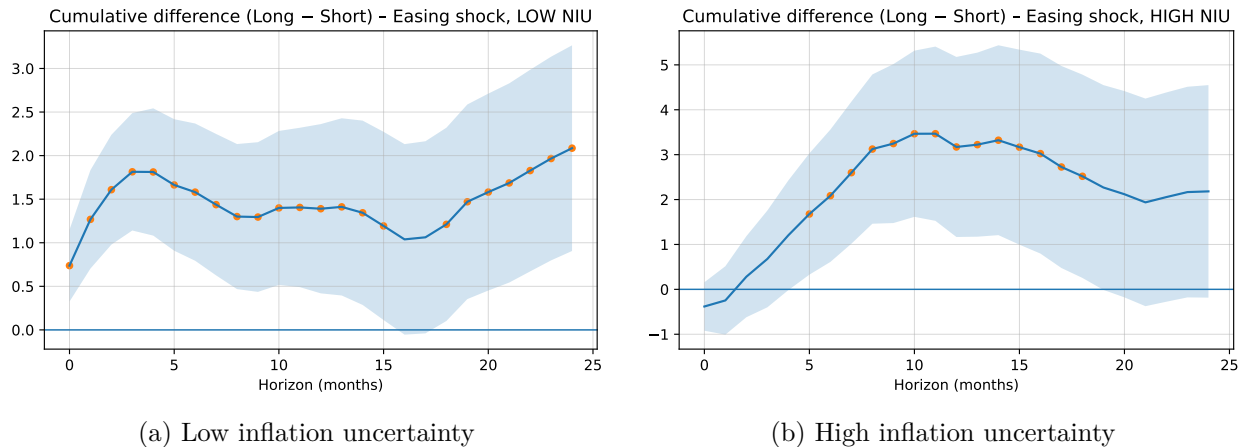
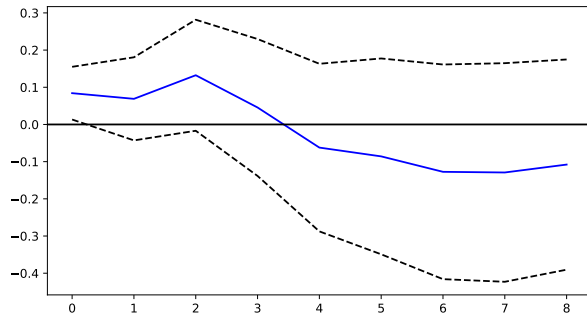


Figure 15: Easing episodes: cumulative maturity differential in NFC loan spreads by inflation-uncertainty regime. Same construction as Figure 14 (easing panel), with easing shocks interacted with an NIU indicator. The low (high) regime corresponds to  $NIU_t$  at or below (above) its sample median.  $NIU_t$  is the normalized inflation uncertainty measure from the ECB-SPF, linearly interpolated from quarterly to monthly frequency.  $NIU_t$  also enters in levels as a control. 95% confidence bands from Newey–West HAC standard errors (maxlags =  $h$ ); markers indicate significance at the 5% level. Horizon: 24 months; 6 lags.

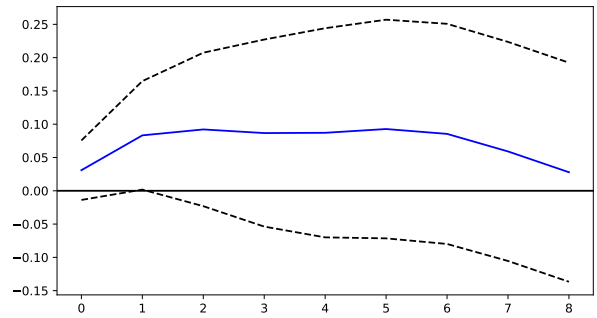
Table 11: Pseudo out-of-sample inflation forecasting: relative MSFEs

$h$	AR(AIC)	AO	IMA( $\theta=0.65$ )	AR+NIU	AR+ACI	AR+NIU+ACI	AR+IU <sup>raw</sup>	AR+Asym. <sup>raw</sup>
1	1.000	0.936 (0.488)	0.915 (0.510)	<b>1.092</b> (0.030)	0.951 (0.445)	1.045 (0.521)	0.970 (0.752)	0.976 (0.604)
2	1.000	0.907 (0.227)	0.829 (0.121)	1.044 (0.298)	0.859 (0.123)	0.927 (0.467)	0.934 (0.632)	0.916 (0.216)
4	1.000	0.942 (0.397)	<b>0.821</b> (0.029)	1.136 (0.122)	0.759 (0.109)	0.855 (0.303)	1.267 (0.104)	0.995 (0.874)

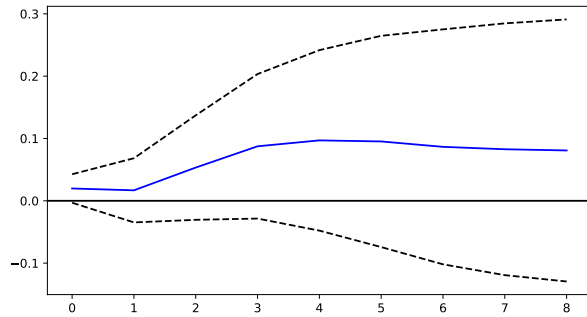
*Notes:* Relative MSFEs for euro-area HICP inflation, normalized to AR(AIC) = 1. Two-sided Diebold–Mariano  $p$ -values against AR(AIC) in parentheses. Bold: significant at 10%. Out-of-sample evaluation from 2003Q1 (expanding window). AO: Atkeson, Ohanian et al. (2001) random walk on the level of inflation. IMA: integrated moving average with fixed  $\theta = 0.65$ . NIU: Normalized Inflation Uncertainty (cross-sectional mean of individual  $CV^*$ ). ACI: Asymmetry Coherence Index. IU<sup>raw</sup>: raw inflation uncertainty (cross-sectional mean of individual SPD variances). Asym.<sup>raw</sup>: raw aggregate asymmetry (Bowley’s skewness). All models use direct  $h$ -step-ahead projections; AR lag order selected by AIC within the recursive window. Adding raw IU worsens accuracy; ACI lowers MSFEs at every horizon, with the largest reduction at  $h = 4$  (relative MSFE = 0.759).



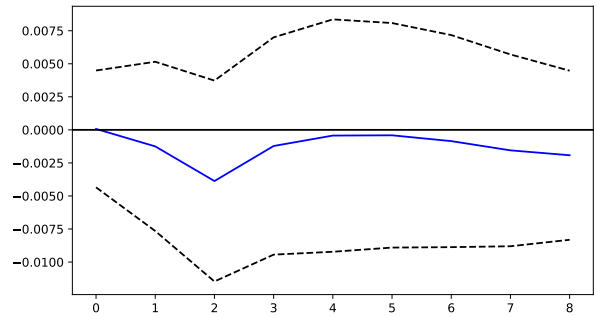
(a) Response of inflation (INFL)



(b) Response of the ECB deposit facility rate (DFR)



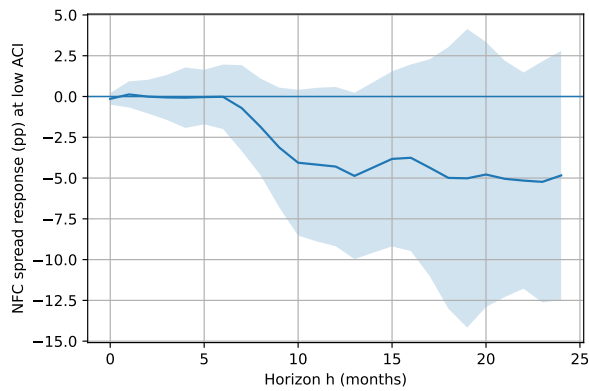
(c) Response of unemployment (UNEMP)



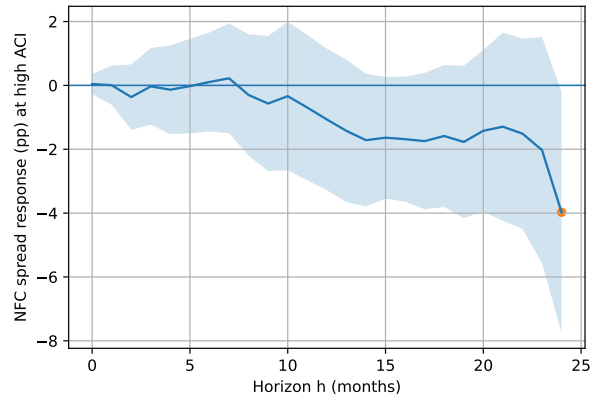
(d) Response of industrial production (log IP)

Figure 16: **Impulse responses to an Asymmetry Coherence shock (VAR 2).** Orthogonalized impulse responses (Cholesky identification) from a quarterly VAR with ordering  $(EPU_t, NIU_t, ACI_t, \pi_t, DFR_t, u_t, \log IP_t)$ . The shock is a one-standard-deviation innovation to standardized ACI.

*Notes:* ACI denotes the Asymmetry Coherence Index for inflation, constructed from ECB-SPF one-year-ahead density forecasts and standardized prior to estimation. NIU (Normalized Inflation Uncertainty) is included in the system but ordered before ACI. Variable definitions and estimation details are as in Figure 10. Shaded areas denote Monte Carlo error bands (1000 replications, 10% significance level). Horizon: 8 quarters.

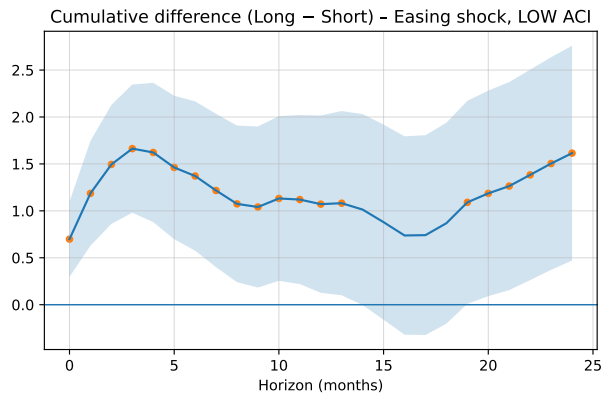


(a) Low ACI ( $-1\sigma_{ACI}$ )

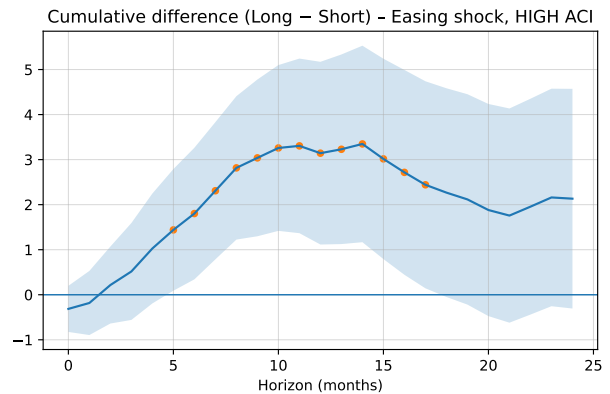


(b) High ACI ( $+1\sigma_{ACI}$ )

Figure 17: Local projections: response of the NFC overnight overdraft–deposit spread to a monetary policy shock across Asymmetry Coherence states. Impulse responses are evaluated at one standard deviation below (left) and above (right) the sample mean of ACI. Monetary policy shocks are “pure” shocks from Jarociński and Karadi (2020). ACI is linearly interpolated from quarterly to monthly frequency and enters both as a control and interacted with the shock. Horizon: 24 months; Newey–West HAC standard errors with horizon-dependent lag truncation.



(a) Low ACI



(b) High ACI

Figure 18: Easing episodes: cumulative maturity differential in NFC loan spreads by Asymmetry Coherence regime. Same construction as Figure 15, with easing shocks interacted with an ACI indicator instead of NIU. The low (high) regime corresponds to  $ACI_t$  at or below (above) its sample median.  $ACI_t$  is the monthly interpolated Asymmetry Coherence Index from the ECB-SPF.  $ACI_t$  also enters in levels as a control. 95% confidence bands from Newey–West HAC standard errors ( $\text{maxlags} = h$ ); markers indicate significance at the 5% level. Horizon: 24 months; 6 lags.